Mechanical Performance Prediction and Retrofitting Technique of Heritage Timber Beams

Reza Abbasi Malekabadi

A Thesis

In the Department of

Building, Civil, and Environmental Engineering

Presented in Partial Fulfillment of the Requirements

for the Degree of

Doctor of Philosophy (Civil Engineering) at

Concordia University

Montréal, Québec, Canada

October 2025

CONCORDIA UNIVERSITY

SCHOOL OF GRADUATE STUDIES

This is to certify that the thesis is prepared by:

Reza Abbasi Malekabadi

Entitled: Mechanical Performance Prediction and Retrofitting Technique of Heritage Timber Beams

Submitted in partial fulfillment of the requirements for the Degree of

Doctor of Philosophy (Civil Engineering)

Comply with the regulations of the University and meet the accepted standards with respect to originality and quality.

Signed by the final examining committee:

_____ Chair

Dr. Behrooz Yousefzadeh

_____ External Examiner

Dr. Sam Salem

_____ External to Program

Dr. Mehdi Hojjati

_____ Examiner

Dr. Biao Li

_____ Examiner

Dr. Fuzhan Nasiri

_____ Thesis Supervisor

Dr. Ghazanfarah Hafeez

_____ Graduate Program Director

Approved by: Dr. Chunjiang An/ Dr. Po-Han Chen

Date of Defence: Dec. 10, 2025

Dr. Mourad Debbabi, Dean of Faculty

ABSTRACT

Mechanical Performance Prediction and Retrofitting Technique of Heritage Timber Beams

Reza Abbasi Malekabadi, Ph.D.

Concordia University, 2025

Heritage timber buildings with cultural value often suffer from age-related deterioration, serviceability issues, load modifications, and gaps in code guidance for assessment and strengthening. This thesis developed an integrated framework to (i) predict the mechanical performance of in-situ Heritage timber beams and (ii) retrofit them using practical, minimally destructive techniques while retaining residual capacity if strengthening is lost. The methodology is executed in two Phases. Phase I (Evaluation) compiles a database for 44 full-scale Heritage beams (collected from Quebec and Ontario) with Non-Destructive Tests (NDTs), including density, dynamic MOE, cavity, and destructive bending test. Then, the material properties and mechanical performance of beams are assessed through two different methods. The first method established a comparison pathway via New/Simulated New Counterpart (SNC) beams for statistical inference testing. A Null-hypothesis protocol is used to investigate whether Heritage and New/SNC beams are mechanically comparable in terms of flexural strength, supporting a novel method that substitutes for NDTs. The technique allows destructive tests to be conducted on New beams and their results to be attributed to in-situ Heritage beams. The second approach developed and formulated NDT results in relation to mechanical performance to directly obtain the required assessment needs.

Phase II (Strengthening) evaluated Near-Surface-Mounted Glass Fibre Reinforced Polymer (NSM-GFRP) retrofits on full-scale Heritage members, varying rebar length, ratio, and configuration. The four-point bending procedure measured capacity gains, neutral-axis shifts, and failure modes. Furthermore, an allowable-strengthening criterion is derived by adapting ACI 440.2R to timber to maintain a safe residual capacity if FRP is suddenly lost. Beyond testing, complementary analytical formulations, Bernoulli-based sections, moment–curvature models

with simplified equilibrium, and a Whitney-type compression block calibrated to the experiments, support design and interpretation. These models bridge the gap between measured behaviour and design prediction, incorporating plasticized depth and neutral-axis movements.

Future work proposes a dual system (local post-tensioning and FRP) for cases where the flexural demand exceeds the allowable FRP limit, aiming to increase stiffness, enhance drift control, and incorporate self-centring capabilities.

The results show that calibrated NDT and destructive data enable Heritage-friendly assessment, and NSM-GFRP retrofits deliver substantial flexural gains, ranging from 30% to over 140%, depending on development length and configuration, while altering damage progression (e.g., delaying tension-governed rupture and changing failure modes). The proposed maximum allowable FRP limits provide a conservation-minded bound on intervention. Collectively, the thesis contributes to: (1) a full-scale Heritage beam database; (2) an NDT-to-mechanics and statistical equivalence pathway for in-situ assessment; (3) evidence-based NSM-GFRP guidance at full scale; and (4) allowable-strengthening and analytical tools with a proposed post-tensioned dual system concept for durable, reversible, and safer conservation practice.

Acknowledgements

First and foremost, I would like to express my sincere appreciation and gratitude to my supervisor, Dr. Gazanfarah Hafeez, for her continued support and encouragement during my doctoral studies. I am thankful to her for considering me worthy of pursuing a doctoral degree program and accepting me into her research team. I am grateful for the foundation he laid, which proved crucial in the successful completion of my thesis. Furthermore, I sincerely express my gratitude to Dr. Hafeez for inspiring me to achieve more than my potential and work hard with honesty in that respect. Overall, this academic journey would not have been possible without her kind support and supervision. I want to express my sincere gratitude to my committee: Dr. Sam Salem, Dr. Fozhan Nassiri, Dr. Emre Erkmen, Dr. Mehdi Hojjati, Dr. Behrooz Yousefzadeh, Dr. Biao Li, and Dr. Hafeez for their careful review of the thesis and for providing valuable insights and feedback, which have significantly enhanced my work. I would also like to thank the faculty members of the BCEE Department, including Dr. Khaled Galal and Dr. Lan Lin, among others, for their help and support during my doctoral studies. I sincerely thank the BCEE Department staff and executives, including Ms. Jenny Drapeau, Ms. Caroline Durand, Mr. Tiberiu Aldea, Ms. Elena Castigliano, and others, for their kind assistance and support. I would like to take this opportunity to thank my lab colleagues, Mr. Alex, Riff and Vito, for their ongoing support and assistance throughout my journey. I am especially grateful to my former supervisor, Dr. Kiachehr Behfarnia, for the exceptional attitude that inspired me to pursue my way in academia. In my life and during my doctoral studies, friends have played a massive role as a support system. I want to take this opportunity to thank all my friends, especially Masoud Bagheri, for always believing in me, helping me, and keeping me going. I would like to thank my wife, Hanieh Shahmohammadian, who stood firmly by my side, providing unwavering support during difficult times and creating a serene atmosphere for me to thrive in my PhD journey, all with unconditional love, for all these years. I could not have pursued this journey without her immense mental and emotional support throughout the years. I appreciate my daughter, Parmis, for bearing with me and all my shortcomings. Last but certainly not least, I want to express my profound gratitude to my parents, Masoomeh Sadeghi Malekabadi and Mokhtar Abbasi Malekabadi. Their constant support and encouragement in each of my life's endeavours have enabled me to reach this stage in my life.

“Don’t settle; keep going. Stay hungry, stay foolish.”

Contributions of Authors

This thesis has been prepared in accordance with the regulations and guidelines for the manuscript-based thesis format. It presents experimental, modelling, and analytical work conducted by Reza Abbasi. Throughout this process, the academic supervisor, Dr. Ghazanfarah Hafeez, provided advice and guidance for the entire thesis. The whole work is divided into two Phases: Phase I involves evaluating the mechanical performance and material properties of Heritage timber beams. At the same time, Phase II focuses on reinforcing the Heritage timber beams using the Near-Surface-Mounted (NSM)- FRP method.

The contribution of this thesis helps conservation engineering for timber Heritage through five integrated contributions. First, it assembled a unique database of 44 full-scale Heritage beams with measured material and mechanical properties, providing unique empirical baselines for assessment and research purposes. Second, it developed two practical, non-destructive evaluation pathways: (i) a Null-hypothesis, equivalence-based approach that safely infers MOR/MOE of in-situ members from tests on their new SPF counterparts (first ever done), and (ii) direct NDT-to-strength correlations for field use. Third, it validated minimally destructive NSM-GFRP retrofits on full-scale beams, identifying effective rebar length/ratio/configuration and documenting associated failure-mode transitions to propose suitable retrofitting guidance while preserving appearance. Fourth, it adapted ACI 440.2R concepts to timber to define Heritage-appropriate allowable strengthening limits (to the best of our knowledge, the first adapted method), explicitly addressing residual capacity if FRP is suddenly lost (e.g., de-bonding, fire, vandalism). Fifth, it proposes analytical models (moment–curvature with equilibrium and a simplified Whitney-type compression block, followed by data-driven models from experimental data) that predict strengthened bending capacity and connect experiments to design, while outlining a dual system with post-tensioning to extend capacity and control residual demand in future work. Collectively, these contributions deliver data, methods, design limits, and models that can be used directly in assessment, retrofit design, and the evolution of Heritage timber guidance.

Three main articles and a paper as a result of contributions:

- Article 1 (addressing Phase I), Submitted to Journal of Materials and Structures, Springer

Abbasi Malekabadi, Reza & Hafeez, Farah (2025). From Non-Destructive to Structural Insights of Heritage Timber: A Combined NDT and Destructive Testing Approach

- Article 2 (addressing Phase I), Submitted to Journal of Engineering Structures, Elsevier

Abbasi Malekabadi, Reza & Hafeez, Farah (2025). Experimental and Statistical Inference Approaches for Evaluating the Mechanical Performance of Heritage Timber Beams

- Article 3 (addressing Phase II), Preparation (Drafts)

Abbasi Malekabadi, Reza & Hafeez, Farah (2025). Strengthening Heritage Timber Beams employing NSM-GFRP: Influence of Rebar Configuration and Length
The authors have been reviewing and developing the manuscript content.

- Paper 4 (addressing Phase I), CSCE 2024

Abbasi Malekabadi, Reza & Malik, Hassan & Hafeez, Farah (2024). Evaluating the Mechanical Properties and Failure Modes of Timber Heritage Beams. *Canadian Society for Civil Engineering. Conference Niagara Falls, 2024.*

<u>Other articles and papers contributing to wood science and timber structure:</u>

- Article 5, Journal of Wood Material Science and Engineering 2025

K.G.M. Kandethanthri, **Reza Abbasi Malekabadi**, Ghazanfarah Hafeez, and Zhiyong Chen4. Effect of critical parameters on structural performance of balloon-type self-centring mass timber wall system. *Journals - Taylor & Francis, 2025*

- Article 6, Journal of Earthquake Engineering 2025

K.G.M. Kandethanthri, **Reza Abbasi Malekabadi**, Ghazanfarah Hafeez. Seismic Assessment of CLT-Steel Hybrid Structures with Mass and Vertical Geometric Irregularities Using Modal Response Spectrum Analysis. *Journals - Taylor & Francis, 2025*

- Article 7, Journal of Measurement, (2023)

Nikoo, M., **Abbasi, R**., & Hafeez, G. (2023). Estimating the mechanical properties of Heat-Treated woods using Optimization Algorithms-Based ANN. *Journal of Measurement*, *207*, 112354.

- Paper 8, CSCE 2023

Abbasi, R, Nikoo, M, Hafeez, G, Bagchi, A (2024). Flexural Performance of Cross-Laminated Timber Panels Using Evolutionary Artificial Neural Networks. *CSCE-Moncton, 2023*

- Paper 9, WCTE 2023

Nikoo, M., **Abbasi, R**., & Hafeez, G. (2023). PREDICTING MODULUS OF RUPTURE OF HEAT-TREATED WOODS BY ARTIFICIAL NEURAL NETWORK COMBINED WITH GENETIC ALGORITHM. *World Conference on Timber Engineering 2023 (WCTE2023).*

- Paper 10, SHMII-11 2022

Nikoo, M, **Abbasi, R**, Hafeez, G, Firefly Algorithm-Based ANN to Predict Modulus of Elasticity (MOE) of Heat-Treated Woods. *SHMII-11: 11th International Conference on Structural Health Monitoring of Intelligent Infrastructure 2022, Montreal, Canada*

- Paper 11, CSCE 2022

Kalantari, R., **Abbasi, R**., & Hafeez, G. (2022). Lateral Performance of Log Wall with Butt-and-Pass Corner Style. In *Canadian Society of Civil Engineering Annual Conference* (pp. 375-382). *Cham: Springer Nature Switzerland, 2024.*

- Paper 12, Last draft

Abbasi, R., Hafeez, G. Estimating Out-of-Plane Bending Properties of Cross-Laminated Timbers Employing Optimization-Based Algorithm

Table of contents

List of Figures xiii

List of Tables xvi

Abbreviations and Symbols xvii

CHAPTER 1: Introduction 1

General 1

1.1 Material and Mechanical Properties 5

1.1.1 *Effect of Aging* 10

1.2 Research Motivations and Needs (Problem Statement) 11

1.3 Research Questions and Thesis Contributions 13

1.4 Research Objectives 14

1.5 Research Methodology 15

1.5.1 *Phase I: Investigating the Material and Mechanical Properties* 17

1.5.2 *Phase II: Strengthening of Heritage Timber Beams* 17

1.6 Scope and Limitations 19

1.7 Thesis Organization 19

CHAPTER 2: Literature Review on the Mechanical Performance Assessment and Strengthening 21

General 21

2.1 Review of Studies on Strengthening with FRP 22

2.2 Review of Studies on a Statistical Inference Method 30

2.3 Review of Studies on NDTs 35

2.3.1 *Worldwide Codes and Standards for the Evaluation of Heritage and Old Buildings* 36

CHAPTER 3: Evaluation-Phase I: Investigating Material Properties and Mechanical Performance of Heritage Timber Beams (Approach 1) 44
General 44
Abstract 45
3.1 Introduction 46
3.2 Background 47
3.2.1 *Effect of Aging on Mechanical Properties of Wood* 48
3.3 Research Significance 50
3.4 Experimental Program 50
3.4.1 *Non-Destructive Testing* 50
3.4.2 *Destructive Testing* 52
3.5 Results and Discussion 53
3.5.1 *Study of the MOE (Static), MOEdyn, and MORs* 54
3.5.2 *Correlation between Density- MOE* 57
3.5.3 *Mechanical Performance of the Heritage Beams* 58
3.5.3.1 *Failure Modes in Identical Beams* 58
3.5.3.2 *Failure Modes in Unidentical Heritage Beams* 60
3.6 Conclusion 64
CHAPTER 4: Evaluation- Phase I: NDT Based on Statistical Inference (Approach 2) 67
General 67
Abstract 68
4.1 Introduction 69
4.2 Research Background and Rationale 70
4.3 Materials and Methodology 73

4.3.1 *Database on Material and Mechanical Parameters of Heritage and New SPF Beams* 73
4.3.1.1 *Non-Destructive Test (NDT)* 74
4.3.1.2 *Destructive Test* 75
4.3.1.3 *Simulation of New SPF* 76
4.3.2 *Statistical Inference to Correlate Mechanical Performance of Heritage and New Beams* 78
4.3.2.1 *Defining Null, Alternative, and Relevant Hypothesis Parameters* 80
4.4 Results and Discussion 81
4.5 Conclusion 86
CHAPTER 5: Strengthening-Phase II: Strengthening of Heritage Timber Beams Using NSM-FRP 89
General 89
Abstract 90
5.1 Introduction 91
5.2 Background 92
5.2.1 *Grooving, Adhesive Application, and Bonding Behaviour* 94
5.3 Research significance 94
5.4 Experimental 95
5.4.1 *Material and NSM timber preparation* 97
5.4.2 *Test setup* 98
5.5 Results and discussion 101
5.5.1 *Load Deflection Curve and Strengthening Performance (among configurations)* 101
5.5.2 *Strain distribution* 105

5.5.3 *Failure modes* 106

5.5.4 *Maximum allowable strengthening* 111

5.6 Conclusion 113

CHAPTER 6: Analytical Insights into the Bending Capacity Formulation of Heritage Timber Beams 115

General 115

6.1 Proposed Bending Capacity for Heritage Timber Beams 115

6.2 Proposed Dual Strengthening System 123

CHAPTER 7: Summary and Conclusion 127

7.1 Summary 127

7.2 Conclusion 129

7.3 Recommendations 131

References 132

Appendix A 150

Appendix B 154

Appendix C 158

List of Figures

Figure 1.1: Examples of two historic buildings. a) Neglected architectural building, b) Well-maintained architectural building ……..…….... 1

Figure 1.2: The old building depicting four historic periods, Turkey. (Photo via Instagram/@architectanddesign)[5] …… 2

Figure 1.3: Collapsed Heritage buildings. a) Ottawa [6], b) Halifax [7]…….…….. 3

Figure 1.4: Schematic illustration of wood cell wall formation, adapted from [13,14] ..…… 6

Figure 1.5: Water contents and transportations [16] …… 7

Figure 1.6: Major mechanical properties of wood under loading [17] ……. 8

Figure 1.7: Three principal axes in wood, differing in material and mechanical properties …. 9

Figure 1.8: Methodology framework to address the main objectives of the research (Phase I and Phase II) ……..…… 16

Figure 1.9: Research methodology; a) approach 1, b) approach 2 ……... 18

Figure 2.1: Cross-section of the reinforced beams [2] …… 26

Figure 2.2: Cross-sectional equilibrium for two configurations of composite section [10] ... 29

Figure 2.3: Null Hypothesis concept [63] …… 33

Figure 2.4: General notes from national and Canadian codes addressing Heritage structures 41

Figure 3.1: Non-destructive tests (Ultrasonic measurements) ……. 52

Figure 3.2: Destructive tests on Heritage beams ……. 53

Figure 3.3: Variation of MOEs and MORs. a) Static and dynamic MOEs, b) Comparison of MORs for all tested beams …….. 56

Figure 3.4: Correlation between MOR and static MOE. a) Current study, b) Combined studies ……. 57

Figure 3.5: Correlation between density-MOE. a) MOE-Density correlation based on data from the current study (Flexure Failure and Shear Failure), b) MOE-Density correlation based on data from the current study and available literature [97] …… 58

Figure 3.6: Mechanical behaviour of five identical Heritage beams …….. 60

Figure 3.7: Visual shear, flexural, and coupled failures ……. 61

Figure 3.8: Force-Deflection correlation for all Heritage/old beams …… 62

Figure 3.9: Deflection-force correlation for all tested beams failed under a) shear Failure, b) bending failure c) shear- flexure coupled failures …….. 64
Figure 3.10: Overview of the framework concluded in the research ……. 65
Figure 4.1: Framework of adopted methodology ……... 73
Figure 4.2: Measurements from ND tests for Heritage and New beams. a) Density, b) MOE 75
Figure 4.3: Heritage and New beam destructive testing.a) Heritage beam,b) New SPF beam 76
Figure 4.4: Measurements obtained from destructive tests on Heritage and New SPF beams 76
Figure 4.5: Results from the destructive tests of Heritage, New SPF, and SNC …… 77
Figure 4.6: Safety factor for Heritage and New beams, as well as from literature [19] …… 78
Figure 4.7: Null hypothesis main conceptualization to address the problem …… 80
Figure 4.8: An overview before Null results. a) comparison of MOE static and dynamic b) the ratio of F_{max}(H/N) …… 82
Figure 4.9: Maximum force (kN)- frequency distribution for Heritage beams (tested) ……. 83
Figure 4.10: Flow chart demonstrating the importance of current research …….. 88
Figure 5.1: a: Specimen groups, b: Grooving of the test specimens, c: placement of the reinforcements, d: application of the epoxy …….. 98
Figure 5.2: a: Cross-sectional reinforcement placement illustrating rebar position within specimen groups, b: Longitudinal reinforcement layouts demonstrating varying lengths and positions of GFRP reinforcement within each specimen group …… 100
Figure 5.3: Four-point test setup …… 101
Figure 5.4: Comparison of the load-deflection results, a: Reference Group, b: Group A, c: Group B, d: Group C, e: Group D, f: Group E, g: Group F …… 102
Figure 5.5: Strain distribution for the recorded test specimens …… 106
Figure 5.6: Visualization of failure modes for the different reinforcement configurations ... 109
Figure 5.7: Maximum allowable for strengthening, considering the ACI recommendation ..112
Figure 6.1: Cross-section of strengthened beam under bending moment [10] ……... 117
Figure 6.2: Proposed Whitney-type stress profile of strengthened beam with GFRP …….. 117
Figure 6.3: Strain profile and compatibility …… 119

Figure 6.4: Stress profile in the cross-section of the strengthened beam …… 120
Figure 6.5: Non-linear Stress profile in the cross-section of the strengthened beam [133] 121
Figure 6.6: Typical Whitney-type Stress profile in the cross-section of a reinforced concrete beam [133] …… 122
Figure 6.7: Support post-tensioning technique in shear panel. a) Practical implementation [134], b) Concept [69] ……..... 123
Figure 6.8: Stiffening connection rigidity as a proposed dual system ……. 124
Figure 6.9: Effect on drift control as a measure of practicality …… 124
Figure A.1: Destructive and NDTs (pertinent to Chapters 3 and 4) ……. 153
Figure C.1: Experimental pictures of strengthened Heritage beams, along with associated failures …… 159

List of Tables

Table 1.1: Research questions, followed by attempts to answer (Contributions) …….. 14

Table 2.1: Available standards and guidelines for existing timber structures [74] …… 38

Table 2.2. Summary of the studies on Statistical Inference ……. 41

Table 2.3. Summary of studies on FRP strengthening ……. 42

Table 3.1: Material properties and failure modes of five identical Heritage timber beams ... 59

Table 4.1: Descriptive statistics for Heritage and New beams …….. 83

Table 4.2: Pearson correlation …… 84

Table 4.3: Results showing the group statistics ……. 85

Table 4.4: Results showing independent t-statistic …… 85

Table 4.5: Results showing effect size ……... 86

Table 5.1: Mechanical properties of MST-BAR® grade III GFRP reinforcement …… 95

Table 5.2: Mechanical properties of FRP bars ……... 96

Table 5.3: Specimen details and reinforcement configuration …….. 99

Table 5.4: Failure modes for the different reinforcement configurations …… 106

Table A.1: Results of full-scale Heritage beams under bending test (pertinent to Chapters 3 and 4) …… 150

Table B.1: Results of destructive tests on Heritage and SNCs (pertinent to Chapter 4) …. 155

Table B.2: Results of destructive tests on New beams ……. 157

Abbreviations and Symbols

ρ_0	Dry Density
A_{ft}	FRP Cross-Sectional Areas at Tensile Zone
ASTM	American Society for Testing and Materials
EI	Bending Stiffness
EB	Externally Bonded
CSA O86	Canadian Standards Association Standard O86
CWC	Canadian Wood Council
CSPG	Compression Strength Parallel to Grain
σ	Compressive Stress
F_{exp}	Experimental Force
FRP	Fiber-Reinforced Polymer
FE	Finite Element
FEM	Finite Element Methods
I_t	Transformed Second Moment of Area
M_{max}	Maximum Bending Moment
$M_{u,theor}$	Ultimate Theoretical Moment
F_{max}	Maximum Applied Force
MOE	Modulus of Elasticity
MOR	Modulus of Rupture
M	Moment
NBCC	National Building Code of Canada
NCC	National Construction Code
SPF	Spruce-Pine-Fir
NSM	Near Surface Mounted
NDT	Non-Destructive Test
SNC	Simulated New Counterpart
PR	Polyester Resin
W	Section Modulus

CHAPTER 1

Introduction

General

Wood is one of the oldest materials available for construction, known for its favourable physical, chemical, and mechanical properties, including a high strength-to-weight ratio, ease of use, and durability. When exposed to optimum moisture conditions, timber structural components offer a long lifespan and low maintenance costs. However, natural loads, non-uniform anisotropy, fungus, insects, and seasoning expose lumber, as a construction material, to a variety of defects such as knots, shakes, twisted fibres, and shrinkage-related issues. Old timber buildings are more susceptible to age-related inefficiencies and destructive issues. These concerns, in addition to the latter-mentioned defects, include splitting, biological deterioration, and changes in chemical contents leading to strength loss.

The literature does not clearly distinguish between "old" and "Heritage." While all Heritage structures are old, not all old structures qualify to be Heritage. Heritage buildings have architectural, historical, or cultural values and significance, so that they have been listed as a protected cultural Heritage in numerous nations [1]. Heritage timber buildings often feature key timber components, particularly within their floor and roof structures, that need regular maintenance to ensure their stability [2]. Fig. 1.1 presents a comparison between a well-maintained and a neglected Heritage building, highlighting the impact of preservation efforts on structural and aesthetic integrity.

a) Neglected architectural building [3]

b) Well-maintained architectural building [4]

Fig. 1.1. Examples of two historic buildings

Fig. 1.2 illustrates a remarkable structure in Istanbul's Fatih district, exemplifying the world's dedication to conservation. This building, with its layers from the Roman, Byzantine, Ottoman, and Republic periods, not only clearly showcases the architectural evolution of one of the world's most historically significant cities but also suggests the imperative need for adaptive preservation.

Fig. 1.2. The old building depicting four historic periods, Turkey. (Photo via Instagram/@architectandde-sign) [5]

Unfortunately, some Heritage timber buildings have deteriorated and been damaged over the years due to excessive deflections, load modifications, and inadequate maintenance, leading to diminished functionality. The recent collapse of the Heritage building depicted in Fig. 1.3a, built in the 1840s in Ontario, Canada, highlights the serious consequences of inadequate inspection, maintenance, and reinforcement [6]. Similarly, another collapse in Halifax, Canada, depicted in Fig. 1.3b, happened when a Heritage building from 1861 was moved without the necessary reinforcement [7].

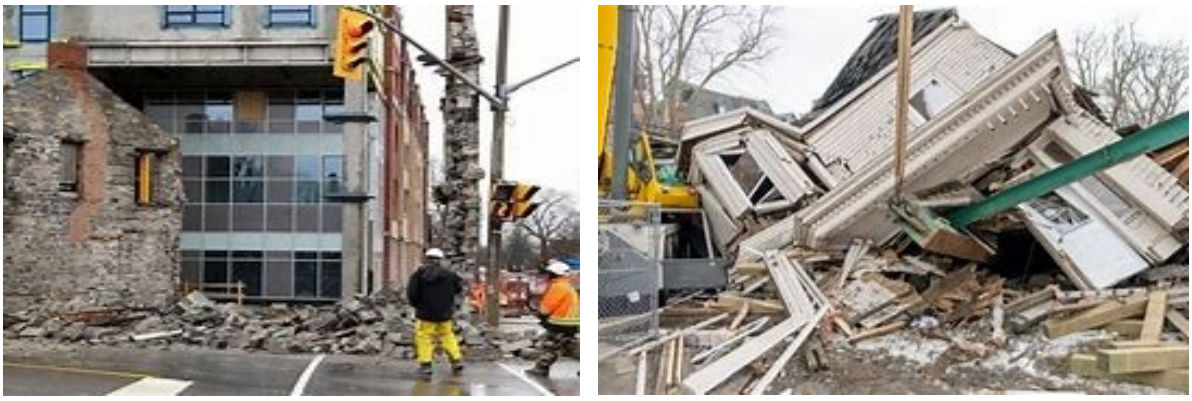

a) Ottawa [6] b) Halifax [7]

Fig. 1.3. Collapsed Heritage buildings

Assessing the physical and mechanical properties of timber members (beams, columns) in Heritage buildings helps provide a comprehensive understanding of the condition of old timber-framed structures, as well as how these materials adapt and respond under long-term loads. Currently, the main evaluation parameters for monitoring ancient timber members include dry density (ρ0), modulus of rupture (MOR), modulus of elasticity (MOE), and compressive strength parallel to grain (CSPG) [8], some of which are destructive and practically feasible.

In-situ evaluations and tests are recommended for Heritage buildings since their functionality, appearance, and features should not be disturbed or altered. This is where non-destructive (ND) methods could aid engineers. As the structure ages and degrades, it may need retrofitting and reinforcement. The decline in performance parameters of timber structures and components requires reinforcement or retrofitting [1]. When comparing old and Heritage structures, any retrofitting techniques involving the restoration of old elements can be implemented. However, selecting a retrofitting approach is critical for Heritage structure elements, as they must maintain their integrity and appearance. When choosing a suitable strengthening method for timber structures, various variables must be carefully evaluated to ensure structural efficiency and real-world practical application. Longevity is an important consideration because the chosen retrofitting/strengthening technology must retain its efficiency over time with minimal degradation, especially in fluctuation of environmental loads and moisture. Ease of installation is critical, especially for in-situ, on-site retrofitting of Heritage timber elements. The approach

should be adaptable to various timber dimensions, geometries, and loading conditions without requiring significant modifications. Furthermore, adaptability is essential in addressing a range of structural defects, including flexural weakness or localized damage, across various wood species and building styles. Finally, for historic or visually sensitive constructions, it is crucial to preserve the appearance of the timber while also respecting architectural considerations, selecting solutions that are visually harmonious with the existing elements. Balancing these requirements enables the development of a strengthening plan that is both technically sound and culturally relevant. It's crucial to recognize that any sudden or gradual removal of strengthening techniques should not lead to the failure of Heritage buildings. This consideration is often overlooked in existing studies, yet it is essential for preserving these unique structures.

Therefore, in this study, the wise recommendation of ACI 440-2R [9] for concrete structures is adapted, interpreted, and applied to timber buildings, ensuring that the Structure will not fail after the sudden removal of Fibre Reinforced Polymer (FRP). Implementation of the proposed advice in timber structures needs a dual-strengthening system, such as post-tensioning and FRP. Only beams under critical moments and deflections are examined to narrow the scope of the study. Post-tensioning helps transfer a portion of the critical mid-span moments to near support zones, while the FRP resolves the remaining extra and residual deflections and moments. To be concise, external post-tensioning alone will split the timber and should be avoided. Worldwide, the structural protection and reinforcement have been enhanced by adding additional components such as independent structural reinforcement, suspended structural reinforcement systems, or reinforcement that works with the existing structural system [1]. The most common practices for strengthening timber beams can be accomplished using the following practical methods:

- Strengthening timber beams along their entire length by attaching components like planks or logs to the sides and adding reinforcement to the tension zone of the beam. Also, reinforcing the side of the beams with full-depth steel plates
- Reinforcement of a beam section involves replacing the damaged part with a

supplementary element, removing the damaged beam end, and supporting the floor beam with steel stirrups

- Using Self-Tapping Screws (STS) as a local remedy, specifically for cracked members
- Reinforcement involving the composition of the floor reinforced concrete slab and beam reinforcement using tie rods [1]
- Reinforcing with composites, mainly FRP, through different applications (such as rods, mats) and methods (such as NSM, insertion in predrilled holes)
- Injecting the epoxy resin-based mixtures to reinforce wood elements [1]

Among the various reinforcement methodologies explored, the technique of attaching steel plates along the full length of timber beams is expected to increase the risk of wood splitting. Further, the use of FRP in the form of mats and bars shows strong potential to enhance load-carrying capacity, improve ductility, and reduce deflections. However, for Heritage buildings, aesthetic preservation is the main priority. While FRP mats offer structural benefits, their surface coverage can compromise the visual integrity of historical elements. Therefore, only FRP bars are deemed acceptable, as they can be discreetly embedded or applied in ways that maintain the original appearance of the timber components. The Near Surface Mounted (NSM) method, a well-known technique for strengthening concrete structures, involves inserting FRP bars into a grooved line with structural epoxy and has recently been applied to timber structures. This method, in particular, preserves the appearance of Heritage timber elements with minimal damage. However, there is no standard method to predict the flexural capacity of NSM-FRP timber [10]. Experimental studies and literature data stand out as the sole resources available for both small Heritage samples and New wood elements.

1.1 Material and Mechanical Properties

The properties of wood and wood-based materials are heavily influenced by the characteristics of the fibres, particularly the properties of the cell walls [11]. Therefore, it is essential to effectively characterize these cell walls to gain insights into the relationships between Structure and properties [11]. Wood cell walls are primarily composed of the polymers cellulose,

hemicellulose, and lignin. As new cells develop in the cambium, these components form a primary wall and a middle lamella (intercellular layer), both containing pectic substance compounds. As the cell matures, cellulose and hemicellulose are deposited on the main wall to create the secondary wall, while lignification begins at the cell corners and progresses over the primary wall and lamella. Lignin is eventually absorbed into the secondary wall, and the cell dies. The final stage deposits cytoplasmic residues within the lumen as a terminal lamella or warty membrane, completing the formation of the wood cell wall [12]. Fig. 1.4 illustrates the wall formation of wood in terms of its chemical components.

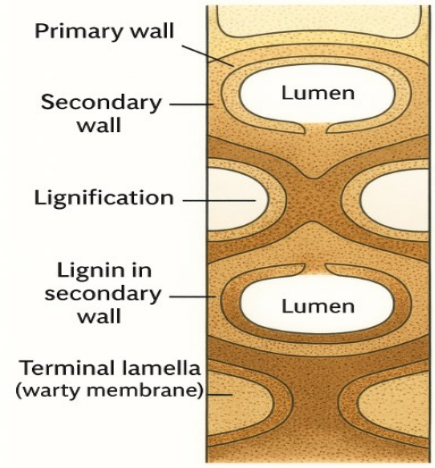

Fig. 1.4. Schematic illustration of wood cell wall formation, adapted from [13,14]

Understanding moisture movement in wood is also critical for its longevity, use, and product quality. Fig. 1.5 illustrates the water contents and transportation within the wood cell. Researchers distinguish between bound water in cell walls and unbound water in lumens/vessels. Experiments on pine, oak, and teak demonstrated that during the absorption of water, bound water saturates the cell walls before the entry of free water into the lumen. However, during the drying process, free water is expelled before bound water is lost. This observation indicates a local thermodynamic equilibrium between bound and free water, suggesting that diffusion within the fibres of the cell wall is a key mechanism influencing moisture transportation [15].

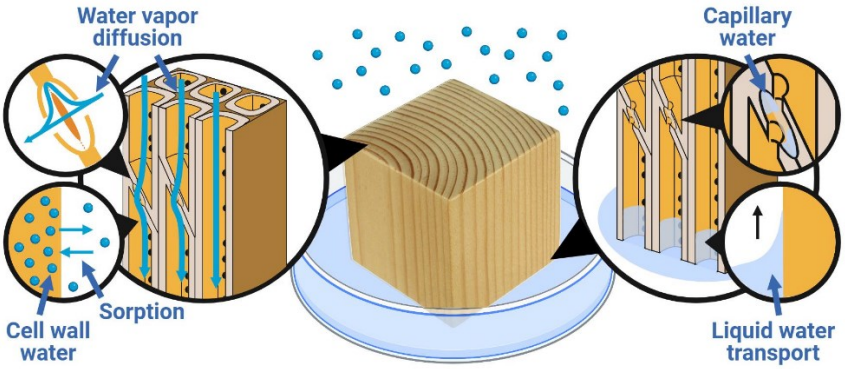

Fig. 1.5. Water contents and transportations [16]

Wood, as a construction material, is categorized as an anisotropic substance, exhibiting varying mechanical properties including tension, compression, shear, and bending, dependent on the orientation of the applied load relative to the wood fibres. The structural strengths and stiffness of wood elements vary along the longitudinal, radial, and tangential directions. Furthermore, the material properties of wood vary depending on the species, growing conditions, density, moisture content, and grain orientation. The key mechanical and material properties of wood include:

- Strength (tensile, compressive, shear), which governs the load-carrying capacity of structural members
- Stiffness (MOE), which affects deformation under loads, specifically in bending
- Fracture behaviour, which is governed by natural defects such as knots, shakes, and grain deviations
- Moisture-dependent behaviour, which directly affects dimensional stability, hygroscopic changes, and strength

Among the various material and mechanical properties of timber members, bending, compression, and tension are the most critical for structural performance. Fig. 1.6 illustrates the key mechanical behaviors of wood under different loading conditions [17].

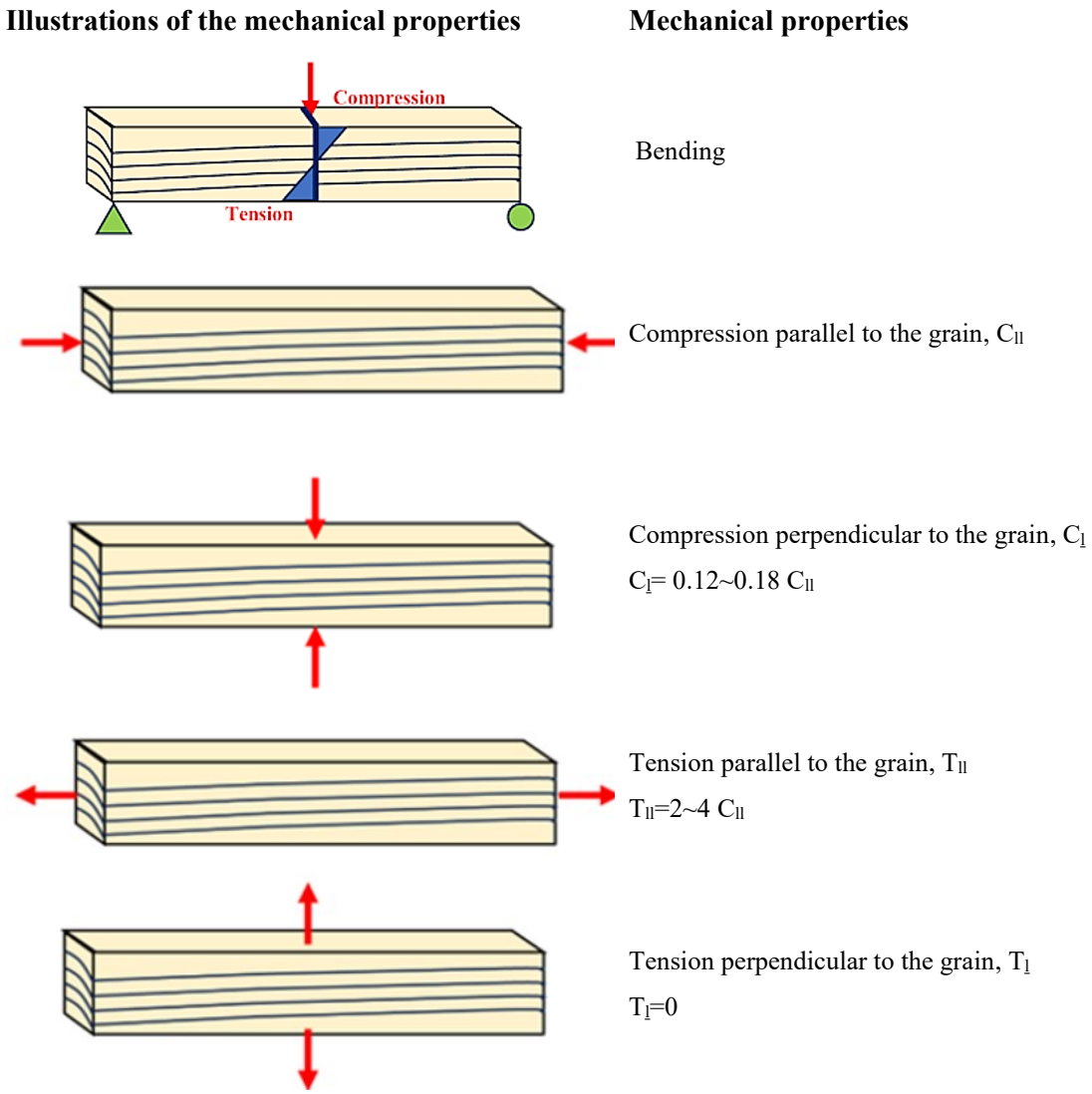

Fig. 1.6. Major mechanical properties of wood under loading [17]

To address the concepts of parallel and perpendicular to grain, Fig. 1.7 illustrates the three principal material directions in wood: i) Longitudinal direction, parallel to the wood fibres (grain). This direction has the highest strength and stiffness in both tension and compression as fibres transfer loads most effectively along their length. ii) Radial direction extends from the tree's centre (pith) to the bark, perpendicular to the growth rings. Strength and dimensional stability in this direction are moderate compared to the longitudinal axis. iii) Tangential direction, parallel to the growth rings and perpendicular to the radial direction. Due to the construction of the yearly rings, this route often exhibits the lowest strength and dimensional stability.

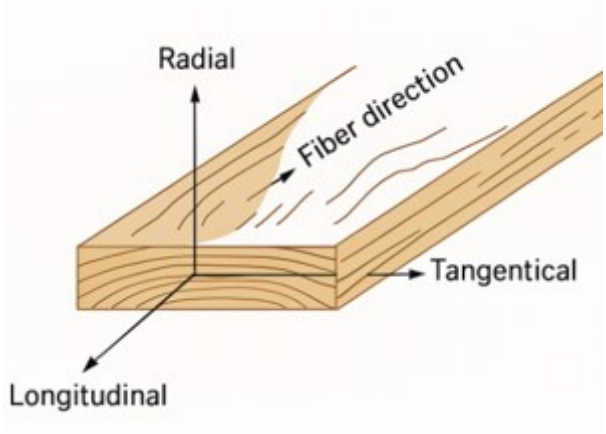

Fig. 1.7. Three principal axes in wood, differing in material and mechanical properties

The fibre direction affects how loads are carried in timber members. Since wood properties differ significantly along these three axes, predicting mechanical performance requires considering anisotropy. For example, the longitudinal axis primarily influences flexural strength and stiffness, while shrinkage, swelling, and shear are more critical in the radial and tangential directions. To determine and describe the elastic properties of wood, a total of 12 constants is needed, of which nine are independent. These include three values of Young's modulus, three values of the modulus of rigidity (G), and six Poisson's ratios (μ) [18]. Handbooks provide Equations or tables that relate these constants to one another [18].

For design purposes, data concerning compressive strength (both parallel and perpendicular to the grain), MOR, and shear strength parallel to the grain are often the most recorded from actual destructive tests. The MOR represents the maximum load that a wood element can withstand in bending and is proportional to the peak bending moment. However, it does not reflect the actual stress experienced beyond the elastic limit. Compressive strength parallel to the grain reflects the highest stress a short specimen can withstand along the fibres, whereas compression perpendicular to the grain is evaluated at the proportionate limit because a clear ultimate stress is challenging to establish. Shear strength parallel to the grain indicates the wood's ability to resist internal movement along its grain and is averaged over radial and tangential planes. Understanding how wood behaves under standard structural loads is vital, and these measurements play a key role in gaining that insight [18].

Various additional mechanical properties are crucial in assessing wood's potential for different applications, such as impact bending strength, which is evaluated through a drop test by measuring the height required to induce failure or a designated level of deflection. The work to maximum load in bending assesses both strength and toughness by determining how much energy a sample can absorb before exhibiting permanent distortion. Tensile strength perpendicular to the grain measures the wood's resistance to splitting forces across the grain, taking an average from multiple grain orientations. On the other hand, tensile strength parallel to the grain is less frequently reported, which measures the maximum tension that wood can bear along its fibres [18]. To investigate material and even mechanical properties and behaviour of timber elements, understanding chemical components and structures also plays a vital role.

Aging is considered one of the significant criteria affecting the chemical characteristics of wood. Understanding MOR from mechanical behaviour and MOE from material properties is crucial for predicting wood behaviour and assessing its suitability for retrofitting or preservation, especially in Heritage structures due to aging, environmental exposure, and prior loading histories.

1.1.1 *Effect of Aging*

Wood is remarkably durable, as evidenced by the condition of centuries-old timber in standing trees, such as redwood [18]. The mechanical properties of wood show only minor changes over time when kept dry, at moderate temperatures, and protected from decay. Research on ancient timbers indicates that the strength of clear wood significantly declines only after several centuries under typical aging conditions [18]. While wood undergoes both physical and chemical changes as it ages, its performance can be compromised by prolonged exposure to fluctuations in humidity, biological deterioration, and mechanical stress.

Generally, these changes can be categorized as:

- Physical changes: Over time, wood naturally loses its bound water, leading to shrinkage and microcracking that result in increased brittleness and reduced ductility

- Mechanical changes: Repeated loading cycles (creep and fatigue) weaken stiffness and load-bearing capacity. Ageing also worsens the effects of natural defects such as knots and cracks
- Biological degradation: Fungal decay, insect attacks, and bacterial actions degrade and diminish the strength of cell walls, resulting in weak wood texture and Structure
- Chemical changes: Hemicelluloses and lignin, essential components of wood's Structure, eventually break down under oxidative and UV exposure, resulting in loss of toughness

Age-related degradation of Heritage timber beams can lead to reduced flexural and shear strength, excessive deflections, and unexpected brittle failures. However, several investigations revealed that the mechanical performance of Heritage timber elements either remains steady or experiences a minor reduction over time [19–22]. Therefore, accurately predicting their mechanical and material performance requires models and methodologies that consider long-term performance. Compliance with building codes for some old/ Heritage buildings, which make up a significant portion of the housing stock in many areas, while addressing sustainability, may still pose a challenge: how to preserve cultural value while ensuring structural safety and adherence to modern standards and building codes?

Lightweight materials, energy retrofitting, and hybrid construction techniques have all been adopted as part of the modernization of wood construction; yet, structural retrofitting remains critical for timber, especially Heritage or aged structures. Retrofitting timber beams may be necessary for various reasons, including safety, serviceability, conservation, and sustainability. The applied technique should enhance the flexural and shear performance of age-affected timber elements with minimal visual impact, making them ideal for Heritage applications.

1.2 Research Motivations and Needs (Problem Statement)

Canada is home to thousands of old wood-based buildings, mainly due to Canada's historical reliance on timber as a primary building material, especially before the widespread availability of other construction materials such as steel and concrete.

Heritage timber structures are an essential part of architectural and cultural history. However, they lack comprehensive standards or guidelines, posing significant challenges for maintenance, assessment, and retrofitting without compromising their appearance and cultural significance. Reliable, ND methods for evaluating and strengthening these structures remain underdeveloped. Additionally, most existing strengthening techniques do not address the critical issue of potential failure following the sudden removal of retrofitting materials.

A particular concern is the difficulty in evaluating the mechanical performance of aged timber members, which often exhibit varying degrees of degradation due to environmental exposure, biological decay, or historical loading conditions. Traditional destructive testing is not suitable in such cases due to the damage it can cause. Therefore, there is a strong need for reliable ND evaluation methods that address the complex nature of Heritage structures.

While modern strengthening techniques, such as the use of FRP techniques, have gained attention, they are often designed without fully considering the long-term consequences of adhesive failure, reversibility, or compatibility with the aged substrate. Particularly, the potential for structural failure following the sudden de-bonding or removal of reinforcement materials is rarely addressed in existing literature or guidelines. This research is driven by recent incidents [6,7] that highlight the importance of establishing proper procedures to protect our architectural Heritage and address current gaps by proposing an integrated framework for the assessment and reinforcement of Heritage timber buildings.

The methodology combines non-destructive testing (NDT), statistical inference, and experimental works to develop a robust, data-driven approach. By focusing on the mechanical behaviour of Heritage beams and introducing the NSM-FRP technique as a minimum-destructive strengthening solution, this study aims to provide practical tools and insights that support both the conservation and structural safety of Heritage timber buildings.

On another platform, it is well known that the construction industry, which accounts for 38 percent of total global energy-related CO_2 emissions, plays a vital role in achieving the goal of limiting global warming to well below 2°C [23]. Therefore, retrofitting old and Heritage buildings not only ensures their preservation for future generations but also aligns with sustainable

development goals by promoting the reuse of existing infrastructure rather than new construction.

1.3 Research Questions and Thesis Contributions

Ageing timber beams in Heritage structures often lack proper documentation and need maintenance, assessment, and reinforcement that do not compromise their structural integrity, appearance, or cultural significance. Additionally, there is a gap in reliable and comprehensive methods for predicting mechanical performance, designing, and retrofitting, which are limited to destructive methods.

The significance of this research lies in its dual contribution to the assessment and rehabilitation of Heritage Timber structures. First, by integrating experimental, NDTs, and statistical approaches, the study enhances our understanding of the material properties and structural performance of Heritage timber beams. Second, it explores the application of NSM-FRP techniques as a means of strengthening Heritage beams while preserving them. Together, these methods aim to support preservation efforts while maintaining the structural integrity and historical value of timber elements. This thesis aimed to address the identified research questions while navigating the constraints and time limitations. Table 1.1 provides a summary of the research questions and their corresponding answers, also referred to as contributions.

In straightforward words:

Table 1.1. Research questions, followed by attempts to answer (Contributions)

Research Questions	Answers (Thesis Contribution)
How can the mechanical performance and material properties of in-situ Heritage or old beams be evaluated non-destructively?	This thesis proposes two methodologies based on: a) Null hypothesis, which uses destructive tests on the New counterpart timber beams and contributes results to the existing Heritage beams b) A developed method to correlate NDT to required properties
How can we expand the data on full-scale Heritage mechanical performance for research, maintenance, and strengthening purposes?	This thesis provides a comprehensive database (Chapters 3 and 4) on the material and mechanical properties of 44 full-scale Heritage timber beams, expanding the existing data in the literature.

How can we determine the allowable FRP-strengthening and provide suggestions for the remaining required strength to address Heritage (vs old) concerns?	In this thesis, the maximum allowable strengthening capacity of Heritage beams is determined based on ACI recommendations [9], addressing safety concerns related to de-bonding, vandalism, and fire (Chapter 5).
How effectively can NSM-FRP retrofit the bending capacity of existing in-situ Heritage beams?	Conducting experimental and analytical investigations to reinforce historic beams with GFRP and studying their failure modes (Chapter 5).
How can the bending capacity of strengthened beams be assessed, and what actions should be taken when the demand exceeds the allowable limit?	This thesis presents: a) Formulating analytical models for composite Heritage timber-FRP beams (complementary work, chapter 6) b) Proposing a post-tensioning method to provide residual load-carrying capacity (dual-strengthening system; future work- chapter 6)

1.4 Research Objectives

Recognizing the existing research gaps and pertinent research questions in the field, while recognizing the current absence of comprehensive and reliable non-destructive evaluation methods, and standardized guidelines for the preservation and strengthening of Heritage timber structures, this research aims at achieving the following specific objectives:

- To establish a comprehensive database of mechanical and material properties of full-scale Heritage timber beams to support conservation, research, and maintenance
- To develop and validate NDT methods for assessing the mechanical and material properties (MOE, MOR) of in-situ Heritage timber beams
- To propose allowable strengthening criteria for timber beams based on ACI 440.2R guidelines as a valuable insight into Heritage conservation
- To establish statistical correlations between New and Heritage timber beams, enabling indirect performance assessment
- To investigate and recommend effective retrofitting methods for Heritage beams to restore their functionality

1.5 Research Methodology

To achieve the objectives of this thesis, the proposed methodology integrates experimental, numerical, and analytical approaches to fulfill the research goals. This methodology involves two main Phases: evaluation (Phase I) and strengthening (Phase II). In the evaluation Phase, two distinct approaches, approach 1 and approach 2, are employed to assess the material properties and mechanical performance of existing in-situ timber beams. Approach 1 develops a correlation between material properties and the mechanical performance of in-situ beams by NDTs, while approach 2 establishes a statistically indirect performance assessment by testing New beams destructively.

During the strengthening Phase, these beams are retrofitted with FRP in various lengths and configurations, and their enhanced bending capacities are examined. This process involves inserting NSM-FRP bars into pre-grooved lines in the timber elements, followed by the application of a structural epoxy.

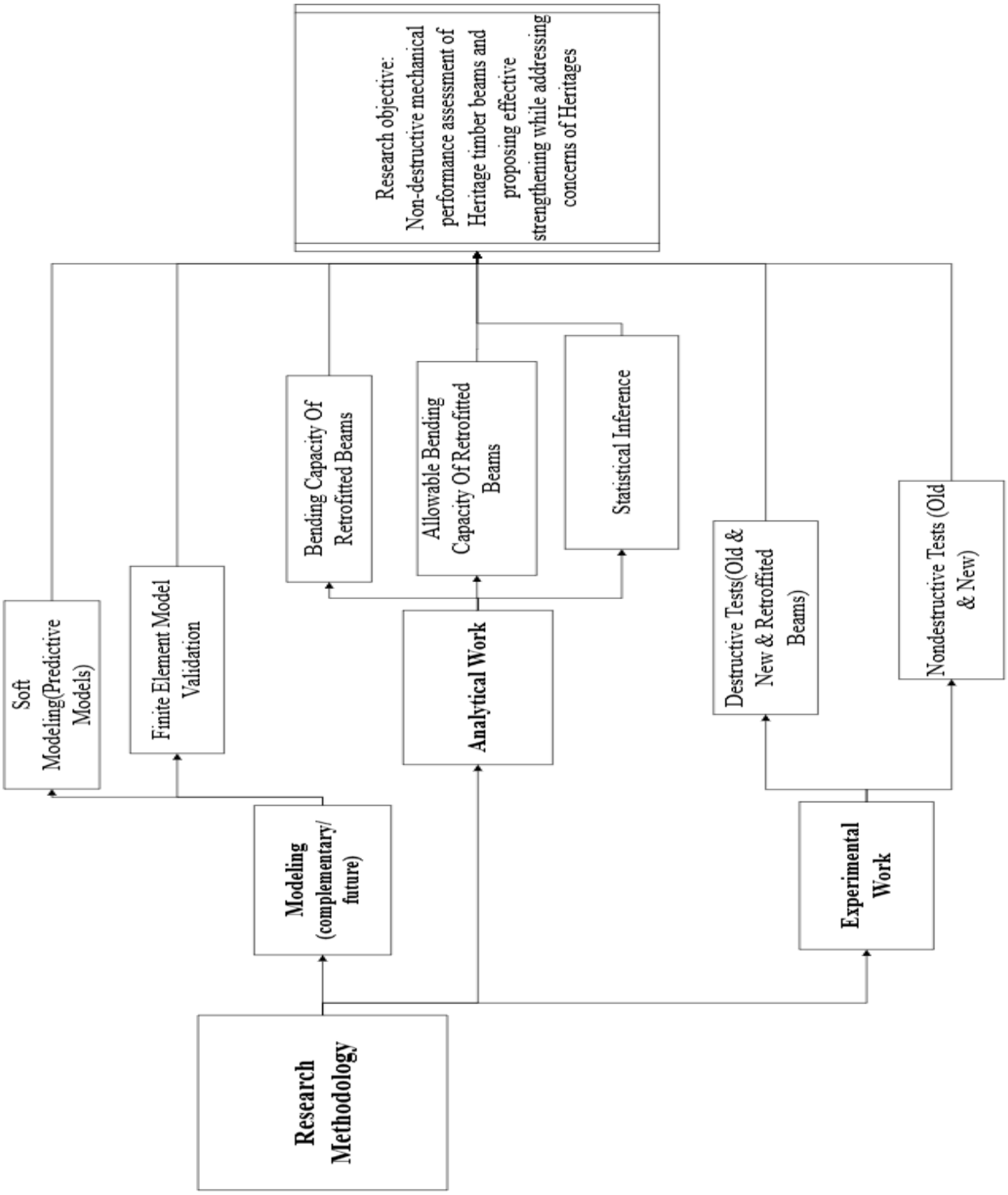

Fig. 1.8. Methodology framework to address the main objectives of the research (Phase I and Phase II)

1.5.1 *Phase I: Investigating the Material and Mechanical Properties*

This Phase is designed to improve the comprehension of the material properties and structural performance of in-situ Heritage timber beams. While destructive testing and NDTs are standard practices for evaluating new timber, their application to Heritage elements is frequently restricted or prohibited. This assertion is supported by the relevant codes, which are described in detail in Chapter 2 [24–28]. A correlation is established between NDT results and mechanical behaviour, allowing for the indirect assessment of mechanical performance criteria, including MOE and MOR. Statistical analysis, including the Null hypothesis technique, is used to evaluate the equivalence of Heritage and newly fabricated beams, justifying the use of simulated "equivalent New beams" as benchmarks. This dual approach not only enhances diagnostic accuracy but also helps establish standardized procedures for assessing Heritage timber, addressing a critical gap in current codes and standards.

1.5.2 *Phase II: Strengthening of Heritage Timber Beams*

This Phase examines not only the bending capacity of reinforced beams but also their failure modes in various configurations, enabling evidence-based optimization of retrofitting techniques. During this Phase, an evaluation of the bending capacities of both reinforced and unreinforced full-scale Heritage timber beams was conducted. Various configurations were examined to investigate the failure modes of these beams. The NSM-FRP technique was employed to enhance the structural integrity of the beams, providing a minimally invasive retrofit solution that offers significant structural improvements. Following the assessment of MOR and MOE in Phase I, certain Heritage beams are strengthened by inserting GFRP bars into pre-grooved lines with epoxy, using variable rebar lengths, ratios, and configurations. The required replications depend on the availability of beam samples and engineering judgment; however, previous studies have used 3-5 replicates [10,29–31]. The configuration providing the best possible bending capacity will then be used to propose the formulation.

As discussed earlier, the primary concern regarding “Heritage” was the sustainability of retrofitting to ensure that, under any circumstances, a strengthened Heritage structure would not collapse if the technique were suddenly removed due to de-bonding, fire, moisture effects,

vandalism, or other similar situations. To address this concern, in this Phase, analytical estimations of the maximum allowable strengthening, based on wise recommendations of ACI 440 standards (for concrete), are considered as theoretical boundaries, while experimental validation provides practical application. The entire framework of the methodology, including the two Phases in this thesis, is demonstrated in Fig. 1.8. Phase I involves assessment through two different approaches, while Phase II focuses on strengthening.

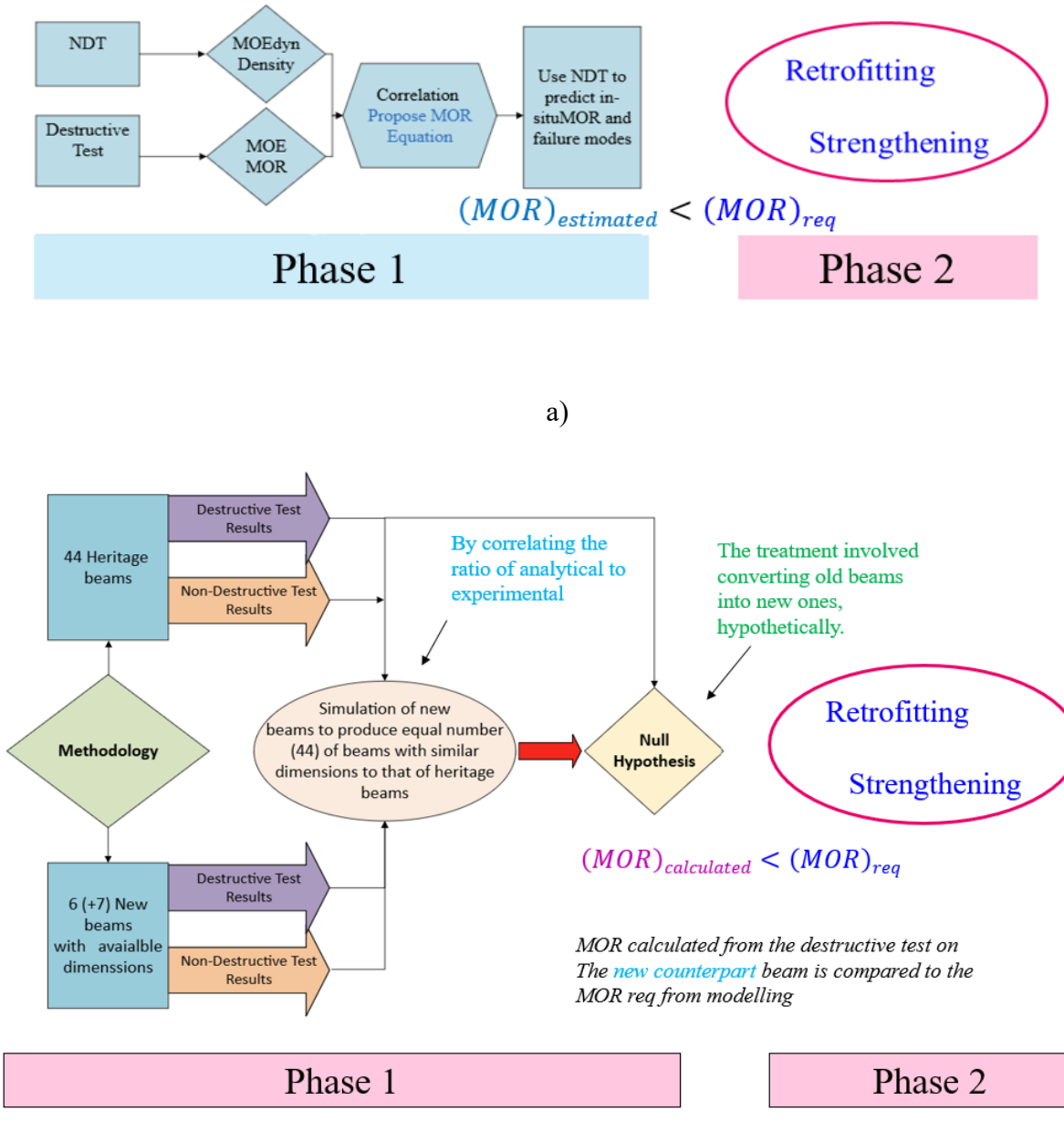

Fig. 1.9. Research methodology; a) approach 1, b) approach 2

1.6 Scope and Limitations

The study focuses on a limited sample of 44 Heritage timber beams collected from demolished buildings in Ontario and Quebec for data-driven assessment, as well as New SPF lumber (grade 2 and higher) available in the market. Since the findings mainly pertain to Eastern Canada's Heritage building stock, they may not accurately represent other regions with different environmental conditions and tree species.

This study examines explicitly the flexural performance of materials, focusing on metrics such as MOE, MOR, and bending capacity. It does not address other aspects of structural behaviour, including shear resistance, long-term creep, or performance under cyclic and seismic loads. Due to a lack of identical Heritage beams, only 18 full-scale, unknown species (some of which were affected by fire) were also collected from an old building in Montreal for strengthening research.

Further, in real-world settings, access to in-situ beams may be challenging, requiring floor and ceiling openings for assessment purposes and strengthening techniques.

1.7 Thesis Organization

This thesis consists of seven chapters, including the current one. Each chapter focuses on a specific aspect of the thesis, addressing Heritage timber beams for NDT evaluation, strengthening, and Heritage conservation concerns.

Chapter 1: establishes a foundation for understanding timber structures and introduces the characteristics of wood as a material. Additionally, it outlines key topics, including the problem statement, research objectives, research methodology, and the thesis organization.

Chapter 2: provides a literature review and background on ND testing, statistical inference, and strengthening with FRP as three major areas of research covered in this thesis.

Chapter 3: presents the first article, which is submitted to the Structures journal titled **"The Report of Experimental Investigations to Evaluate the Mechanical Behaviour and Failure Modes in Heritage Timber Beams."**

Chapter 4: presents the second article submitted to the Structures journal, titled **"Evaluating Mechanical Properties of Heritage Timber Beams: A Statistical Inference Approach."**

This chapter presents a novel method to evaluate the mechanical properties of in-situ Heritage timber beams through destructive tests on their new timber counterparts.

Chapter 5: presents the third article, intended to be submitted to the Structures journal titled **" Retrofitting Heritage Timber Beams Employing NSM-GFRP: Influence of Rebar Configuration and Length ."**

Chapter 6: includes bending theory, complementary and proposed methodology.

Chapter 7: reports the summary, discussion, conclusion, and recommendations.

This concluding chapter presents a comprehensive overview of the research, highlighting the key findings and essential discussions. It also offers recommendations and outlines future work needed to improve the research, addresses any existing gaps, and ensures both accuracy and practicality.

CHAPTER 2

Literature Review on the Mechanical Performance Assessment and Strengthening

General

This chapter offers a comprehensive review of the existing literature pertinent to the study, with a particular emphasis on NDT methods used to assess the mechanical performance and material properties, specifically bending characteristics, of in-situ Heritage timber beams. Additionally, it explores various strengthening techniques, with a focus on the application of FRP composites. The aim is to establish a strong background for understanding the mechanical performance and enhancement techniques of existing and functional Heritage beams in structures.

The chapter begins by providing an overview of wood as a construction material, emphasizing its historical significance, structural advantages, and limitations. It also introduces statistical inference methodologies and their applications, followed by a discussion of current practices regarding the retrofitting of Heritage timber beams.

The application of FRP involves various reinforcement configurations in wood, including Externally Bonded (EB), NSM, and protected insert systems, with emphasis on fire safety and durability. In this chapter, the qualities of FRP composites, covering their typical components (fibres and matrices), classification types like carbon, glass, and aramid fibres, and their mechanical properties are reviewed. The benefits of using FRP in structural contexts, such as its high strength-to-weight ratio, corrosion resistance, and ease of installation, are highlighted, particularly for timber strengthening elements.

Based on the Methodology implemented in this study, the literature survey involves three main distinct topics: 1) FRP strengthening, 2) A statistical inference method, and 3) ND assessment of Heritage timber.

2.1 Review of Studies on Strengthening with FRP

Wooden structures are often damaged or impacted by earthquakes, load variations, and environmental factors such as moisture, temperature fluctuations, fungi, and insects. Natural aging also causes a decline in their physical and mechanical properties, which negatively affects the stability and safety of Heritage timber beams. Timber structures and elements must be reinforced or retrofitted due to a reduction in their performance criteria [1]. Since the 1970s, enhancements in epoxy adhesives used to attach composite reinforcing elements have led to an increase in timber structural reinforcement methods.

Using FRP to reinforce timber beams is a significant advancement in structural engineering, providing a highly effective method to enhance the load-carrying capacity and durability of timber structures. The high tensile strength, lightweight nature, specific thermal coefficient, and ease of installation make FRP materials preferable for retrofitting old and Heritage timber beams. In this approach, these composites are bonded onto the wood surfaces or inserted inside to mechanically strengthen the beams, thereby improving their bending and deflection resistance. These methods not only extend the lifespan but also help preserve aesthetic appeal and historical significance, as seen in Heritage buildings. Additionally, the flexibility of FRP allows it to be adapted in various configurations to address structural deficiencies. However, challenges such as long-term de-bonding, fire resistance, and vulnerability to vandalism must be managed appropriately to ensure the durability and effectiveness of reinforced timber beams. As a result, overall improvements are necessary when considering how FRP might be used to enhance its lifespan and efficacy in beam reinforcement within wooden constructions. FRP strengthening presents a robust and innovative method for preserving and enhancing the structural integrity of timber beams in both contemporary and historical structures. These composites are engineered using various fibre types, including Glass Fibres (GFRP), Aramid Fibres (AFRP), Carbon Fibres (CFRP), and hybrid materials that combine different fibre types, such as carbon and glass fibres [1,32]. The use of fibreglass and cork plates, bonded with epoxy resin, dates back to the 1960s [33].

Several studies have explored the use of FRP as a wood reinforcement material, aiming to enhance durability, aesthetics, and mechanical performance. Researchers generally utilize GFRP to strengthen solid wood beams in various configurations (lengths and locations) parallel to the grain [2][34]. The proper location of reinforcement is a critical feature when constructing a reinforcement solution; accurately identifying the places that require reinforcing ensures the efficiency and efficacy of the method [2]. Another alternative for reinforcing or repairing beams is to make grooves into the structure's surface or sides and insert FRP bars as armour within the cross-section. This method aims to enhance the overall strength and durability of the structure by carefully strengthening critical locations [35]. Research findings revealed that the use of NSM-GFRP bars successfully mitigates the impacts of local defects in the timber while significantly increasing the bending strength of the members, resulting in an increase of 18% to 46% [34]. Overall, using FRP reinforcements enhances the mechanical properties of reinforced timber elements [36].

Plevris & Triantafillou (1992) applied a thin unidirectional CFRP sheet to the tension face of timber beams and showed that bending strength rose linearly with the number of fibres until it reached a critical threshold. Furthermore, the authors discovered a relatively constant moment beyond the critical point, indicating that the volume of FRP applied impacts the bending failure of beams [37]. It is demonstrated that incorporating GFRP sheets in beams can considerably improve their stiffness, with improvements in bending stiffness (EI) ranging from 1.05 to 1.53 times the initial value [38] and between 1.20 and 1.30 in bending resistance [39]. Regarding the percentage of FRP in strengthening, several studies have been conducted so far.

Studies looking into the use of CFRP for the reinforcement of solid timber beams and glulam have shown that the usage of a modest proportion of reinforcement in the range of 1.5% to 2.5% can lead to increases in stiffness and bending strength of up to 90% and 100%, respectively [40–42].

According to André and Kliger (2009), who utilized external bonding of FRP sheets on the tension side of timber to compare GFRP (1% of the volume of lumber) and CFRP (0.4%),

flexural stiffness increased by 15% to 30%. The failure happened due to timber crushing on the compression side, followed by shear or tensile failure [43].

Al-Hayek (2014) claimed that timber beams reinforced with CFRP bars increased strength and stiffness by 47% and 28% for ρ= 0.22%, and 29% and 22% for ρ= 0.11%, respectively [44].

The NSM method, a well-known strengthening technique in concrete structures, has recently crept into timber structures. The process involves cutting grooves into structural lumber and bonding the FRP bars or plates to the prefilled adhesive [45]. However, there is no standard method for predicting the NSM-FRP timber flexural capacity [10]. Yeboah and Gkantou (2021) proposed a theoretical model for the ultimate strength of NSM-FRP reinforced timber beams, which was evaluated based on test results and collected data, revealing a satisfactory comparison between the experimental and theoretical results. The NSM reinforcement resulted in a significant increase in the ultimate load (33-69%) and flexural stiffness (22-33%) of the timber beams. The authors also confirmed that the major failure mechanism found in both NSM-FRP reinforced and unreinforced specimens was the brittle tensile failure of the timber at the tensile zone, without any compression failure in the compression zone [10].

For strength performance, a study BY Yeboah and Gkantou (2021) proposed that 25% and 75% of the reinforcement be located at the top and bottom of the wood beam section, respectively, while for stiffness, equal reinforcement was recommended at both the tensile and compression zones. All of the reinforcement was advised to be positioned at the bottom for optimal ductility [10]. Johnsson et al. (2007) investigated the impact of inserting two NSM carbon fibre pultruded rods on the underside of a glulam beam, resulting in a reinforcement ratio of roughly 1.0%. This reinforcement resulted in three benefits: an increase in flexural strength of 44-63%, a 10% increase in stiffness, and a change in failure mode from tensile (brittle) to compressive (ductile) [29]. Fossetti et al. (2015) showed this improvement using a reinforcement ratio of around 1.0%, achieving a 25% increase in flexural capacity [46].

When it comes to groove and epoxy selection, the literature provides with a handful of information. Generally speaking, the studies have not identified the composite action/behaviour

between epoxy, FRP, and the member. Most studies have focused on the direct pull-out strength, with a limited studies on the bonding between FRP rods and timber. Corradi et al. (2015) examined the pull-out strength of CFRP rods installed near the surface in hardwoods and softwoods from the United Kingdom; as a result, pull-out capacity increased with bond length [47].

Compared to square grooves, circular grooves improved rigidity and moment capacity more significantly [48]. The essential structural performance of the groove filler in the current technology is the transfer of shear and tensile strength. Although phenol-resorcinol, Sikadur, and epoxy resins have been utilized, the most popular adhesive for the NSM process is a 2-part epoxy [10,34,48,49]. In two-part epoxy adhesives, one component is the base, which contains epoxy resin, and the other is the curing agent or hardener. Epoxy adhesives exhibit excellent shear strength and can withstand temperatures ranging from 40°C to 100°C, and are also cost-effective and easy to apply [10,50]. Sikadur 31 Hi-mod is the finest choice because it is insensitive to moisture before, during, and after curing. It also shows excellent adherence to concrete, masonry, metals, wood, and other structural materials. Furthermore, there is no tensile stress limit, and the structural paste adhesive has a high modulus and strength [48].

The reinforcing pattern for fracture mechanisms and the use of structural glue for bond action are essential features that heavily influence the efficiency of the reinforcement [51]. The main problem with reinforcement is that the wood and the reinforcing chemical are incompatible [52]. Therefore, research findings demonstrated low to no degradation in the bonding strength of traditional structural epoxy adhesives when subjected to moisture content values as high as 22% [53]. Considering the discussed facts, several factors, including the type of fibre used, the layout of the reinforcement in the element, and the integrity of the bonding surface between the FRP and the timber, play a critical role in determining the performance and behaviour of the structure during the test until fracture [54].

Due to the variety in the type of fibre used, reinforcement arrangement, and bonding surface integrity, the results obtained in research efforts may vary substantially, making direct comparisons between studies difficult [2].

Morales et al. (2015) identified various modes of fracture in the old beams, including the commonly observed beam fracture due to the failure of the lower fibres when subjected to tension or a combination of tension and shear forces. Some reinforcement systems, surprisingly, did not show a correlation between the length of the reinforcement plates and the fractured load. The authors deployed the transformed method shown in Fig. 2.1 to construct the bending capacity formulation, concisely presented through Equations (2.1) to (2.4) [2].

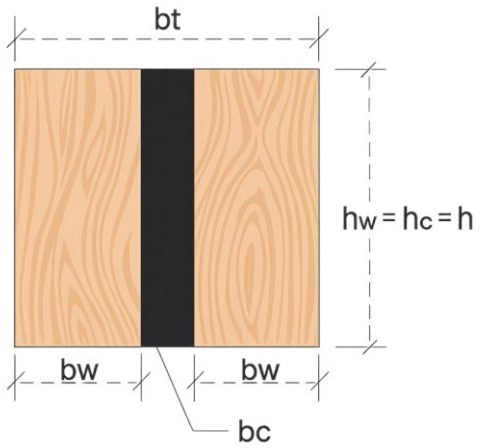

Fig. 2.1. Cross-section of the reinforced beams [2]

All tested beams were intended to have an epoxy-bonded GFRP and Polyester Resin (PR) matrix in the critical zones. Consequently, the maximum bending strength was determined as follows:

$$\sigma_{w,max} = \frac{aFmax}{2W} \quad \left(\frac{N}{mm^2}\right) \tag{2.1}$$

Where:

a: Distance between a load point and the nearest support, in millimetres (mm); F_{max}: Fracture load of the specimen in Newtons (N); W: Section modulus in cubic millimetres (mm^3) equal to $I_t/(h/2)$, where I_t is the transformed second moment of area (mm^3).

$$b_t = 2b_w + t_c \frac{E_c}{E_w} = 2b_w + t_c n \tag{2.2}$$

$$I_t = 2\frac{b_w h_w^3}{12} + \frac{nth_c^3}{12} \tag{2.3}$$

As an important outcome, the authors claimed that although the section modulus (W) was the same for all series of beams with different reinforcing, which led to the theoretical fracture load to be the same in each case, the experimental results (F_{exp}) exhibited significant variation over the series [2].

A study by Brol and Postulak (2019) on retrofitting over-century-old larch beams revealed a significant improvement in bending load-carrying capacity when reinforced with various fibrous materials, including CFRP, AFRP, BFRP, and GFRP. The tests aimed to estimate the reinforcement effect and potential improvement in the performance of existing structures. As a result, the reinforcement of the beams with CFRP mats showed the highest increase in bending capacity, with a 60.66% increase compared to their unreinforced counterparts. On the other hand, beams reinforced with GFRP (10 mm in diameter) exhibited the lowest flexural bending capacity, with only a 19.04% increase compared to unreinforced counterparts [1].

The bending strength of the tested beams was calculated based on symmetrically loaded beams with two concentrated forces (four-point bending test). Equation (2.4) shows the bending resistance of the tested beams.

$$\mathrm{f_m} = \frac{3\mathrm{Fa}}{\mathrm{bh^2}} \tag{2.4}$$

Where: f_m is the bending resistance (N/mm^2); F represents load (N); a is the distance of the applied force point from the nearest support (mm); b is the section width (mm); and h is the sample height (mm).

The authors also discussed two methods of repair for timber beams, depending on the type of damage, including the use of CFRP strips and mats. The results demonstrated the dependency of the repair method on the specific kind of damage to the timber elements. The study

concluded that repairing the beams with carbon fibre strips regained the load-carrying capacity of the beams up to 80% while maintaining the stiffness of the original beams. However, it should be noted that the strip used for reinforcement was eventually damaged due to loosening in the anchorage zone. To prevent delamination in previously damaged beams, mats were wrapped around the beams. This repairing method significantly (90%) restored the load-carrying capacity of the beams [1]. Although this method is developed, simple, and practical, it is not suitable for Heritage beams due to its destructive nature.

Yeboah and Gkantou (2021) employed a generic theoretical model to assess the moment resistance of NSM-FRP timber beams, as a standardized technique for predicting the flexural capacity of these beams, which is currently lacking. The theoretical analysis involved the application of fundamental behavioural principles of wood and FRP materials. The model was based on pure bending theory and the assumption of a plain section without considering debonding between bars and timber. Non-linear response was detected for specific reinforced beams, in which the neutral axis appeared to be somewhat lowered. Fig. 2.2 depicts the equilibrium of the reinforced beam cross-section for both configurations, with F representing the force of the subscript. The depths of the compression and tension zones are denoted by x_c and x_t, respectively, and x_{c1} and x_{c2} represent the timber part in the plastic and elastic regions. Additionally, z_{ft} and z_{fc} represent the distance between the centre of the FRP bars and the edge of the beam for tensile and compression bars. By taking a moment around the neutral axis, Equation (2.5) allows for the calculation of the ultimate theoretical moment ($M_{u,theor}$) [10].

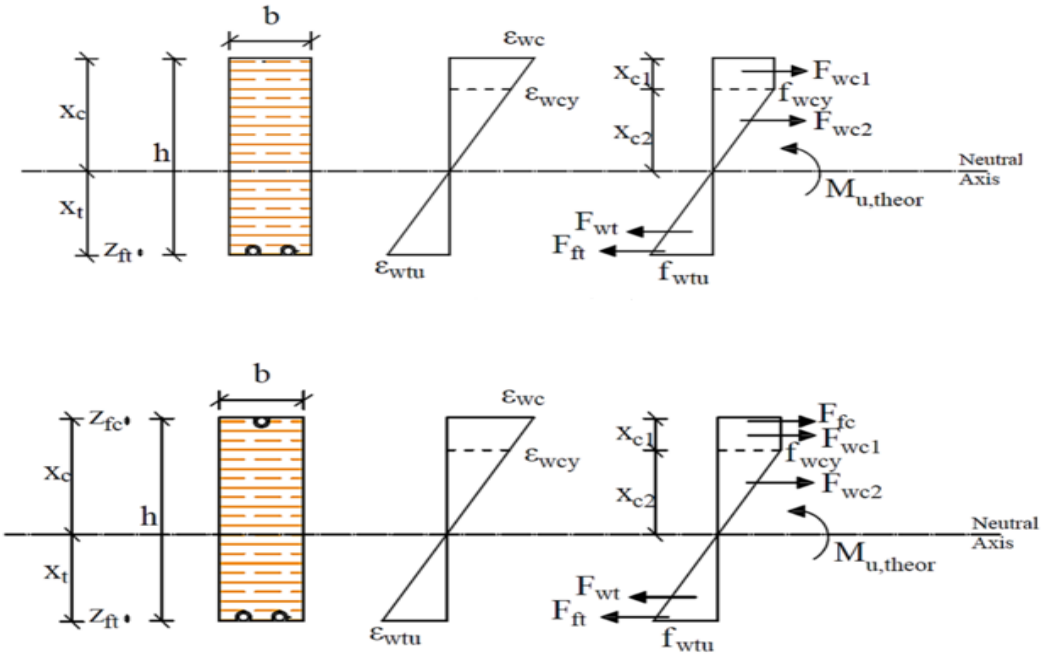

Fig. 2.2. Cross-sectional equilibrium for two configurations of the composite section [10]

$$M_{u,theor} = F_{wc1}\left(x_c - \frac{1}{2}x_{c1}\right) + \frac{2}{3}F_{wc2}x_{c2} + F_{fc}\left(x_c - Z_{fc}\right) + \frac{2}{3}F_{wt}x_t + F_{ft}\left(x_t - z_{ft}\right) =$$

$$bf_{wcy}x_{c1}\left(x_c - \frac{1}{2}x_{c1}\right) + \frac{1}{3}bf_{wcy}x_{c2}^2 + f_{wcy}\frac{E_f}{E_w}A_{fc}\left(x_c - z_{fc}\right) + \frac{1}{3}bf_{wtu}x_t^2 + f_{wtu}\frac{E_f}{E_w}A_{ft}(x_t - z_{ft}) \quad (2.5)$$

Where A_{ft} and A_{fc} are FRP bars' cross-sectional areas at tensile and compression zones, respectively. It is clear that A_{fc} is zero for the first configuration of beams in Fig. 2.2.

To produce the maximum moment capacity, Equations (2.6) and (2.7) are extracted from the geometry and followed by rational calculations of Equations (2.9) and (2.10):

$$x_c + x_t = h \quad (2.6)$$

$$x_{c1} + x_{c2} = x_c \quad (2.7)$$

$$\frac{x_t}{x_{c2}} = \frac{\varepsilon_{wtu}}{\varepsilon_{wcy}} \tag{2.8}$$

$$F_{wc1} + F_{wc2} + F_{fc} = F_{ft} + F_{wt} \text{ , so:} \tag{2.9}$$

$$bf_{wcy}x_{c1} + \frac{1}{2}bf_{wcy}x_{c2} + f_{wcy}\frac{E_f}{E_w}A_{fc} = \frac{1}{2}bf_{wtu}x_t + f_{wtu}\frac{E_f}{E_w}A_{ft} \tag{2.10}$$

Using Equations (2.6) to (2.10), material laws, modulus of elasticity of lumber, BFRP, and GFRP, and ultimate tensile strain values from non-reinforced beams, the theoretical moment resistance ($M_{u,theor}$) and associated force ($F_{u,\ theor}$) were evaluated. All studied beams had x_{c1} equal to zero, indicating an elastic condition for the compressive component of the timber. The failure happened when the ultimate tensile strain was achieved, consistent with experimental observations. The theoretical moment resistance ($M_{u,theor}$) for the analyzed beams was compared to the experimental values ($M_{u,exp}$). The average ratio of $M_{u,exp}/M_{u,theor}$ is 1.09, indicating that theoretical predictions are in good agreement with experimental results. As a notable finding, the increase in maximum load ranged from 33% to 69%, the displacement at failure ranged from 9% to 41%, and the global flexural rigidity and stiffness increased by 22% to 33% [10]. The latter analytics will serve as the basis for formulating strengthened beams, proposed in Chapter 6.

Post-tensioning, another method for strengthening timber structures, can be applied to the connection zone. The literature discusses the development of structural frame beams and columns connected by unbounded post-tensioning for multi-story timber buildings. The focus is on the deformations within shear panels of timber beam-column joints, providing lateral resistance. Beams exhibited higher stiffness and minor deformations; they can also achieve ductility, even though timber is a brittle material [55].

2.2 Review of Studies on a Statistical Inference Method

The Null hypothesis, a powerful statistical tool, has recently transitioned from behavioural science, specifically psychology and social science, to engineering fields. According to Woodside (2017), management research continues to rely heavily on symmetric modelling and Null Hypothesis Statistical Testing (NHST) [56]. However, some researchers argue that the method

may not be accurate. According to Tryon (2001), NHST has been widely discussed but consistently effectively defended [57]. Balluerka et al. (2006) investigated the controversy around the Null hypothesis in psychological research. It examined concerns of NHST and alternative approaches proposed by the APA Task Force on Statistical Inference to improve statistical analysis and data interpretation. The essay argues that, while NHST remains helpful, it should be used judiciously and in conjunction with other methods to address its limitations. Adherence to rational usage criteria is critical for thorough research [58]. According to Nathoo and Masson (2016), simulations that compared the Bayesian Information Criterion (BIC) method to two Bayesian processes for ANOVA designs, as well as the classic Null hypothesis, revealed that Bayesian approaches consistently supported the Null model when no effects were evident, particularly with large sample sizes. Furthermore, Bayesian posterior probability with NHST values indicates that approaches are more cautious with small effect sizes [59].

Galvão Patriota (2017) analyzed how Bayesian and conventional statistical methods evaluate evidence differently. It criticizes classical hypothesis testing, mainly using p-values, for occasionally yielding surprising results. The author analyzed the limitations of p-values and proposed s-values as a more logically coherent alternative. It describes how to compute s-values and uses examples to demonstrate their advantages over p-values, providing a more straightforward and trustworthy measure of evidence [60]. Harrison et al. (2020) believed that, despite some controversial issues, including the use of p-values without considering effect sizes and confidence intervals, many experts argue that some problems with NHST are often due to misuse and misunderstanding rather than inherent flaws in the method itself [61].

The Null hypothesis is the fundamental concept that any statistical hypothesis testing begins with. It starts from the assumption that there is no significant difference or effect between certain populations or variables, essentially assuming that any observed differences are due to random chance or sampling variability. The baseline for the alternative hypothesis (H1), which posits a significant difference or relation, is tested against the Null hypothesis (H0) using a Z-test statistic. To establish if enough evidence exists to reject the Null hypothesis in favour of

the alternative hypothesis, data can be subjected to some tests of statistical significance. To do so, one must compute a statistical test and then compare it with critical values or use p-values to establish how likely it would be for such data to have occurred, assuming that H0 was true. However, rejecting the Null Hypothesis implies that an observed effect is statistically significant, unlike failing to reject it, which implies insufficient support for a significant difference or effect. This ensures that the objectivity and rigour of statistical analysis are maintained by having a clear framework of scientific inquiry and preventing false conclusions using a hypothesis.

The Null hypothesis, in engineering, is a key factor that guarantees the authenticity and validity of experimental results and design decisions. When engineers test new materials, processes, or structures, they may use the Null hypothesis as a starting point for comparisons. For example, in evaluating the mechanical performance of timber beams, the Null hypothesis may assert that there is no significant difference in strength or durability between Heritage timber beams and New ones. It is through conducting experiments and applying statistical tests that an engineer can determine whether observed differences in performance are statistically significant or merely due to random variation.

The following are the most essential fundamental components of hypothesis testing. The Null hypothesis (H0) and alternative hypothesis (H1) should be mutually exclusive for the population value of the test statistic. For the test statistic t = T(D), the population value of "t" is represented by "Θ." When examining the sample distribution, calculate/estimate the probability distribution of the test statistic using either Z-score or T-score, assuming the Null hypothesis is true. A significance level (α) should be chosen to assess the likelihood of producing a Type 1 error (false positive). The significance level (α) can range from 0 to 1, denoted as $\alpha \epsilon [0, 1]$. The equation can also be written as α = P (Type 1 error) = P (reject H0/H0 true). Determining P-values, which show the possibility of receiving more extreme values under the Null hypothesis, is vital. In the form of formulation in Equation (2.11):

$$\alpha = \int_{\theta_c}^{\infty} f_n(x'|H0\ true)\, dx' \tag{2.11}$$

It is worth noting that the test statistic and the P-value are both random variables, as they are dependent on the specific data sample analysis [62].

The final and crucial stage is to decide on the Null hypothesis. Determine whether to reject or accept the Null hypothesis using the P-value or a pre-defined threshold (Θc), as defined in Equation (2.12):

$$If\ t_n > \theta_c, \qquad reject\ H_0 \tag{2.12}$$

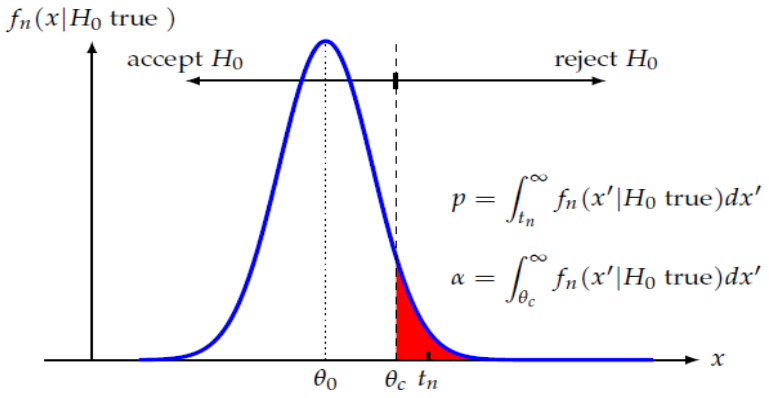

Fig. 2.3. Null Hypothesis concept [63]

All required steps and the whole concepts are summarized in Fig. 2.3. Note that if the statistical analysis does not provide sufficient evidence to reject the Null hypothesis, it will be taken as the default assumption; accepting the Null hypothesis does not imply proof of its truth [63]. It simply indicates that there is insufficient evidence to reject it based on the analyzed data.

When comparing old wood to New wood, several factors come into play, including age-related issues, density, inherent strength, and defects. From a background perspective, it has been suggested that old timber beams, over 150 years in age, may possess superior mechanical properties, such as MOE, MOR, and CSPG, compared to Newer timbers. Cavalli et al. (2016) suggest that differences between old and New wood are more related to the original quality of the

material rather than just the effect of aging itself [64]. Several factors contribute to this, including environmental influences such as increased air pollution and global warming [65]. Also, due to the smaller scale of the furniture industry during that time, most hardwoods were primarily used in building construction.

Considering these facts and the literature, if old timber beams are not biologically deteriorated, their mechanical performance may remain consistent despite natural aging, defects, and cracks. According to Brol et al. (2012), reusing old floor beams from demolished buildings is possible, as demonstrated by the testing of 130-year-old timber beams from a notable building. The beams showed adequate strength for reuse despite unknowns regarding the original timber characteristics [19]. Thaler et al. (2013) showed that the mechanical performance of Oak wood does not deteriorate over time. Also, no significant differences in the mechanical properties of old and New spruce wood were considered. In general, it is confirmed that most of the relevant properties of wood do not deteriorate over time, and they can be reused after decades of service [20]. Additionally, Gómez et al. (2019) indicated that wave velocities and mechanical resistance could be equivalent between old and New wood of the same species under certain conditions [66]. When comparing the mechanical properties of old timber beams to their New counterparts, it is essential to consider the impact of aging on the material. Old timber beams, due to their inherent mechanical properties and the presence of extractives that protect against insects, are often more durable and superior to New timber beams [67]. Kránitz et al. (2010) claimed that the modulus of elasticity of 200-year-old oak and spruce, if not deteriorated biologically, and their New counterpart wood was almost the same [22].

Due to the abundance of resources and the construction style, old wooden buildings constructed 120-150 years ago used massive beams. When retrofitting these intact beams, it's essential to find New lumber beams that match the performance of the original ones in terms of size and strength to perform destructive testing of these correlated New beams. The literature offers limited full-scale test data on the mechanical and material properties of old/Heritage beams, hindering the development of a unique computational approach as an alternative to destructive tests at this stage.

Statistical analysis can effectively and scientifically compare New and old/Heritage beams, focusing on mechanical properties such as bending strength, modulus of elasticity, and load-carrying capacity. The implementation of a Null hypothesis to investigate the possibility of equivalence between New and Heritage is not further explored in the literature. The results of this part of the research are expected to influence the practices associated with Heritage preservation, restoration, and maintenance.

2.3 Review of Studies on NDTs

The behaviour of timber is known for its high variability and complex, non-linear nature, making its assessment troublesome. In-situ NDT, or the evaluation of wood's mechanical and material properties under operational settings, has gained popularity in recent years [68]. Over the last two decades, numerous studies have investigated the application of NDT methodologies to assess the mechanical performance and material properties of old timber members [8,21,22,66,69]. These strategies are critical in historic restoration, where preserving structural integrity and cultural value requires little physical or appearance changes.

Generally, several NDT methods, such as stress wave propagation, ultrasonic testing, resistance drilling, X-ray and CT imaging, acoustic emission, and infrared thermography, are used to estimate parameters including MOE, MOR, density, and internal decay. Stress wave and ultrasound technologies are among the most widely used due to their portability and sensitivity to interior defects, as well as their potential for development and more reliable results. However, Studies have found that standardizing these approaches is difficult, as moisture content, grain orientation, species diversity, and surface aging and deterioration all impact the results. Research has focused on correlating NDT results with destructive mechanical testing results to increase prediction accuracy, as well as establishing empirical and statistical models that relate material parameters to mechanical performance. More recent studies have investigated the complementary use of numerous NDT methods or their integration with artificial intelligence (e.g., ANN, SVM) to improve diagnostic reliability, particularly for in-situ structures. Overall, the literature demonstrates encouraging contributions, but emphasizes the importance of

calibration frameworks, consistent datasets, and validated models adapted to Heritage timber, which are currently missing.

A number of NDT approaches have recently been proposed, including colour measurement [68], tomography [70], micro-drilling resistance [71], acoustic wave velocity [72], and active thermography [8], for wood material characterization. Currently, the primary evaluation indicators for evaluating old timber members are dry density (ρ_0), MOR, MOE, and CSPG [8].

2.3.1 *Worldwide Codes and Standards for the Evaluation of Heritage and Old Buildings*

Within the study of building reliability, the reliability-based assessment of existing structures has been identified as a critical topic. At the same time, most available codes specifically address only the design situations of new structures [73].

Visual inspection is commonly acknowledged as the critical first step in the assessment of Heritage timber structures, providing an ND, cost-effective way for identifying vulnerability, safety concerns and structural performance issues; as Riggio et al. (2018) emphasized, visual examination serves as the foundation for additional investigative procedures, such as NDTs. However, present inspection methods are not consistent across countries, with only a few, such as Italy, providing precise national standards. While the authors admit that a globally uniform inspection form is unrealistic due to structural and cultural diversity, a shared ontological framework is essential to enhance consistency, comparability, and flexibility across different contexts and assessment objectives [74].

General structural codes rarely address existing timber constructions or assess them for their structural integrity. Although new codes are available, their application in Heritage sites is problematic, as the need to improve strength may necessitate alterations to the original structure [74]. To address this gap, ISO 13822 [25] *Bases for Design of Structures, Assessment of Existing Structures* (2010), was introduced to serve as a basis for the establishment of national standards [74]. Although the document provides general requirements for assessing any existing structure, Heritage structures are also highlighted in the annex.

Macchioni, et. al (2011) reviewed the limited criteria for in-situ evaluation of timber structures, noting that ISO 13822:2001 (New version-2010) [75] only provides basic guidelines aimed at safety rather than conservation. Italy provides the most comprehensive framework addressing Heritage. The Swiss SIA 269 [24] series, particularly SIA 269/5 [76], introduces probabilistic approaches for reassessment and maintenance. The need for a coordinated, conservation-driven code is emphasized, while existing techniques remain fragmented and poorly applied [77].

Considering the evaluation and retrofitting of timber structures, considering earthquake and seismic performance, the only guidance document exclusively dedicated to timber structures is FEMA 807 [27], *Seismic Evaluation and Retrofit of Multi-Unit Wood Frame Buildings with Weak First Stories* [74]. Similarly, *New Technical Rules for the Assessment and Retrofitting of Existing Structures* [28] is a concise review of National Technical Codes of European Countries, some of which are particular to timber structures that address existing structures [74]**.** National standards vary in their level of detail. The Italian National Design Code, NTC 2008, establishes general guidelines for the maintenance of timber roofs and timber floor slabs in traditional buildings [74]. In contrast, the Swiss Code, SIA [26], provides a document devoted to the evaluation of existing structures, featuring a section (part 5) on timber constructions; this section is based on either Bayesian techniques for observed individual variables, or conditional failure probabilities due to measured/observed variables (cracks) and/or expected variables (extreme loads) [73,74]. Table 2.1 provides an overview of the available codes that address existing timber structures.

Table 2.1. Available standards and guidelines for existing timber structures [74]

Code	Main Objective	Scope of Evaluation	Level of Assessment
FEMA 807:2012	Seismic evaluation and retrofit	B	1,3
ISO 1382:2010	Assessment of existing structure	C	1,3
ISO 2394:2015	Reliability of structures	C	2,3
CSN 730038:2014	Assessment of existing structure	C	2,3
SIA 269/5:2011	Assessment of existing structure	C	1,2,3
UNI 11138:2010	Intervention on timber structure	C	2,3
UNI 11118:2004	On-site inspection	C	3
EN 335: 2013	Durability of wood and wood-based products	B	2
ASTM D 245:2012	In situ grading of structural timber	C	3
COST ACTION IE0601	Assessment of timber structures	C	1,2,3
COST E55	Assessment of timber element	C	3
ICOMOS ISCARSAH	Assessment of timber structures	A-C	1,2,3
ICOMOS IWC	Assessment of existing structure	A-C	1,2,3

The classifications of these standards are based on three primary targeted assessments, including documentation, vulnerability, and safety. The level of assessments also includes preliminary, general, and detailed.

Several common concepts arise among national and international Heritage conservation regulations and guidelines. Understanding the significance is crucial to ensuring that any intervention respects the structure's historical, architectural, and cultural characteristics. Minimal intervention is continually emphasized, with strengthening confined to what is necessary and carried

out in a manner that protects original materials and historical authenticity. ND assessment approaches are encouraged, with sophisticated technologies that allow structural evaluation without causing harm.

Where possible, traditional techniques and materials are used and promoted to ensure continuity with the building's original construction practices. Interventions should also aim for reversibility, enabling future removal or modification without damaging the originality. In circumstances when new work is required and unavoidable, it must be compatible with existing materials and systems, including modern requirements, while respecting Heritage values. Finally, sustainability is acknowledged as a guiding concept, with energy efficiency and environmental concerns incorporated into interventions as long as they do not compromise Heritage significance. Together, these fundamental principles form the core of conservation practice worldwide, guiding both the assessment and structural strengthening of historic timber and other structures.

Despite the existence of several standards and guidelines for detecting structural safety and vulnerability, many are limited to specific structural systems or building categories. As a result, many Heritage timber structures do not fall within their scope. Only a few nations (such as Italy) have rigorous inspection criteria, which often focus on timber components. Notably, the Swiss standard SIA 269/5:2011 [26] and the COST Action IE0601 guidelines are among the rare documents that explicitly address hierarchical levels of investigation, thereby providing valuable models for developing inspection forms where no national procedures exist. These findings emphasize the critical need for standardized, Heritage-specific assessment methodologies. Additionally, COST Action FP1101 developed a specialized inspection form to bridge the gap between general evaluation standards and specialized on-site methods. However, it currently only applies to traditional timber roofs within a specified, though vast, geographical region [74].

The Standards and Guidelines for the Conservation of Historic Places in Canada (Second Edition, 2010) establishes a Canadian framework for the preservation of historic places through a

values-based and methodical approach. The standards promote minimal intervention, repair over replacement, and incorporate sustainability while preserving values and authenticity. It describes three major conservation treatments, including preservation, rehabilitation, and restoration, that prioritize the preservation of Heritage value and aspects while allowing for suitable adaptation. The document also includes standards for cultural landscapes, archaeological sites, buildings, engineering projects, and materials, such as wood and wooden structures. It emphasizes that conservation is a continuous process of understanding, planning, and intervening, led by Statements of Significance and sustained by ongoing maintenance. The guidelines are widely adopted by federal, provincial, and municipal authorities, serving as a benchmark for assessing interventions, integrating sustainability considerations, and balancing technical requirements with Heritage protection, thus providing a consistent reference for decision-making in Heritage conservation [78].

In 1986, the Canadian Association for the Conservation of Cultural Heritage (CAC) published its first Code of Ethics and Guidance for Practice for those involved in the conservation of cultural property in Canada. The guide emphasizes the importance of limiting intervention and prioritizing preventive conservation over direct interventions. According to Article 18 of this Code of Ethics, if restoration is deployed, it must be done with little involvement.

In Canada, there are no dedicated Heritage codes within the National Building Code (NBC), meaning that Heritage projects must comply with the same regulatory framework as other projects. To address the special needs of historic buildings, the Standards and Guidelines for the Conservation of Historic Locations in Canada (Parks Canada, 2010) established a national reference framework that has been widely adopted by federal, provincial, and municipal governments. These guidelines outline principles of preservation, rehabilitation, and restoration, emphasizing the protection of Heritage value. At the local level, additional provincial and municipal regulations supplement the federal guidelines; for example, the Ville de Montréal has developed bylaws and practical guidelines for the protection of Heritage buildings, ensuring that conservation practices reflect both national standards and regional priorities. Fig. 2.4 illustrates

the general notes from national (global) and Canadian codes regarding Heritage structures. These notes provide an overview and framework for assessing and retrofitting existing Heritage buildings.

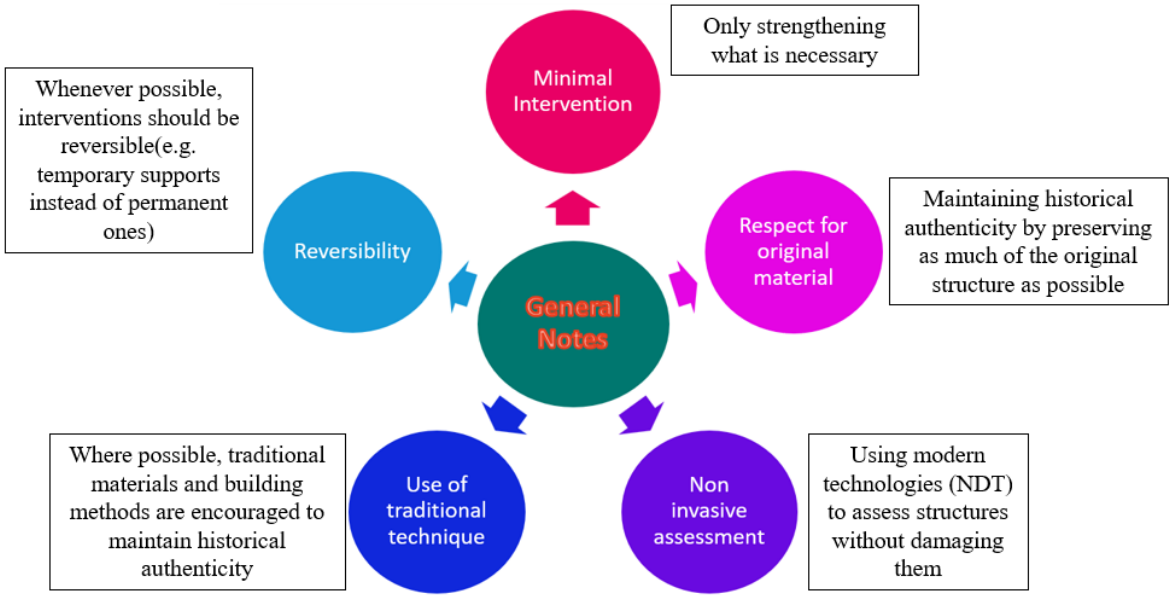

Fig 2.4. General notes from the national and Canadian codes addressing Heritage structures

The literature on statistical inference and FRP-reinforced wood beams is summarized in Tables 2.2 and 2.3.

Table 2.2. Summary of the studies on statistical inference

Authors' Names	Points
Tryon (2001)	Null hypothesis statistical testing (NHST) has been widely discussed but consistently and effectively defended.
Nathoo and Masson (2016)	Bayesian approaches consistently supported the Null model when no effects were evident.

Woodside (2017)	Management research continues to rely heavily on symmetric modelling and Null hypothesis statistical testing (NHST).
Harrison et al. (2020)	Despite some controversial issues, including the use of p-values without considering effect sizes and confidence intervals, some problems with NHST are often due to misuse and misunderstanding rather than inherent flaws in the method itself.

Table 2.3. Summary of studies on FRP strengthening

Authors'	Main Objective	Main Result
Wheeler and Hutchinson (1998)	Investigated Resin repairs to timber structures.	Showed that there is low to no degradation in the bonding strength of epoxy adhesives subjected to moisture as high as 22%.
Dagher (2000)	Investigated High-performance wood composites for construction.	Claimed main problem with reinforcement and wood is chemical incompatibility.
Gentile et al (2002)	Mitigates the impacts of local defects in the timber.	Increased the bending strength of the members by 18% to 46%.
Johnsson et al. (2006)	Investigated Glulam members strengthened by carbon fibre reinforcement.	Increased in flexural strength of 44-63% with a reinforcement ratio of 1%.
Kliger et. al (2008)	Strengthening timber with CFRP or steel plates	Increased stiffness and bending with reinforcement in the range of 1.5% to 2.5% up to 90% and 100%, respectively.
Schober et. al	Reinforcement of timber and engineered wood.	
Alam et. al (2009)	Investigated the Mechanical repair of timber beams fractured in flexure using bonded-in reinforcements.	Found that the reinforcing pattern for fracture mechanisms and the glue for bond action heavily influence the efficiency of the reinforcement.
Yusof and Saleh (2010)	Investigating the application of the GFRP sheet.	Improved bending resistance between 1.20 and 1.30.

Raftery and Whelan (2014)	Investigated improved arrangements of bonded-in GFRP rods.	Found that circular grooves improved rigidity and moment capacity more significantly; also claimed Sikadur 31 Hi-mod is the finest choice because it is insensitive to moisture before, during, and after curing for concrete, masonry, metals, wood, and other structural materials.
Al-Hayek (2014)	Strengthening timber beams with CFRP.	Increased the strength of the members with reinforcement of 0.22% by up to 47%.
Franke and Franke (2015)	Investigated failure modes and reinforcement techniques for timber beams.	Proposed 25% and 75% of the reinforcement to be at the top and bottom of the wood beam section, respectively (for strength).
Fossetti et al. (2015)	Investigated the flexural behaviour of glulam timber beams reinforced with FRP.	Resulted in an increase in flexural strength of 25% with a reinforcement ratio of 1% (early de-bonding).
Morales-Conde et. al (2015)	Investigated bending and shear reinforcements for timber beams using GFRP plates.	Claimed that results of research may vary substantially, making direct comparisons between studies difficult; also, commonly observed beam fractures are due to failure of the lower fibres under tension or a combination of tension and shear.
Brol and Wdowiak (2019)	Investigated reinforcement effectiveness of old timber beams employing CFRP and AFRP mats and strips, as well as BFRPs and GFRPs.	Showed that the highest flexural capacity occurred in samples CFRP mats (60.66% flexural bending increase) and the lowest capacity occurred with GFRP (increased by 19.04%).
Yeboah and Gkantou (2021)	Investigating NSM-FRP capacity and failure modes.	Claimed that there is no standard method for the prediction of the NSM-FRP timber flexural. Constructed a formulation based on test results. Reported an increase in bending capacity of 33% to 69%.

CHAPTER 3

Evaluation-Phase I: Investigating Material Properties and Mechanical Performance of Heritage Timber Beams (Approach 1)

General

Chapter 3 is part of the Phase I (Evaluation) of the thesis methodology, which describes the experimental program used to establish the baseline material properties and mechanical performance of full-scale Heritage timber beams before any strengthening. In accordance with the framework of Methodology (Sec. 1.6.1), this chapter documents the specimen source and conditioning, as well as records the density and moisture content. The chapter explains controlled bending tests (with instrumentation to capture load-deflection, stiffness (MOE), strength (MOR), and failure modes). The generated dataset enhances the thesis's Heritage-beam database. It gives the calibrated inputs and targets required for the two assessment approaches described in the Methodology: (i) the non-destructive/indirect indicators used subsequently to correlate in-situ data with mechanical performance, and (ii) the Null-hypothesis/equivalence comparisons between Heritage and New counterparts created in Chapter 4. The findings from Chapter 3 establish realistic demand and variability for the NSM-GFRP strengthening investigation in Chapter 5, serving as a baseline for the complementary analytical formulations developed in Chapter 6. Finally, the chapter paves the path to functionality of the Phase I workflow, correlates the mechanical performance of in-situ Heritage beams to NDT results, relying on validated experimental evidence.

Additional information and pictures pertinent to Chapter 3 are provided in Appendix A.

Status: Under review. Submitted to Journal of Materials and Structures, Springer

From Non-Destructive to Structural Insights of Heritage Timber: A Combined NDT and Destructive Testing Approach

Reza Abbasi Malekabadi [1] Ghazanfarah Hafeez [2, *]

[1] Department of Building, Civil and Environmental Engineering, Concordia University, Montréal, Canada, H3G1M8

reza.abbasimalekabadi@mail.concordia.ca

[2] Department of Building, Civil and Environmental Engineering, Concordia University, Montréal, Canada, H3G1M8

*Correspondence: ghazanfarah.hafeez@concordia.ca ; Tel.: +15148482424; ext.: 8703

Abstract

Heritage and old timber structures are desired to be conserved, necessitating a comprehensive understanding of their mechanical behaviour and failure mechanisms. This study presents an experimental investigation to comprehensively investigate the mechanical and material properties of aged timber beams. The mechanical properties and the failure modes of 44 full-scale Heritage timber beams sourced from Canada are assessed through both destructive and non-destructive testing (NDT) methods. The beams are evaluated for their maximum bending capacity, deflection, static and dynamic Modulus of Elasticity (MOE, MOE_{dyn}), Modulus of Rupture (MOR), and density, along with their failure modes, emphasizing their structural integrity and potential for continued use. The outcomes of this study indicated variability in mechanical performance due to aging, environmental exposure, and inherent material properties. Correlations between MOE, MOR, and density are recognized, supporting predictive assessments. Measuring material properties through NDT enables in-situ evaluation of the mechanical properties of old timber elements, aimed at extending the lifespan of Heritage wooden structures, preserving their structural functions and cultural values, while also contributing to sustainability and low carbon emissions.

Keywords: MOE; MOR; Maximum Load-Deflection; Failure Modes; Full-Scale.

3.1 Introduction

Wood is recognized as a readily available and highly versatile building material, experiencing significant growth in its application within the construction industry over the past twenty-five years [79]. Wood utilization, including both conventional and engineered products, is increasingly recognized as an environmentally wise and sustainable choice. It is actively promoted by government bodies as part of broader sustainable development strategies aimed at mitigating climate change [80], and it has even been verified as a carbon-negative substance [81]. As one of the oldest construction materials, wood possesses superior material and mechanical properties, including strength and low specific weight. Moisture and temperature fluctuations, fungi, and insect activities are common contributors to the deterioration of wooden structures. When exposed to optimal moisture conditions, timber structural elements have a long lifespan and require low maintenance costs. However, natural aging and imperfections such as cracks, splitting, knots, shakes, and twisted fibres, complemented by non-uniform anisotropic features, necessitate that existing timber elements to be evaluated and assessed. Timber structures and elements may require reinforcement or retrofitting due to reduced performance criteria over time [1]. Some Heritage timber buildings have deteriorated and suffered damage due to severe deflections, load adjustments, and inadequate maintenance, resulting in reduced functionality. The initial step for strengthening or maintenance of old timber buildings is the mechanical and material evaluation of their structural members, ensuring they remain responsive to loads while also preserving their cultural value.

The ISO 13822:2010 [75] standard serves as the sole guideline for the in-situ evaluation of timber structures on a global scale, considering all building materials, including wood [77]. However, in Canada, while specific regulations for Heritage structures are not outlined in the building codes, Heritage projects must still adhere to the National Building Code of Canada (NBC) [82]. Currently, the major evaluation parameters for monitoring and evaluating ancient timber members are dry density (ρ_0), Modulus of Rupture (MOR), Modulus of Elasticity (MOE), Compressive Strength Parallel to Grain (CSPG) [8], and specifically Nod-Destructive Tests (NDT) including colour measurement [68], tomography [70], micro-drilling resistance

[71], acoustic wave velocity [72], active thermography [8], and ultrasonic velocity tests. Visual strength grading is also considered an NDT [74,83,84]. It has been noted that the irregular geometry typical of timber structures complicates the application of NDT, consequently leading to increased inspection duration, costs, and variability in results [85]. Therefore, Xin et. al [21] suggested deploying several NDT techniques and ML approaches to precisely evaluate the properties of old timber members. Due to the significant variability and nonlinearity inherent in timber behaviour, data are often presented in a statistical format.

This study aims to analyze the mechanical and material properties of Heritage timber beams, and to establish the correlations between MOE, MOR, density and beam failure modes. The methodology employed in this study involves a comprehensive approach, utilizing both NDTs and destructive tests to address relevant concerns through a total of 44 full-scale beams from historic residential buildings in Ontario and Quebec, Canada, dating back to 1875. Additionally, the observed failure modes in the beams are discussed in relation to these structural characteristics.

3.2 Background

Reusing, maintaining, and protecting old timber buildings highlights the historical significance of wood in architecture, preserves heritage structures, particularly those carrying cultural importance, and presents an opportunity to promote sustainability. Assessing their structural integrity, load-carrying capacity, actual condition, and impacts of aging and weathering over time are multidirectional, challenging, and crucial concerns in Heritage timber engineering. Understanding the mechanical performance of Heritage structural elements is crucial for their strengthening and for making informed decisions on restoration or adaptive reuse projects [2]. Additionally, a thorough comprehension of the materials used, construction methods employed, historical modifications made, and the current state of the structure is essential for effective conservation efforts [86].

Evaluation of the material and mechanical properties of wood during operational conditions, also known as in-situ ND testing, has become a flourishing topic nowadays [8,87]. NDTs are the preferred methods, unless the structure is demolished and destructive tests can be conducted

on full-scale members. However, the majority of the available results are from testing small wood samples [1,2]. Research has shown that many structures often have load capacities that surpass what analytical models estimate. This observation can be confirmed through NDTs, which serves as an assessment tool for evaluating the load-carrying capacity of aging timber beams [88].

It is advisable to enhance the correlations between NDT and destructive methods for Heritage conservation [89]. Marzo et al. [89] proposed a linear correlation to relate the MOE to the MOR, yielding an R^2 value of 0.41, indicating insignificant statistical correlation between the results obtained from NDTs and those from DTs. According to Thaler et al. [20], few studies have examined the long-term performance of wood materials over time. The authors confirmed that most of the relevant characteristics of wood, including MOE and MOR, do not deteriorate with time and can be reused after decades of service [20]. Kránitz et al. [22] reported that the MOE of 200-year-old oak and spruce, if not damaged biologically, and their New counterpart wood were nearly the same. Although aging itself may not directly affect the strength and stiffness of beams under moderate loading conditions, various factors, including environmental loads, overload situations, fire events, and restoration efforts, can all contribute to a decline in performance over time. Further, as materials age, their inherent heterogeneity tends to increase, impacting structural integrity [90].

3.2.1 *Effect of Aging on Mechanical Properties of Wood*

The correlation between MOE, representing timber stiffness, and MOR, indicating strength in bending, is essential for understanding the structural integrity and performance of timber, particularly when comparing old and new timber elements.

To assess the mechanical performance of Heritage timber beams, the age-related aspects which might be challenging to obtain, need to be measured [8]. Research consistently demonstrates that MOE and MOR correlate strongly across a wide range of timber species, and several studies have found a significant correlation between these entities among different timber species [8,21,91,92]. Firmanti et al. [93] mentioned that the correlation coefficient (R^2) between MOE and MOR of Norway spruce might range from 0.51 to 0.72. In another study the linear

correlation between MOE and MOR was confirmed in various timber species, with R=0.81 (R^2=0.66) [94]. Growth rings and density differences also influence the mechanical characteristics, including MOE and MOR, of older timber [95,96]. Furthermore, imperfections like knots in older timber weaken its overall mechanical performance, thereby complicating the correlations between MOE and MOR compared to new timber, which may be less common or evaluated differently [97]. The experiments using ND testing methods have shown reliable correlations between dynamic MOE (MOE_{dyn}) measurements and static bending tests for MOR, allowing for performance predictions without significant physical sampling [98]. Sequera et al. [85] proposed a linear Equation to correlate MOE to MOE_{dyn} in existing timber structures with variability in cross-section. Wood density has also been reported and proposed to correlate with MOE and MOR [97,99].

Numerous studies agreed that the mechanical performance of Heritage beams either remains stable or experiences a minimal decline over time [19–22]. However, the initial properties of the wood elements are not well-documented, making the comparisons to their current properties challenging. To address these concerns, researchers compared the MOE values of aged wood with those of similar new wood species, providing valuable insights into the performance characteristics of Heritage timber elements over time. Hirashima et al. and Cavalli et al. [64,100] compared the MOE values of wood aged 270 and 290 years to those of new simulated samples and found an increase in the MOE values of aged wood. However, it is noticeable that the samples were small-scale, and new wood was best selected to match the properties. Similarly, literature has reported the increase in MOE values of aged timber for some samples and species [64]. While, Cai et al. [101] compared the MOE of 90-year-old structural joists to those of their newer counterparts and reported a reduction of up to 40% in the MOE values of the old joists. The analysis of the literature indicated that several studies reported MOE has remained almost unchanged or decreased slightly over time [15,16,28–30], while only a handful of studies reported a decrease in MOE [21,101].

3.3 Research Significance

The mechanical performance of Heritage beams should be evaluated through destructive methods. However, NDT based on precise and consistent test data acquired from full-scale samples, while verified through destructive testing, represents a reliable and preferable method for evaluating intact Heritage beams. The limitation of NDT methods is that they are often calibrated using standard, small-sized lumber, and a very few tests can provide quantitative data that genuinely reflects the actual strength of large Heritage beams [90]. A review of available studies highlights a limited number of evaluations conducted on full-scale Heritage samples [99], indicating a lack of reliable data regarding key performance parameters such as MOE, MOR, density, and failure modes of Heritage beams. Therefore, the current study focuses on full-scale assessments to address this gap. Without an appropriate methodology for correlating NDT outcomes with destructive test data, there exists no quantitative framework to pave the way for establishing lifespan and maintenance schedules for Heritage buildings and structures, conducting reliable ND evaluations, and determining the potential need for strengthening Heritage and older timber structures.

This study presents a systematic experimental testing plan based on NDT and destructive tests to evaluate the material and mechanical properties of full-scale undeteriorated Heritage beams, respectively. The study aims to establish a reliable correlation between the performance parameters, MOE (from NDT) and MOR (from destructive tests), of aged wood, allowing for in-situ evaluation of existing ancient timber buildings. Subsequent discussions present the details of the experimental program, along with the test results and analysis.

3.4 Experimental Program

Initially, the timber beams, collected from Heritage buildings in Canada, underwent a thorough visual inspection, including the condition of the wood and natural defect criteria. It's important to note that any deteriorated sections were cut out to prepare for testing beforehand. Subsequently, both ND and destructive tests were conducted on all 44 Heritage beams.

3.4.1 *Non-Destructive Testing*

To estimate the material (and consequently mechanical) performance of in-situ timber structural elements, especially culturally valued buildings, NDTs or semi-destructive methods are

required. Ultrasonic velocity measurements and density evaluation using the oven method are performed as NDTs. The density can be determined from small, clear samples collected from areas with minimal stress, following the required configurations specified in the codes [102]. Samples were weighed before and after drying in the oven, and dry density is computed using Equation 1.

$$\rho_0 = \frac{M}{V} \quad (1)$$

where M is the Weight of the oven-dry mass (g) after being in the oven at 103 ± 2°C, and V is the volume (cm^3) of the specimens.

An ultrasonic test, as an NDT, can be used to determine the species of wood, MOE, and the percentage of cavity by monitoring the speed at which waves propagate between two points. This method is particularly valuable for assessing Heritage and historic beams, where the wood species may not be identifiable. Density testing is integrated to provide the necessary information when the wood species are unknown. In this study, the MOE of the Heritage beams were calculated using the beam density as $\rho_0.v^2$, where ρ_0 is the dry density, obtained from Equation 1, and v is the velocity determined between two points based on specified instructions from the manufacturer. It is noteworthy that the MOE calculated using this method is referred to MOE_{dyn} [92]. The correlation between the MOE_{dyn} obtained from an NDT and that from a destructive test is desired. Based on the literature, a strong correlation exists between static and dynamic MOE, indicating that the MOE_{dyn} can be 5-15% higher than its static counterpart [92,103].

Fig. 3.1 portrays the NDT prior to the destructive tests. Moisture content was measured by a moisture meter, showing 7% to 12%, addressing bending test considerations [104]; however, the exact amount was calculated by the oven dry method, followed by density measurements [105].

Fig. 3.1. Non-destructive tests (Ultrasonic measurements)

3.4.2 *Destructive Testing*

A comprehensive database of the mechanical characteristics of full-scale (44 Heritage) timber beams was established through testing of various sizes at Concordia University. The non-uniformity in the geometry was not a matter of choice, but rather a result of the available old beams. The main goals of this series of tests are to determine the maximum load-bearing capacity of each beam and to evaluate the corresponding deflection. A selected number of identical Heritage beams were also included in this assessment to examine their individual failure mechanisms.

The ASTM standard D198 [106] is widely recognized for evaluating the structural properties of wood through 3- and 4-point testing. In this study, a three-point bending test method was used to measure the mechanical parameters of the beams. The findings indicated that the quality of the wood beams largely conformed to the requirements outlined in the standards for static testing.

The beam specimens were then positioned horizontally between two roller supports, as shown in Fig. 3.2, and potentiometers were placed to record the deflections. A loading nose was set in the middle of the beam specimen, applying a force at a constant rate of 0.02 mm per second. The force was gradually increased until the specimen either failed by breaking or exhibited a significant drop in applied force (more than 15%). The deflection of the specimen was assessed at the point where the force was applied, specifically in the middle span. This measurement is essential for evaluating the flexural properties of the material. To determine the maximum stresses experienced in both the tension and compression zones of the specimen, the simple

concept, presented in Equation 2 was employed. Where P (N) is the force applied at failure, L (mm) is the total span of the beam, and b and d (mm) are the width and depth of the beam specimen, respectively.

$$\sigma=\frac{3pl}{2bd^2} \quad (2)$$

To establish a correlation between the dynamic response, as defined by the MOE_{dyn} in NDT, and its static equivalent, fundamental concepts from the classical mechanics of materials were employed, utilizing the relationship illustrated in Equation 3 [107].Where P is the load up to the elastic limit (N), L is the total span (mm), δ is the corresponding deflection to P in the mid-span (mm), and I is the moment of inertia of the cross-section (mm^4).

$$MOE = \frac{PL^3}{48I\delta} \quad (3)$$

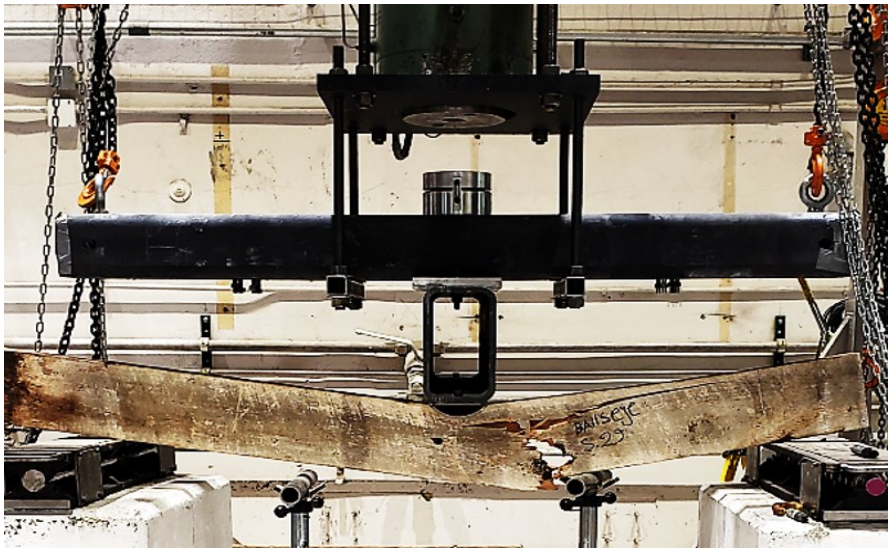

Fig. 3.2. Destructive tests on Heritage beams

3.5 Results and Discussion

This section discusses the correlations of MOEs, MOR and density for the measured beams, along with their mechanical performance and failure modes. The proposed correlations are also compared with existing studies. A comparable evaluation focusing solely on the identical beams among those examined is also discussed.

Since there is no exact value for the elastic limit for wood as a material, the MOE is determined by analyzing total deflections. This MOE is often referred to as the apparent modulus of elasticity. The difference between the two types of MOE (static and dynamic) is illustrated in Fig. 3.3. The results from the various tests, including both destructive and NDTs, are presented in Table A1, included in Appendix A.

3.5.1 *Study of the MOE (Static), MOE_{dyn}, and MORs*

Fig. 3.3a presents the obtained MOE_{dyn} from ND testing methods with their static counterparts derived from MOE_{dyn}, leading to more consistent modulus values. Although the species of the majority of the collected Heritage beams remains unidentified, the range of the MOE is still demonstrating a predictable trend, leading to the fact that timber of the same era, if not biologically deteriorated, shows a similar range of MOEs (5818 to 11817). On the other hand, as seen in Fig. 3.3a, the static MOEs discussed in section 3.2 revealed significant fluctuations, essentially indicating a limitation of the classical formulation (Equation 3) to the elastic range, which is not well defined in wood materials and does not account for the effects of shear deformation that, actually contributes. The fluctuations are prominent in static MOEs, attributed to cracking in old wood, as the real behaviour can be more reflective in static MOEs (obtained from destructive testing). The results also show that fluctuations in static MOEs are frequently evident in longer span beams (more than 1.7 m) due to unavoidable plastic deformations, while acknowledging the diminishing contribution from shear effects. For some beams, the two MOEs are seen in closest proximity. However, to facilitate a fair comparison between dynamic and static modulus values, the loading should be continued up to the maximum elastic limit, which is not specifically known for aged timber beams. Considering MOE_{dyn} in Table A.1 (Appendix A) and the static MOEs obtained from Equation 3, the ratio of MOE_{dyn}/MOE is 1.34, indicating an average difference of 34% between these MOEs. According to the findings of Divos and Tanaka [108], MOE_{dyn} could be as much as 10% greater than the static modulus. Their study further suggested potentially escalating the magnitude of this difference up to 70% when considering the influences of time and creep [108]. Similarly, Nowak et al. [92] have indicated the

variation of MOE_{dyn} from 5% to 15% above the static value. The observed 34% difference in the tested beams, when compared to existing literature [92,103], indicates the impact of aging, time, cracking, potential degradation, and creep.

The MOR, representing the maximum load-bearing capacity of a structural member subjected to bending, is directly proportional to the maximum bending moment experienced by the specimens. This measure is widely acknowledged as a strength criterion, although it does not represent a true stress, as the value is derived using a method constrained to the elastic limits [18]. Therefore, the current study employs the maximum load capacities of the tested samples for calculating the MOR, extending the analysis beyond the elastic range.

Fig. 3.3b displays a comparative peak fluctuation of MOR obtained from the Equations proposed by Caveli et al. [64] and Arriaga et al. [109]. The figure also presents a plot of $0.005(MOE_{dyn})$ as MOR, obtained from the mean results of NDTs conducted during the current investigation ($MOR/MOE_{dyn}=0.005$). This ratio (0.005) reliably represents MOR but is not considered a conservative approach for design or analysis. As illustrated in the figure, it can lead to overestimations of MOR in some cases. This finding is aligned with Marzo et al. [89], who confirmed that NDT alone may overestimate mechanical properties, emphasizing the need for combining NDT and DT for accurate assessments.

Arriaga et al. [109] who investigated the prediction of mechanical properties of timber members in existing structures, proposed Equation 4 to determine MOR using MOE_{dyn}. In this Equation, A and B depend on the method of ND measurement technique and density of the wood samples, which are considered, A=-9.3 and B=0.003 for the current study. Cavalli et al. [99] suggested a formulation to find the MOR, based on an experimental study involving dismantled old structural timbers, shown as Equation 5. Their proposed formulation defines *A* and *B* as the longitudinal MOE (MPa) obtained from the NDT and the defects (wane), which is regarded as zero for the current study due to the absence of wane in the testing samples.

$$MOR = A + (B * MOE_{dyn}) \quad (4)$$

$$MOR = -18.06 + 0.004A + 15.05B \quad (5)$$

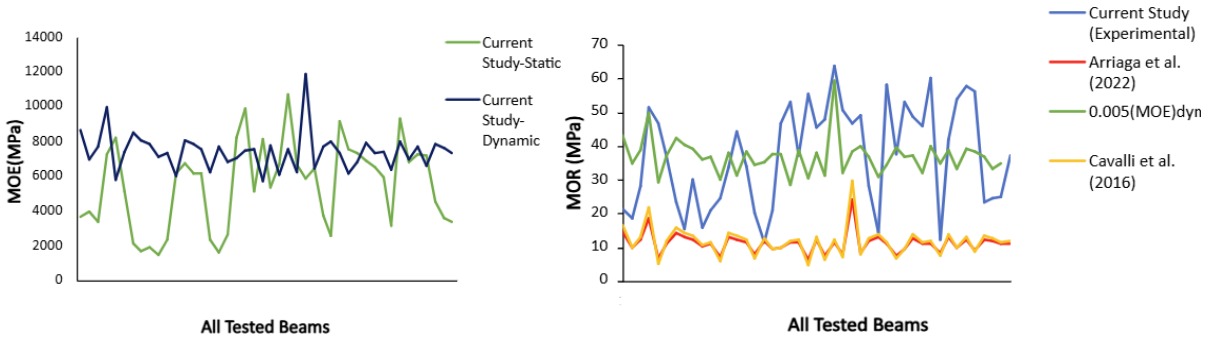

(a) Static and dynamic MOEs *(b) Comparison of MORs for all tested beams*

Fig. 3.3. Variation of MOEs and MORs

Nowak et al. [92] made a similar observation, highlighting a modest correlation between MOR and MOE, with R^2 = 0.61-0.69 in their study. Unlike the current study, which focused solely on full-scale destructive tests, their (Nowak et al. [92]) experimental investigation examined both small-scale and some full-scale samples for testing.

Fig. 3.4a demonstrates a correlation between the static MOE and MOR of the full-scale beams tested in this study, yielding Equation 6 with a coefficient of correlation R^2 = 0.74, indicating a strong relationship between the two entities. By integrating the results from the current study with those available in the literature by Nowak et al. [110], as illustrated in Fig. 3.4b, Equation 7 is produced. This Equation demonstrates a strong linear correlation, with an R^2 value of 0.92, indicating a significant correlation between the MOR and MOE. Ultimately, this relationship (Equation 7) effectively bonds NDT results to a key performance parameter for assessing the mechanical performance of existing timber structures, irrespective of failure modes or the sizes of the specimens.

$$MOR = 5.36\,(MOE) + 7.59 \quad (6)$$

$$MOR = 7.58\,(MOE) - 1.92 \quad (7)$$

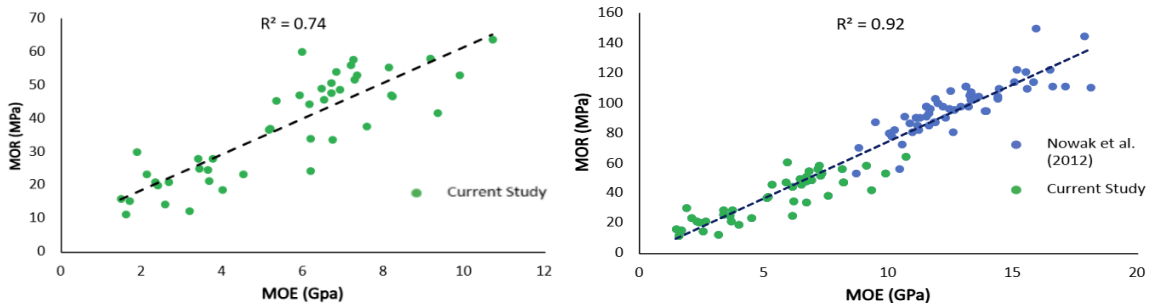

(a) Current study *(b) Combined studies*

Fig. 3.4. Correlation between MOR and static MOE

3.5.2 *Correlation between Density- MOE*

Density, as a semi-NDT metric, is recognized for its correlations with the MOE. Fig. 3.5a illustrates the correlation between density and MOE for all tested Heritage/old beams, indicating that an increase in density correlates with an increase in MOE. This observation applies to all beams, regardless of whether their failure was caused by shear or bending. The density-MOE linear regression for those that failed under flexural and shear yielded formulations provided as Equations 8 and 9 with $R^2 = 0.6$ and $R^2 = 0.86$, respectively, reflecting a stronger correlation for those that failed under shear.

$$MOE=16.11density+541 \quad (8)$$

$$MOE=25.3density-3213 \quad (9)$$

Considering the combined effect of all failure modes, Equation 10 presents the best-fit line to correlate density with MOE with $R^2 = 0.80$.

$$MOE=23.15density-2328.5 \quad (10)$$

Zziwa et al. [97] who conducted research on small-scale samples of Ugandan timbers, proposed a linear Equation as a function of density (kg/m³) for calculating MOE. Their investigations did not distinguish the failure mode, unlike the current study. The resulting Equation is presented below as Equation 11, and the best-fit on the wide scatter is displayed in Fig. 3.5b. The lower R^2 value of 0.3405 represents variability in the limited dataset. This Equation (11) fails to predict MOE based on density in Table A.1 (Appendix A). The reason might be attributed

to Ugandan species, which are quite different from those of North Americans. Equation 11 is also compared with the findings of the current study, which similarly illustrates the best-fit linear correlation corresponding to the tested data of the beams, including those that exhibited failures due to shear, bending, and the coupled effects of shear and flexure. Further, as illustrated, the scatter from the current study is narrower, comparatively demonstrating a modest correlation between the density and MOE of Heritage beams.

$$E=18.618x-1761.5 \quad (11)$$

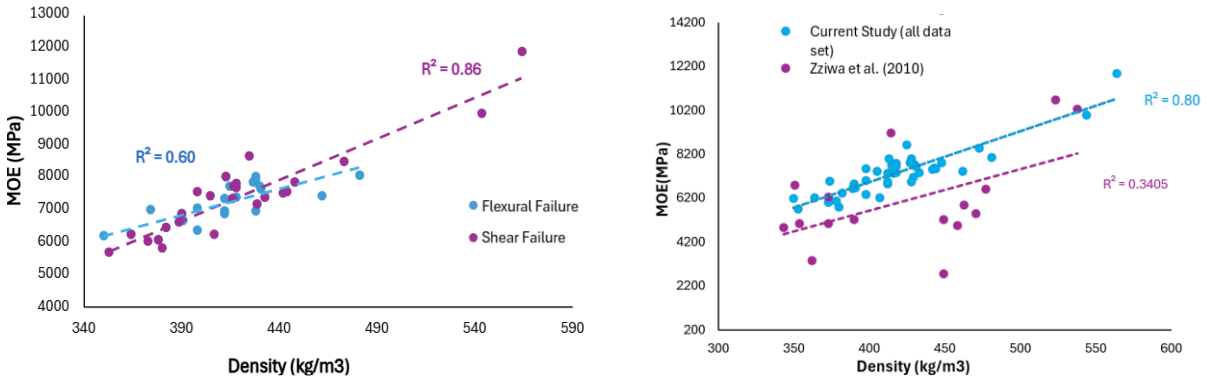

a) MOE-Density correlation based on data from the current study (Flexure Failure and Shear Failure)

b) MOE-Density correlation based on data from the current study and available literature [97]

Fig. 3.5. Correlation between density-MOE

3.5.3 *Mechanical Performance of the Heritage Beams*

This section analyzes the mechanical and material properties (MOE, MOR, ρ_o, force-deflection) of Heritage beams obtained through destructive and NDTs, aiming to correlate these properties with observed associated visual failure modes, including flexural, shear, and coupled shear-flexure.

3.5.3.1 *Failure Modes in Identical Beams*

A comparison of 5 identical Hemlock beams retrieved from a dismantled ancient building enabled an analysis of the correlation between failure modes, density, and MOE, thereby

enhancing the overall comparability of the results. For the reader's information, these five beams are the only ones that are identical among all those tested. The remaining beams have varying geometric features and unidentified species from different locations, yet they share the same age as the identical beams.

The results presented in Table 1 show that the average beam densities vary between 374 and 473 kg/m³, and the average MOE_{dyn} ranges from 6849 to 8092 MPa, determined using NDT methods. On the other hand, the maximum load capacity and corresponding deflection are derived from the destructive test.

Table 3.1. Material properties and failure modes of five identical Heritage timber beams

Beams	Samples	Density (Kg/m^3)	MOE (MPa)	b*h (mm)	Span (mm)	Fmax (kN)	Deflection (mm)	Failure mode
B31	1	412	6862	70*195	1050	25.9	8.4	Bending
	2	398	7021					
	3	391	6663					
B30	1	428	7730	75*190	1080	34.9	9.15	Bending
	2	412	6862					
	3	430	7730					
S32	1	430	7730	70*200	1070	52.3	15.1	Shear
	2	473	8491					
	3	448	8054					
S33	1	429	6961	70*200	1100	39.3	11	Shear
	2	418	7377					
	3	428	6900					
BS36	1	374	6980	75*200	1030	30.9	9.48	Shear-Bending
	2	430	7159					
	3	408	6860					

Fig. 3.6 shows the force-deflection correlation of these identical beams. From this figure, Table 3.1, and various observations, it is evident that the beams that failed under shear (S33, S32) can sustain more load and experience greater deflection compared to the three beams that experienced bending failure. Referring to Table 3.1, shear-dominant beams generally have higher

densities and MOEs. This consistent trend is observed in the two similar beams, B17 and B18, as detailed in Table A.1 of the Appendix A. B18, characterized by its higher MOE and density, demonstrated a failure under shear at a significantly higher load than B17, which exhibited lower performance values attributed to bending failure. A quantitative assessment of the visual examination of failure modes associated with their corresponding criteria, considering imperfections and natural defects, is presented next.

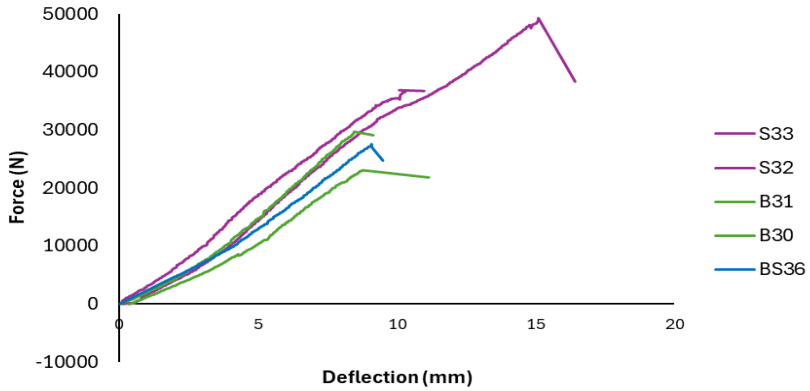

Fig. 3.6. Mechanical behaviour of five identical Heritage beams

3.5.3.2 *Failure Modes in Unidentical Heritage Beams*

The tested beams demonstrated failures attributed to flexural, shear, and their coupled mechanisms. Fig. 3.7 illustrates the typical modes of failure and crack propagation observed in various Heritage beams. Specifically, Figs. 3.7a to 3.7e depict typical flexural failures, while Figs. 3.7f and 3.7g present shear-dominated failures in the beams. The failure modes characterized by coupled shear-flexure are represented in Figs. 3.7h and 3.7i.

Flexural failures consistently originated from the tension zone and progressed toward the compression face at specific angles, resulting in brash failure or splintering through naturally weak areas, as illustrated in Fig. 3.7e. In the cases shown in Fig. 3.7b and detailed in Fig. 3.7c, the failure resulted in distinct compression crushing, with the crack path notably intersecting an existing nail. Pure shear failure, as shown in Figs. 3.7f and 3.7g are characterized by horizontal splitting of the beam. In coupled failure modes, shear cracks generally initiate in the middle of

the beam and propagate outward under load, ultimately resulting in final bending or shear failure. The current study revealed that beams with pre-existing cracks (Figs. 3.7f and 3.7g) are more prone to shear failure, aligning with the literature [111], confirming that the existing cracks lead to shear failure. However, further research is necessary to differentiate the impacts of mechanical performance and the presence of cracks on the failure modes of these beams.

Fig. 3.8 illustrates the correlation between deflection and force for all Heritage/old beams, generally demonstrating that those failing under flexure exhibited more deflection, but fewer loads compared to those dominated by shear.

a) B31 *b) B30* *c) B30*

d) B8 *e) B11* *f) S32*

g) S33 *h) BS14* *i) BS36*

Fig. 3.7. Visual shear, flexural, and coupled failures

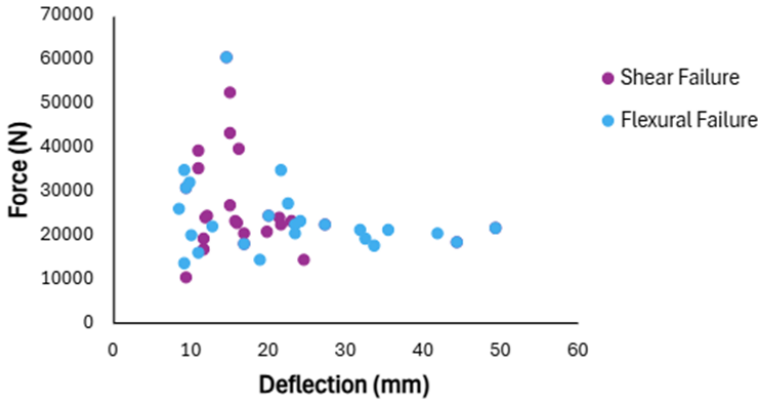

Fig. 3.8. Force-Deflection correlation for all Heritage/old beams

The load-carrying capacity and failure modes were found to correlate with density (ρ_0) and MOE, as presented in Fig. 3.9 and Table A.1 (Appendix A). Figs. 3.9a, b, and c display the force-deflection profiles of all tested beams, directly obtained from the DAS (Data Acquisition System), considering their failure under shear, flexure, and coupled shear-flexure. The observed and measured mechanical and material properties for each beam, along with their associated failure modes, are presented in Table A.1, which is included in Appendix A. Provided the beams were not identical, it is cumbersome to compare their performance; however, the general observations indicated that most beams with the highest densities and MOEs failed in shear. Other beams exhibiting MOE values between the two extremes, the highest and lowest values, also demonstrated coupled shear-flexure mechanisms, Fig. 3.9c and Fig. 3.6 (BS 36). Furthermore, beams exhibiting higher MOE values, which experienced shear failure, were capable of supporting greater loads than those that failed due to bending. It was noted that when shear failures predominated, the resulting member deflections were more significant compared to instances where failure was attributable to pure bending (Fig. 3.7a-e). Remarkably, the final collapse occurred after a series of peak failures in shear, as seen in Fig. 3.9a and Fig. 3.6 (S32, S33), whereas beams subjected to flexural failure typically collapsed rapidly following a single peak failure occurrence in a brittle manner, as shown in Fig. 3.9b and Fig. 3.6 (B30, S31). Further, abrupt decreases (less than 15%) mainly in shear, as shown in Fig. 3.9a, in the force-deflection profile may arise from shear failures or the closure of existing shear cracks as the

load increases. However, distinguishing between these two conditions visually remains a challenging task.

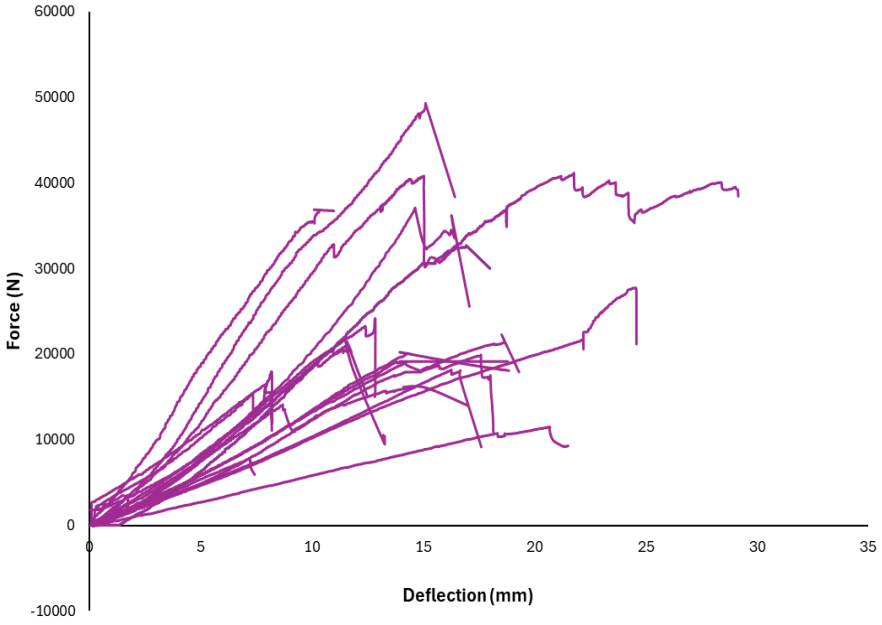

(a)

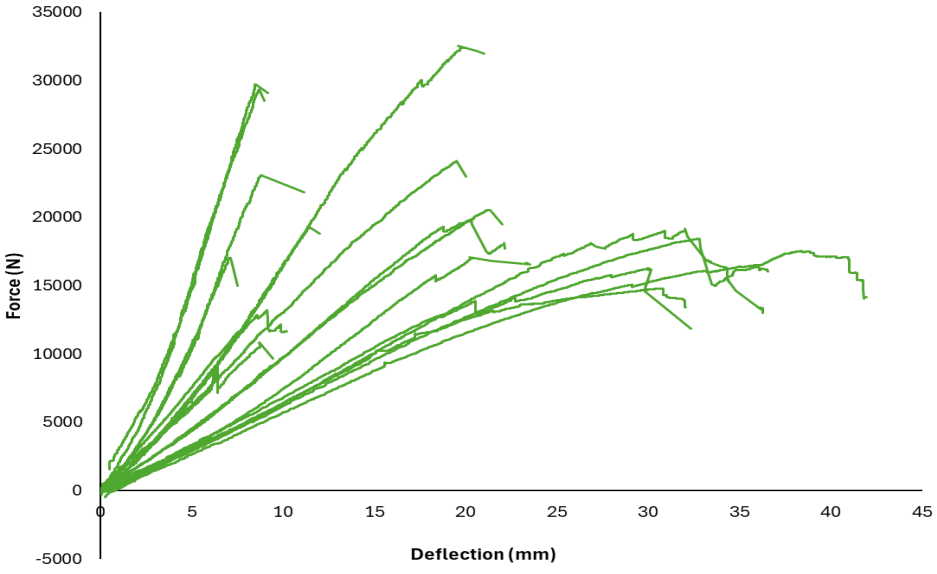

(b)

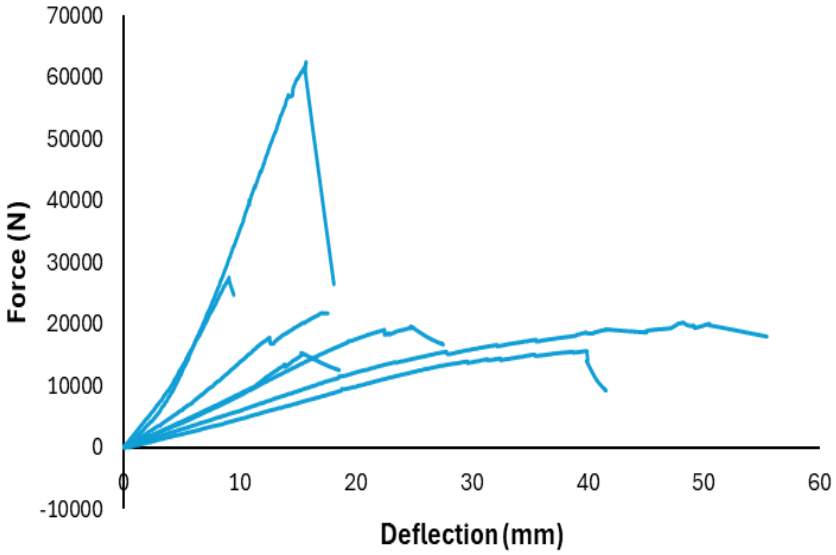

(c)

Fig. 3.9. Deflection-force correlation for all tested beams failed under a) shear Failure, b) bending failure c) shear- flexure coupled failures

3.6 Conclusion

This study experimentally provided a detailed evaluation of the mechanical performance and failure modes of 44 full-scale Heritage timber beams, collected around Canada using destructive and non-destructive testing (NDT) techniques. The findings establish a predictive foundation based on in-situ NDT evaluations of existing heritage buildings, providing valuable insights into their structural performance and supporting preservation, restoration, strengthening, and research purposes. A framework concluded in this study is presented in Fig. 3.10, to predict the strength (MOR) and failure modes of in-situ beams. It also supports and encourages the reuse of aged timber elements, addressing sustainability.

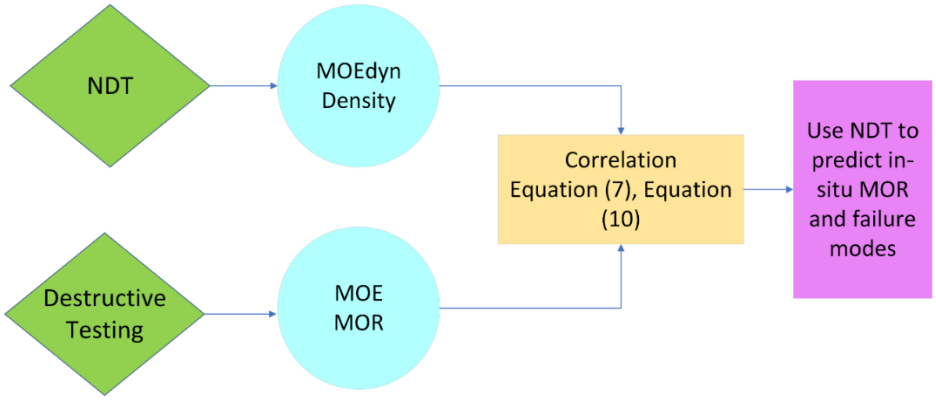

Fig. 3.10. Overview of the framework concluded in the research

The key findings of this study are as follows:

- A comprehensive dataset was developed from full-scale testing of aged Canadian timber beams, which can serve as a benchmark for future evaluations and modelling studies.
- To predict the beam's stiffness, this study proposes Equation (10), with $R^2 = 0.80$, defining a strong linear relationship between density and MOE. This correlation validates density as a reliable indicator of stiffness in Heritage timber.
- The current study recommends (Equation 6, $R^2 = 0.74$) and (Equation 7, $R^2 = 0.92$) to estimate the MOR of Heritage/old beams based on static MOE. The study also suggests $MOR \approx 0.005\ MOE_{dyn}$ for a practical strength estimation of in-situ Heritage timber. However, it may not be conservative for design and structural assessment purposes due to its inherent tendency to overestimate.
- The study found that MOE_{dyn} overestimates static MOE by 34%, which is aligned with the statement in the literature [89]. However, MOE_{dyn} has remained within a consistent range, making it reliable for capturing the inherent stiffness of Heritage/old timber. Further, MOE_{dyn} is more reliable than static MOE, as the effects of plastic deformations and material variability, including defects, are not captured in MOE_{dyn}.
- Beams with existing cracks tend to fail under shear. Shear failures involve gradual strength degradation with multiple peaks in the force-deflection curve until another

failure mechanism occurs. On the other side, bending failures are sudden and brittle, characterized by a single, sharp load drop. Additionally, sudden small load drops can occur due to the closure of pre-existing cracks or microcracks within the interior from shear.

- Beams with higher density, which leads to greater stiffness (MOE), generally demonstrated a higher load-carrying capacity and were more likely to fail in shear, while those with lower MOE tended to show flexural domination.

- In the absence of biological deterioration, the mechanical performance of old/aged timber beams, particularly their load-carrying capacity, remains high, making them viable for reuse in structural and non-structural applications.

Future work

Available data in this study are being used for an innovative method to replace destructive and NDTs of Heritage/old timber buildings, aiming mechanical performance assessment.

Authorship contribution statement

Reza Abbasi: Timber Collection, Experimental, Investigation, Formal Analysis, Validation, Conceptualization, Literature Review, Writing, and Editing. Ghazanfarah Hafeez: Conceptualization, Methodology, Investigation, Formal Analysis, Validation, Writing, Original Draft Preparation, Review, and Editing, Supervision.

Acknowledgments

This study received no support from the public, commercial, or not-for-profit funding agencies.

Conflicts of Interest

The authors declare that they have no conflicting interests concerning the publication of this article.

CHAPTER 4

Evaluation-Phase I: NDT Based on Statistical Inference (Approach 2)

General

Chapter 4 is a part of Phase I (Evaluation) of the thesis methodology and uses the statistical inference approach to evaluate in-situ Heritage timber beams. Building on Chapter 3 dataset, this chapter develops and tests whether Heritage members have mechanical performance comparable to that of their New counterparts by applying a Null-hypothesis framework (t-tests with variance/normality checks) to MOE/MOR and related flexural considerations. While required dimensions were not available in the market, Simulated New Counterparts (SNC) were constructed using grade-specified SPF characteristics and analytical bending relations, allowing for comparisons and the determination of safety factors across matched geometries. The outcome is a defensible method to indirectly infer the attributes of in-situ Heritage beams from calibrated New beams, thereby tightening the uncertainty bounds for the evaluation method discussed in Chapter 3 and supporting downstream strengthening decisions.

Status: Under review. Submitted to Journal of Engineering Structures, Elsevier

Experimental and Statistical Inference Approaches for Evaluating the Mechanical Performance of Heritage Timber Beams

Reza Abbasi Malekabadi [1] Ghazanfarah Hafeez [2,*]

[1] Department of Building, Civil and Environmental Engineering, Concordia University, Montréal, Canada,

reza.abbasimalekabadi@mail.concordia.ca

[2] Department of Building, Civil and Environmental Engineering, Concordia University, Montréal, Canada,

*Correspondence: ghazanfarah.hafeez@concordia.ca

Abstract

Heritage buildings are valuable cultural structures that must be preserved. The lack of proper maintenance, aging, biological threats, weathering, and new code requirements make their assessment and monitoring vital steps for decision-making, including strengthening or maintenance schedules. The initial step, while addressing the preservation value and appearance concerns, necessitates a non-destructive (ND) in-situ evaluation of the timbers' mechanical properties. However, there are no comprehensive methods or practices for assessing their structural performance. To bridge the gap, this study methodologically employs a Null hypothesis approach as a robust statistical tool for correlating the mechanical performance of Heritage beams to their New timber counterparts. As identical New beams are unavailable to match their Heritage counterparts, this study examines the bending performance of both Heritage and New timber beams through experimental and simulation methods, validating the results with existing research and standards.

A Null hypothesis approach is then employed to assess whether the mechanical properties of the unknown Heritage timber beams differ significantly from those of their New timber counterparts, providing valuable insights into the novel ND assessments. A one-tailed testing method was employed to maintain the additional safety margins. The results from the inferential statistics showed that as long as Heritage beams remain biologically intact, their mechanical properties are very

similar to those of New Spruce-Pine-Fir (SPF) timber beams of grade 2, having a bending strength (Fb) of 7.6 GPa or higher, as demonstrated by the statistical t-test (t (86) = 1.67, p=1.57, one-tailed). Therefore, mechanical evaluations of in-situ Heritage beams can be effectively carried out using both destructive tests and ND methods on New identical SPF beams of the same cross-sections and spans. The findings from these tests will then be directly applied to the Heritage beams.

Keywords: SPF Counterpart; Simulation; Null-Hypothesis; MOR; MOE

4.1 Introduction

Wood has been a primary building material for centuries due to its availability, workability, and structural properties. The application and historical usage of wood ranges from unprocessed wood log houses to highly processed and engineered products, facilitating mid-rise to tall wood buildings. Today, with the emergence of green building objectives and the high durability and stability of wood, it has become a widely used construction material worldwide. Spruces, classified as softwoods, are estimated to have about 40 species globally, among which black and white are the most common in North America and have been primarily used for construction [8].

The prevalence of wood-based Heritage buildings underlines the material's historical significance in architecture. Heritage is commonly associated with older or historic buildings, many of which are designated as protected cultural Heritage in various countries [1]. These structures offer insights into past construction techniques, architectural Heritage, and cultural impacts while showcasing the craftsmanship of wood as a traditional construction material. Despite these valuable insights, Heritage buildings have been experiencing structural inefficiencies and serviceability concerns throughout their service life, demonstrating the need for preservation and systematic investigations of structural performance and integrity. Timber elements, generally as part of floor or roof structures, require interventions to ensure stability for possible rehabilitation [2]. Understanding the mechanical performance of Heritage structural elements is crucial for making informed decisions about restoring or adaptively reusing older timber buildings. Comparing Heritage or old beams with contemporary timber counterparts presents

a unique opportunity to contrast their mechanical properties, as potential differences can inform the structural integrity and feasibility of restoration.

Therefore, the possibility for comparing the mechanical performance parameters of these Heritage beams, including dry density (ρ_0), Modulus of Rupture (MOR), and Modulus of Elasticity (MOE) [8] with those of New lumber, for both practical strengthening and research, requires a methodological approach.

This study examines the flexural performance of various Heritage timber beams through statistical inference, drawing upon available experimental research [19] for validation. Supporting background studies are provided to reinforce the presented research.

4.2 Research Background and Rationale

Evaluation of in-situ structural timber elements through ND testing methods is a currently popular research topic [8,87], despite the fact that there remains a lack of a comprehensive approach to assess the structural performance of existing Heritage buildings.

The current literature on destructive testing largely relies on either a limited number of full-scale timber members or small sample sizes [1,2]. When it comes to wood characterization using NDTs, the literature highlights a range of methods, including colour measurement[68], tomography[70], micro-drilling resistance[71], acoustic wave velocity[72], and active thermography[8]. Researchers have proposed various Equations and techniques for comprehensive assessments to relate the results of NDTs, especially MOE and density, to the actual mechanical performance (MOR) of existing timber elements [64,83,85,90,92,97,99,109,110,112]. Despite the progress made in the field through these methods and techniques, they still fall short of consistency and thoroughness, lacking universally accepted standards or guidelines.

Literature also includes limited international standards and guidelines for Heritage buildings based on visual assessments [77,112]. Visual strength grading, although not being an exhaustive procedure, is recognized as an NDT [74,83,84]. The ISO 13822:2001 standard, updated in 2010, is noted for being the only comprehensive guideline specifically addressing Heritage buildings constructed with any materials [77].

To enhance the evaluation of the mechanical performance of Heritage timber of various sizes,

Sousa et al. [112] proposed a combination of visual grading and bending tests.
Several studies have explored the performance comparison between old and New timber elements.

Typically, the mechanical performance of Heritage beams remains stable or experiences only a slight decline, provided the timber has not completely deteriorated, despite aging and the gradual development of cracks over time[19–22].Therefore, A century-old timber beam can still exhibit acceptable structural performance, including MOE, MOR, and Compression Strength Parallel to Grain (CSPG). Additionally, repurposing old timber beams from demolished buildings is feasible, provided that their structural properties meet the necessary standards [19].
Kránitz et al. [22] claimed that 200-year-old oak and spruce showed almost the same range of MOE when compared to their New wood counterparts. Thaler et al. [20] demonstrated that the mechanical behavior of oak wood remains stable over time, while the characteristics of spruce wood showed only minimal changes indicating that the properties of these two types of wood are unlikely to alter or diminish significantly over the time. Carrillo et al. [66] stated that the mechanical and physical properties of old timber beams are comparable to those of New ones. Cavalli et al. [64] suggested that differences between old and New wood are more related to the primary quality of the material rather than just the effect of aging itself. Additionally, it is indicated that wave velocities and mechanical resistance can be equivalent between old and New wood of the same species under certain conditions [66]. The existing literature reveals inconsistencies regarding the stiffness and strength properties of Heritage buildings, while simultaneously suggesting that there are negligible differences in the mechanical performance between Heritage and Newly constructed beams [68]. On the other hand, some studies address a decrease in the mechanical performance of Heritage beams during their service life [70], particularly regarding their MOR, though no clear correlation between age and performance was identified [21]. These inconsistent studies are central to assessing the comparative structural integrity and suitability of Heritage versus New timber counterparts for research, maintenance and strengthening purposes.

The Null Hypothesis (H0), a statistical inference tool, simply claims that there is no significant difference between untreated samples and those that have undergone treatment. This concept is widely employed in behavioral science and has found applications in various engineering and medicine fields.

The accuracy and practicality of the method has been supported highlighting the H0 as a reliable tool for research that depends on symmetric modeling, specifically normal distribution, and Null hypothesis statistical testing (NHST) [56]. The NHST has been widely discussed and consistently defended effectively [57]. However, adherence to rational usage and required criteria are essential thorough the research process [58]. Simulations which compared the Bayesian Information Criterion (BIC) method to two Bayesian processes for ANOVA designs, as well as the classic Null hypothesis, revealed that Bayesian approaches consistently supported the Null model when no effects were evident, particularly with large sample sizes. Additionally, Bayesian posterior probability with NHST values highlights that Bayesian approaches are more cautious with small impact sizes [59]. Further, Galvão Patriota [60] analyzed how Bayesian and conventional statistical methods evaluate evidence differently, criticizing classical hypothesis testing, particularly the use of p-values, for occasionally yielding unexpected results. The author analyzed the limitations of p-values and proposed s-values as a more logically coherent alternative [60]. Despite some debatable issues, including the use of p-values without considering effect sizes and confidence intervals, some experts disagree that some problems with NHST are often due to misuse and misunderstanding rather than inherent flaws in the method itself, as indicated by Harrison et al. [61].

Based on a review of existing literature and considering the variability of wood as a material, there is a gap in this research for precise, comprehensive, consistent, non-subjective methods to evaluate the mechanical performance of in-situ structural timber materials. To address this concern, either a comprehensive ND testing approach or alternative indirect techniques could be proposed. Therefore, this study bridges the gap by examining and comparing crucial mechanical properties, such as bending strength, MOE, and load-carrying capacity, between Heritage timber and New timber beams. This research presents a comprehensive testing plan and

novel methodology, Null hypothesis, designed to assess the structural behaviour of existing timber structures by comparing them to their geometrically New counterparts.

4.3 Materials and Methodology

The methodology in this paper involves both experimental and numerical work. In the experimental Phase, both destructive and non-destructive tests (NDT) are performed on 44 Heritage beams and 6 (+7) New beams to determine their mechanical and material properties. Out of these 13 tested New beams, the results of only six beams are considered in the simulation to test the Null hypothesis due to limitations in the destructive testing results. However, all 13 beams are considered for validation. Visual grading is conducted to identify visible defects and degradation before destructive tests. In the numerical section, in the first step, simulation of 44 New beams resembling their Heritage counterparts is done, followed by the Null hypothesis approach to compare Heritage and New beams. The details and limitations are presented in the following subsections and demonstrated in Fig 4.1.

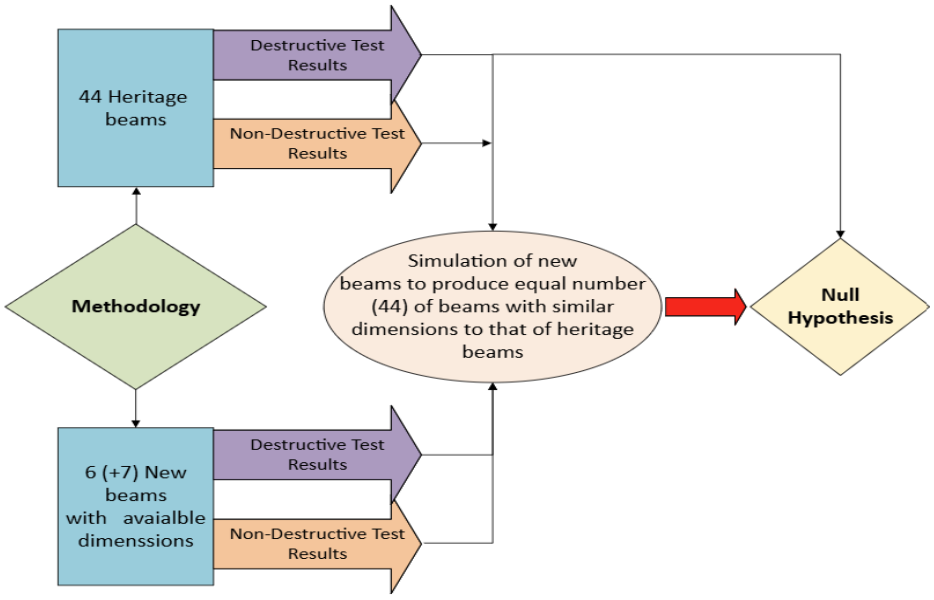

Fig. 4.1. Framework of adopted methodology

4.3.1 *Database on Material and Mechanical Parameters of Heritage and New SPF Beams*

Destructive and ND tests are conducted at Concordia Structural Laboratory to establish a database of the mechanical performance and material properties of Heritage and New beams and to perform simulation of New beams to feed the Null hypothesis.

4.3.1.1 *Non-Destructive Test (NDT)*

Procuring Heritage beams was challenging as it required searching for century-old buildings being dismantled to source the required Heritage beams. A representative number of samples, including 69 unknown (mixed population) Heritage timber beams were collected from demolished Heritage buildings in Canada. All beams underwent a comprehensive visual inspection and were graded into three categories: grade 1, grade 2, and grade 3, corresponding to low, moderate, and high defects, respectively, in accordance with the available guidelines [112]. Beams classified as grade 3 were not considered for NDT and destructive testing. Subsequently, the beams were inspected using an ultrasonic device to determine the MOE and the percentage of defects, followed by measuring the density using the standard method in both the Heritage and New SPF beams. The beams showing more than 20 percent of defects were excluded, leaving 44 Heritage beams with variable span lengths (1050mm to 2030mm), depths (90mm to 202mm), and widths (65mm to 140mm).

The dimensions of timber used in the past vary significantly from those of today's lumber, making it difficult to find New beams (unless customized) that match the size of the Heritage beams. To address this challenge, a simulation of New SPF beams was performed, yielding a similar number (44) of simulated New beams with identical geometric features to those of the Heritage beams. Therefore, 13 New SPF beams, readily available in the market, with variable span lengths (1500mm to 2420mm), depths (88mm to 144mm), and widths (36mm to 70mm), were also collected and underwent NDT, acquiring MOE and Density.

Density and MOE obtained from NDTs for Heritage and New beams are presented in Fig. 4.2. The density parameter is obtained from an oven test at 103 ± 2°C, following applicable standards [105], and the dynamic MOE (MOE_{dyn}) is calculated using $\rho 0 \cdot V^2$, where $\rho 0$ is the dry density and V is the wave propagation velocity measured between two points using Ultrasonic testing according to the specific manufacturers' instructions.

These measurements, portrayed in Fig. 4.2, demonstrate the superior quality of Heritage beams compared to Newer SPF beams, as later confirmed by the Null test. As indicated by the available literature, wave velocities and mechanical resistance (reflected in MOE_{dyn}) can be similar

between old and New wood of the same species, indicating that the material properties of both New and old beams are comparable [66]. Density, MOE, and MOR are indicators of a high-quality Heritage beam, revealing either the use of a hardwood or a denser timber sample from the same species. Wood from old trees may show higher density due to slower growth rates caused by past environmental conditions, including lower air pollutant levels and temperature compared to today [65].

(a) (b)

Fig. 4.2. Measurements from ND tests for Heritage and New beams. a) Density, b) MOE

4.3.1.2 *Destructive Test*

Following the NDTs, the three-point bending test was performed, adhering to the procedure defined in commercial standards, including ASTM D198 [106] and ISO 178 [113]. These destructive tests were conducted adopting a deflection-controlled approach at a constant rate of 0.02 mm/s. Fig. 4.3 illustrates the experimental destructive test setup for Heritage and New SPF beams, followed by Fig. 4.4, which displays the cluster of the maximum resistance forces obtained from the destructive tests. Destructive test results for the Heritage and New beams are also provided in Tables A.1 and A.2, included in Appendix A. Note that the obtained MOE from this destructive test is mainly called the apparent MOE.

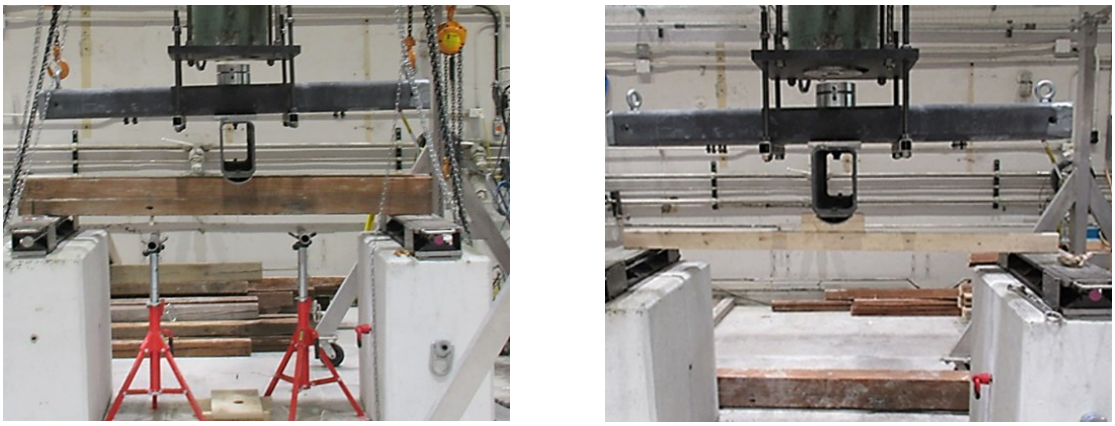

a) Heritage beam b) New SPF beam

Fig. 4.3. Heritage and New beam destructive testing

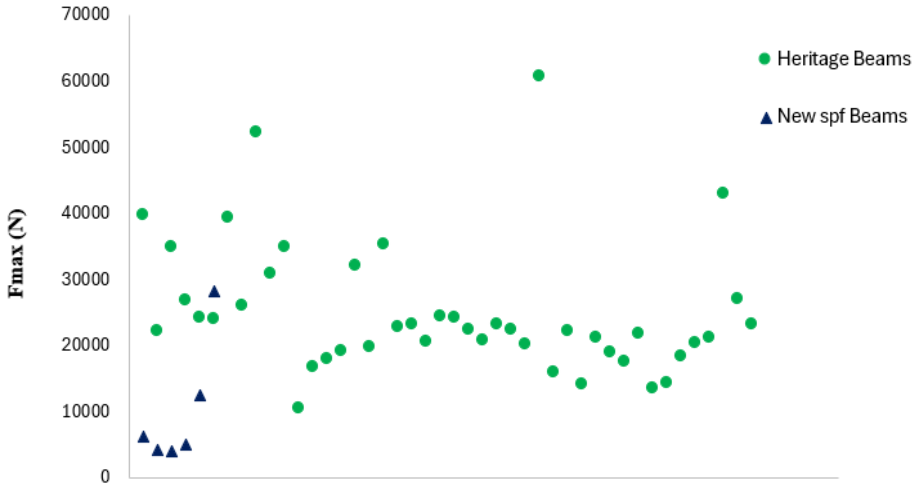

Fig. 4.4. Measurements obtained from destructive tests on Heritage and New SPF beams

4.3.1.3 *Simulation of New SPF*

After obtaining the performance parameters of 13 New SPF beams through destructive and ND tests, a simulation was conducted to create New timber beams with dimensions that closely match those of the Heritage beams. In this study, these beams are known as Simulated New Counterparts (SNC) and were verified in accordance with CWC O86 [104]. The SNC were simulated employing an iterative procedure with variable bending strength (F_b), followed by matching safety factors ($F_{max.}/F_{exp.}$). The SPF beams were considered grade II and better with

F_b= 7.6-11.8 MPa and MOE= 9.5 GPa, as identified in CWC O86. The moment capacity of the Heritage and New beams, followed by maximum force, was calculated to find the safety factor. Fig. 4.5 displays the scatter chart of maximum force obtained as the results of destructive tests on Heritage and New SPF beams, along with SNC beams with the same geometric configurations as the Heritage beams. Results of simulated beams compared to their Heritage counterparts are also provided in Table A.1, included in Appendix A. Out of 13 New SPF beams, only data from the 6 beams are included in this study, excluding the outcomes of the 7 beams that failed due to lateral torsional buckling before reaching their ultimate capacity.

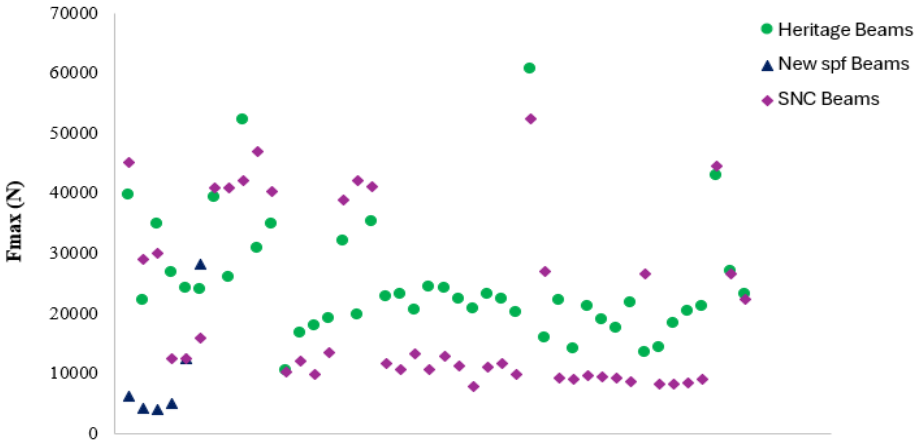

Fig. 4.5. Results from the destructive tests of Heritage, New SPF, and SNC

As clearly shown in this Figure and Table 1, the majority of Heritage beams exhibit higher Fmax in the range of 10000-20000 N compared to their SNC beams. However, some SNCs exhibit superior load-carrying capacity in the range of 40000-50000 N, which makes it challenging to reach an informed decision about the comparison. Therefore, the study employs statistical inference, the robust and right tool, to help establish a correlation between two entities. Furthermore, the safety factors presented in Fig. 4.6 demonstrate that the current methodology of simulating the beams with their old counterparts is more conservative (the difference between 2.9 to3.38 compared to 2.8 to 3.6).

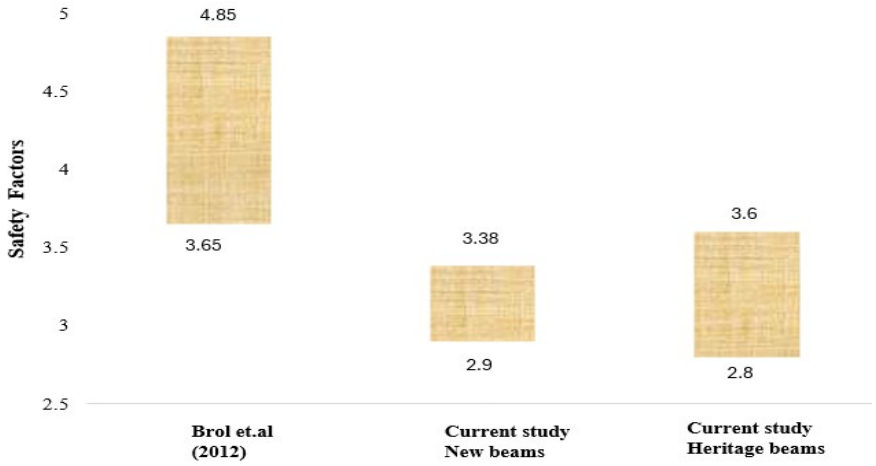

Fig. 4.6. Safety factor for Heritage and New beams, as well as from literature [19]

4.3.2 *Statistical Inference to Correlate Mechanical Performance of Heritage and New Beams*

Implementing the Null hypothesis on the established dataset statistically analyzes and compares the maximum load-carrying capacity and other relevant mechanical characteristics (such as MOE) of Heritage and New timber beams.

The Null hypothesis claims there is no statistically significant difference in the results of samples before and after treatment (a common terminology in the Null hypothesis). In the case of Heritage timber beams compared to their New counterparts, treatment is applied to unknown Heritage timbers to artificially remove cracks, defects, and other natural aging-related effects, thereby ensuring the validity of this statistical criterion hypothetically. By using the Null hypothesis, the test aims to determine whether observed differences between the Heritage and New beams in performance are statistically significant or merely due to random variation. The Heritage beams are compared with lower-strength, lower-quality timber species, such as SPF from grade II, which demonstrates Fb = 7.6 GPa (previously obtained in the SNC process). A one-tailed test will be performed, increasing the probability of observing more extreme numbers [114].

As there was no data available on the population (all Heritage beams in all patrimonial buildings), the t-test was selected over the standard and well-known method of Z-scores, followed

by analysis of variance (ANOVA). The t-testing, using the sample mean, allows for inferences to be drawn about the population mean.

The main steps involved in the Test are portrayed in Fig. 4.7.

The t-test requires adherence to sample values comprised of independent variables/observations, a condition that is satisfied in this study. Further, the population from which the sample is drawn should follow a normal distribution to satisfy the mathematical assumptions underlying the development of the t-statistics. However, violating this assumption tends to have minimal practical impact on the results derived from the t statistic, particularly when the sample size is relatively large. For very small samples, it is important that the population distribution is normal to ensure the validity of the test. With relatively large samples (n>30), the assumption of normality becomes less critical without compromising the integrity of the hypothesis-testing process; however, if suspected, the assumption of homogeneity of variance should be tested [114]. To verify homogeneity, ensuring the treatment is applied and a constant value is added equally to all individual samples, referring to Table 1: F-max = variance (largest)/variance (smallest)= 205322487 /100101105=2.05 which is smaller than the critical value of 2.34 (k=2, df=43, a=0.01). Therefore, the data do not provide evidence that the homogeneity of variance assumption has been violated [114].

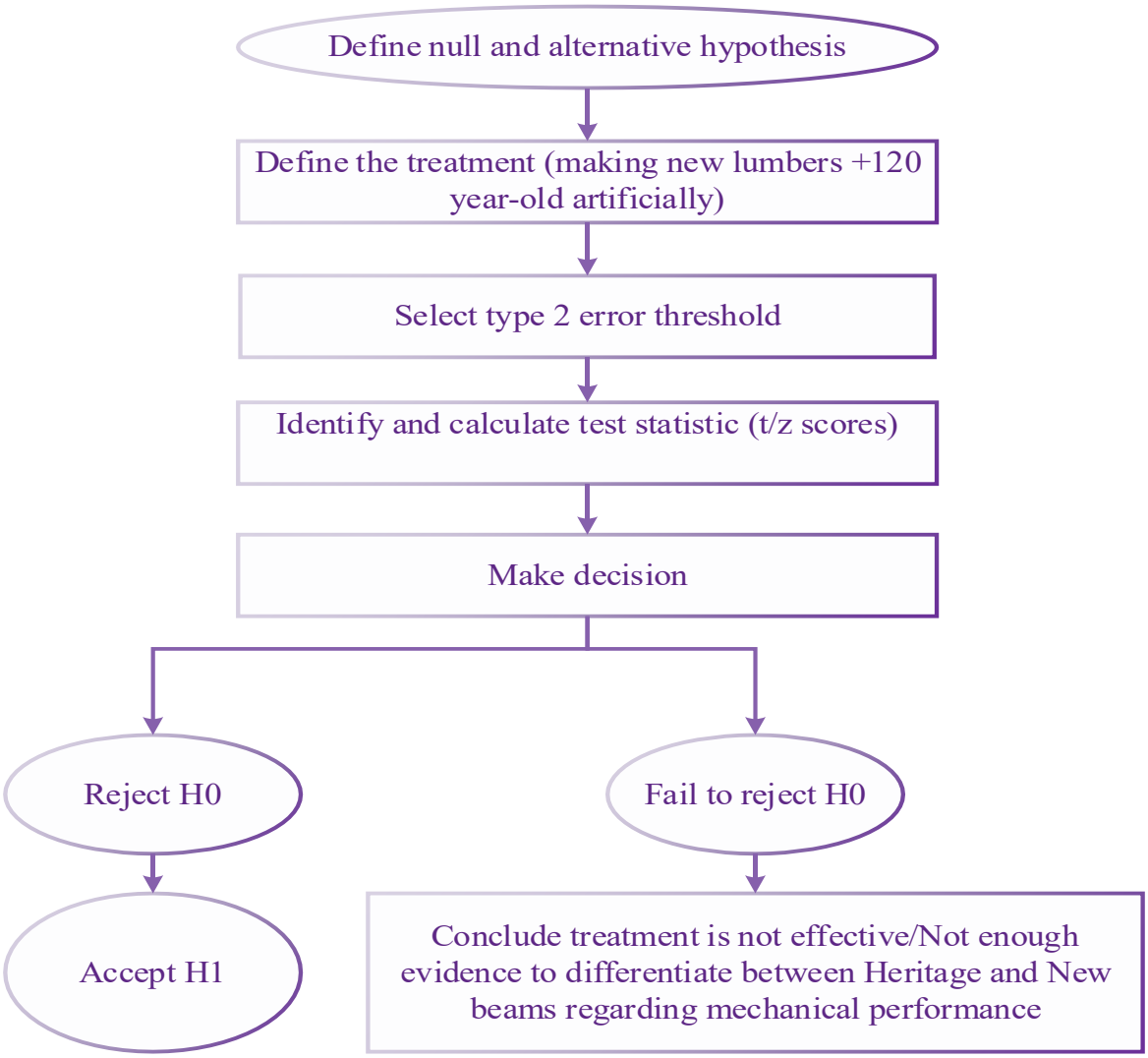

Fig. 4.7. Null hypothesis main conceptualization to address the problem

4.3.2.1 *Defining Null, Alternative, and Relevant Hypothesis Parameters*

Null Hypothesis (H0): There is no significant difference between the mechanical properties of Heritage and New counterpart timber beams.

Alternative Hypothesis (H1): There is a significant difference between the mechanical properties of Heritage and New counterpart timber beams.

The significance level (α\alphaα), as the next crucial step, is typically set at 0.05 to establish the threshold for statistical significance. If the p-values from the tests fall below this level, it indicates that the observed differences are statistically significant; It alerts researchers to the

probability of misinterpreting their research results [114]. With a degree of freedom (df) of 86 and a significance level set at 5%, a one-tailed test to enhance the safety margin was opted for aiding in the potential rejection of the Null hypothesis.

4.4 Results and Discussion

As per the discussion in the background, some researchers claim that the material and mechanical performance of old wood either does not decline or may decrease slightly over time. However, these claims and observations are based on test results and have not been substantiated using statistical tools on a large dataset, unlike the current study. This research verifies the claim of similar performance between Heritage and New SPF beams and proposes a method as an alternative to NDTs for conducting both destructive and NDTs on New timber, rather than its in-situ Heritage counterparts.

Fig. 4.8 a shows the comparison of MOE_{dyn} obtained from NDT and MOE from destructive tests, while Fig. 4.8-b demonstrates the ratio of the maximum load-carrying capacity of Heritage to New beams. Discrepancies are observed in the two MOEs of several beams, such that the MOE obtained from the destructive test is a true reflection of material behaviour, while the MOE_{dyn} does not consider age-related effects. Remarkably, for at least 10/44 beams, it can be observed that when there is a significant difference between two MOEs (Fig. 4.8a), the ratio of maximum load ($F_{max, Heritage}/F_{max, SPF}$) is close to or under 1, indicating that the performance of the two entities is nearly identical. The experimental findings (shown in Figure 4.8) strongly support the scientific outcomes of the Null hypothesis. Clearly, 34/44 beams show ($F_{max, Heritage}/F_{max, SPF}$) ratios of up to 2.5, suggesting that the Heritage beams, if not biologically deteriorated over time, exhibit considerably better structural and material performance compared to their SPF New counterpart beams.

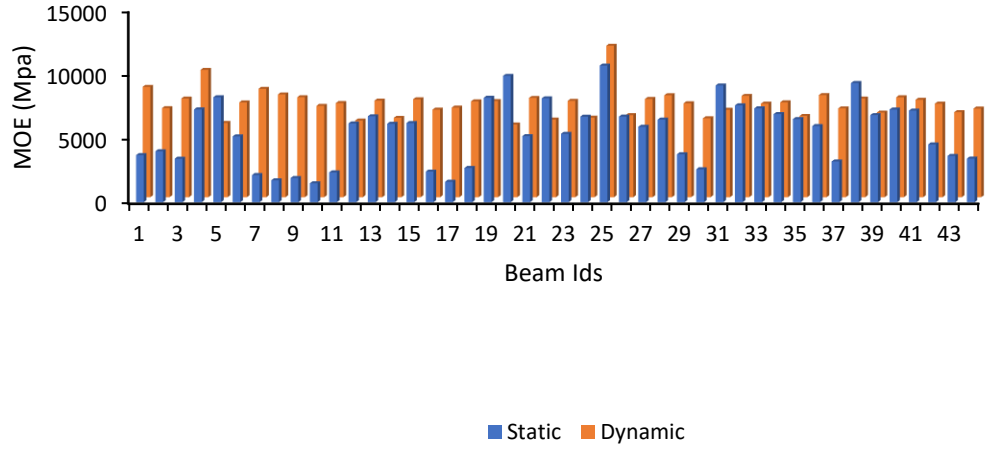

(a)

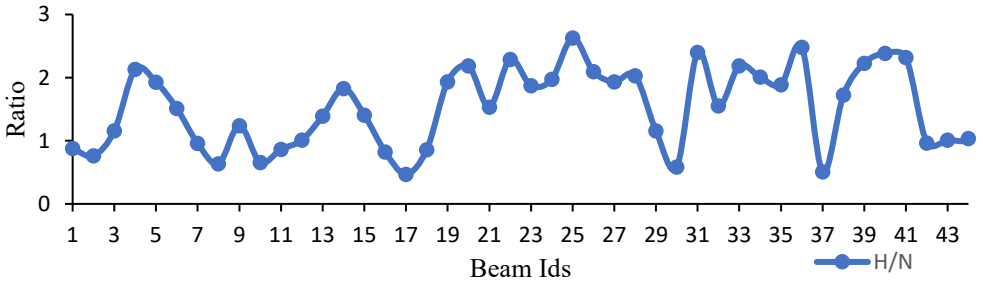

(b)

Fig. 4.8. An overview before Null results. a) comparison of MOE static and dynamic b) the ratio of F_{max}(H/N)

Considering the Null hypothesis, SPSS software was deployed to analyze the data of 88 New and Heritage beams (44N+44H=88). The data for Heritage beams are real and derived from experiments, whereas the data for New beams are simulated, while those of 6 (+7) are real. Table 4.1 presents the maximum, minimum, range, summation, mean, variance, and corresponding standard deviation, where H and N represent Heritage and New, respectively. Note that the standard deviation and variance are calculated based on n-1 for the samples; if the population is intended to be considered, these should be multiplied by the square root of (n-1)/n.

Table 4.1. Descriptive statistics for Heritage and New beams

	No.	Range	Minimum	Maximum	Sum	Mean		Std. Deviation	Variance
	Statistic	Statistic	Statistic	Statistic	Statistic	Statistic	Std. Error	Statistic	Statistic
Force H	44	50203.2	10397	60600	1103170.2	25072	1508.3	10005	100101105
Force N	44	44445.1	7902.8	52347.9	924658.6	21015	2160.2	14329	205322487

Frequency distribution describes the behaviour, overview, and distribution of the data, as presented in Fig. 4.9. As illustrated, most of the values for the maximum force in the Heritage beams are clustered around 20000 N, with the mean values of 25072 N. Table 4.3 provides the value of standard deviation as 10005 for the Heritage beams, whereas New beams show a value of 14329, indicating a stronger strength for the New beams, ultimately making the comparison between New and Heritage beams cumbersome, emphasizing the need to deploy a robust tool, such as the Null hypothesis.

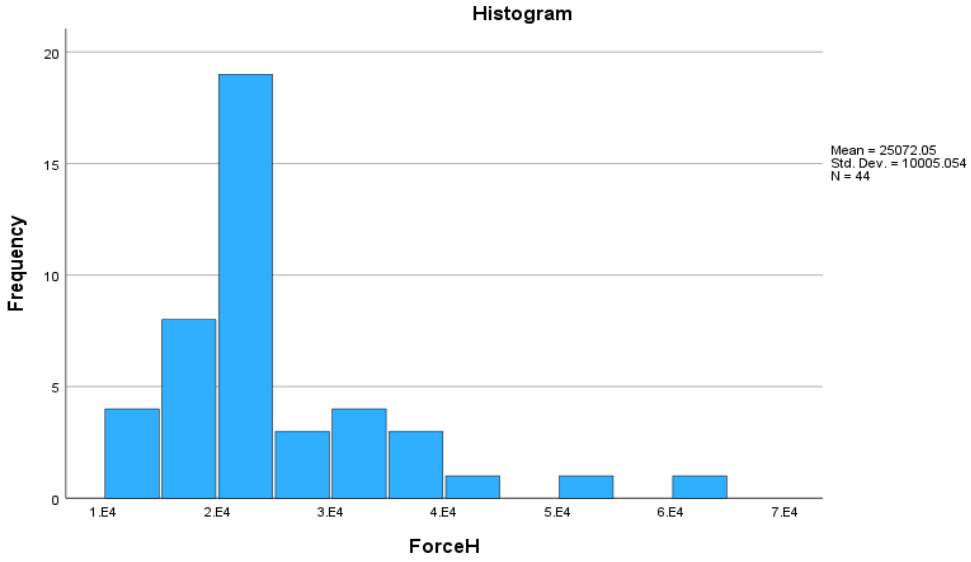

Fig. 4.9. Maximum force (kN)- frequency distribution for Heritage beams (tested)

From Table 4.2, a significant correlation is observed between Heritage and New beams at a significance level of 0.01 (2-tailed). With degrees of freedom (df) totalling 86, calculated as 43H + 43N, and an alpha level of 0.05, the critical t-values at the boundaries of the t-distribution are set at approximately t=2 (which is not conservative), chosen based on the degrees of freedom set at 60, opting for a conservative approach.

Table 4.2. Pearson correlation

Correlations			
		Force H	Force N
Force H*	Pearson Correlation	1	0.754**
	Sig.		<0.001
	N	44	44
Force N*	Pearson Correlation	0.754**	1
	Sig.	<0.001	
	N	44	44
** Correlation is significant at the 0.01 level. H*, N*: Heritage, and New respectively.			

Further, for a more conservative margin, a one-tailed test was then employed, which demonstrated a critical t-value of 1.671. The result, with a t-value of 1.54, falls short of this threshold. Thus, despite the proximity of degrees of freedom to 86, the choice of 60 (to be conservative) for the analysis led to an inability to reject the Null hypothesis, so simply failing to reject the Null hypothesis. The results of stacked (Heritage + New beams) are presented in Table 4.3.

The obtained t-value (t=1.54) is not in the critical region, indicating that the obtained sample mean difference is 1.54 times greater than expected if there is no difference between the two populations. This result shows that the Null hypothesis (H0) is true. Therefore, rejecting H0 failed to conclude that the treatment, aging artificially New beams (from real species in the period) to make them +150-year-old ones, is not working and there is not a significant difference between the reported scores in the Heritage and the scores in the New beams; t (86) = 1.67, p=1.57, 95% CI [-1180.5, 9294.6], one-tailed.

The validation of this ND approach to finding the mechanical performance of in-situ Heritage/old timber beams is a vital contribution. All non-deteriorated historical timber beams (+120-year-old) can be simulated by a New counterpart SPF timber (Fb= 7.6 GPa) beam. The results of staked statistics, including group statistics, independent t-statistics and the effect size, are provided in Tables 4.3, 4.4, and 4.5, respectively.

Table 4.3. Results showing the group statistics

Group statistics					
Var.		No.	Mean	Std. deviation	Std. error mean
Stacked	H	44	25072.1	10005	1508.3
	N	44	21015	14329.1	2160.2

Table 4.4. Results showing independent t-statistic

Independent samples test								
Stacked	Levene's test for equality of variances		t-test for equality of means					
	F	Significance	t	df	Significance 1- sided P / 2-ided P	Mean difference	Standard error difference	95% confidence intervals Lower / upper
Equal variances assumed	15.747	<0.001	1.54	86.0	0.064 / 0.127	4057.1	2634.7	-1180.5 / 9294.6
Not assumed			1.54	76.9	0.064 / 0.128	4057.1	2634.7	-1189.5 / 9303.5

Table 4.5. Results showing effect size

Independent sample effect sizes					
				95% confidence interval	
		Standardizer[1]	Point estimate	Lower	upper
Stacked	Cohen's d	12357.66	.328	-.093	.748
	Hedges' correction	12466.7	.325	-.093	.742
	Glass's delta	14329.1	.283	-.141	.704

1. Cohen's d uses the pooled standard deviation.
Hedges' d uses the pooled standard deviation, plus a correction factor.
Glass's delta uses the sample standard deviation of the control group.

4.5 Conclusion

Through the application of Null hypothesis testing, this study aimed to provide valuable insights into the mechanical performance of unknown Heritage timber beams (mixed in

population) compared to their New counterparts. The results of this research contribute to the overall understanding of the mechanical performance of Heritage timber beams by performing required destructive tests on their New counterpart beams, influencing the practices associated with their preservation, restoration, maintenance, and research purposes. Based on the yielded test results, the Null hypothesis failed to be rejected, demonstrating there are no significant differences between the mechanical performance of Heritage and New SPF beams.

Key findings of this study are as follows:

- This study employed a statistical inference method (t (86) = 1.67, p=1.57, one-tailed), followed by MOEs studies, to scientifically demonstrate that old/Heritage timber beams exhibit superior mechanical performance over time, making them suitable for reuse and supporting sustainability.
- If +120-year-old Heritage/old timber beams are not biologically deteriorated, their mechanical performance can be studied by conducting destructive tests on their New SPF (Fb=7.6 GPa) counterpart timber beams.
- If in-situ Heritage or old beams show up to moderate age-related degradations, MOE_{dyn} from NDTs accurately represents the MOE, required to find MOR.
- If in-situ Heritage/old beams are not deteriorated and also have a few age-affected signs, their mechanical performance can reach up to 2.5 times that of their New SPF counterpart.
- A safety factor ($F_{max.}/F_{exp.}$) of 2.9-3.38 shows this study is stronger than failing to reject the Null hypothesis, making the methodology reliable.

The following result flow chart presented in Fig. 4.10, highlights the importance of the study.

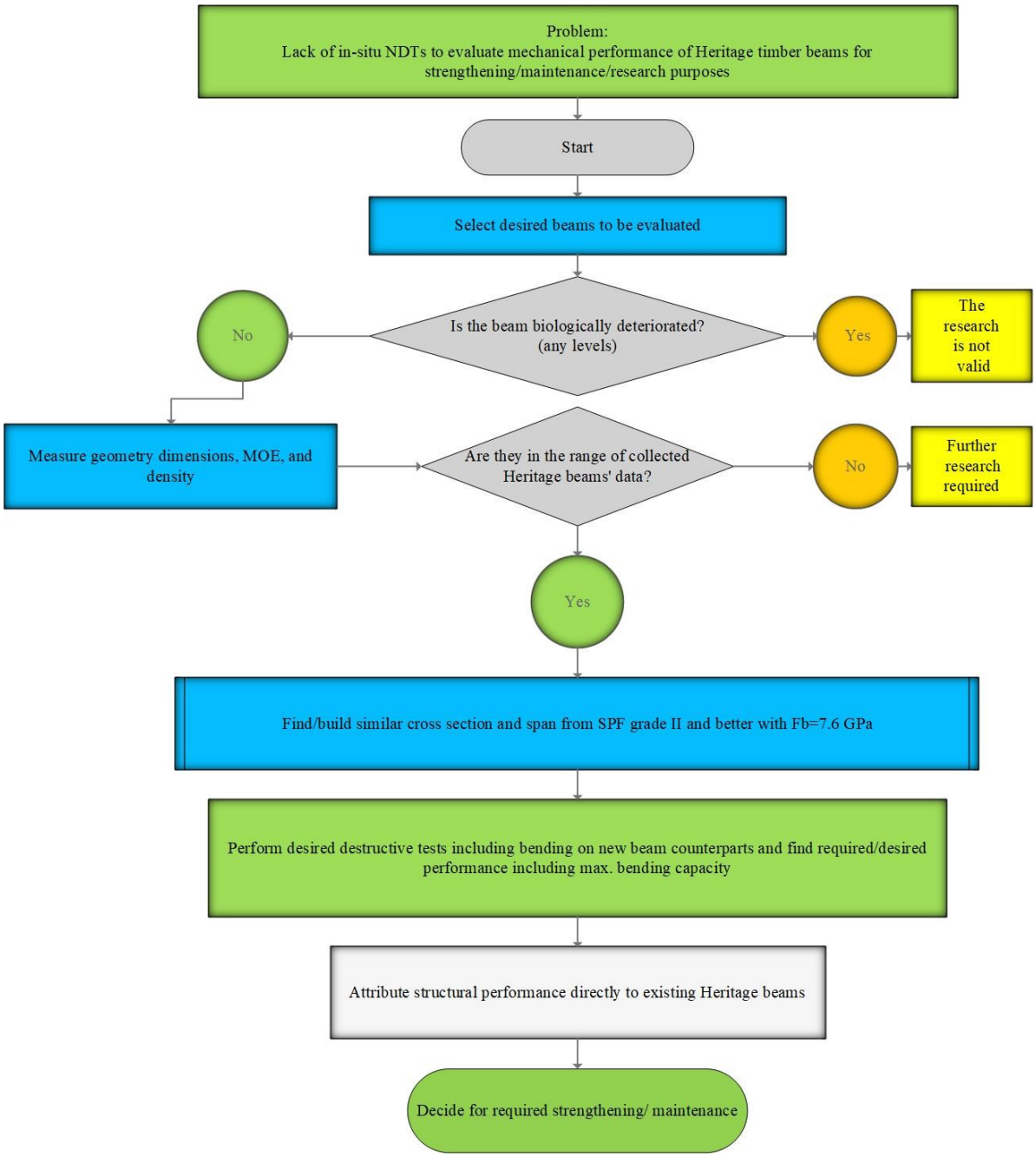

Fig. 4.10. Flow chart demonstrating the importance of current research

Acknowledgments:

This study received no support from the public, commercial, or not-for-profit funding agencies.

Conflicts of Interest:

The authors declare that they have no conflicting interests concerning the publication of this article.

CHAPTER 5

Strengthening-Phase II: Strengthening of Heritage Timber Beams Using NSM-FRP

General

Chapter 5 covers the Phase II (Strengthening) of the thesis by experimentally evaluating NSM-GFRP retrofits on full-scale (~150-year-old) Heritage timber beams, considering both undamaged and fire-affected members. The strengthening program varies the rebar number, position (tension/compression), and development length (50–100%). It employs four-point monotonic bending with strain gauges and deflection measurements in the middle of the span to quantify capacity gain, stiffness response, neutral-axis shifts, and failure-mode transitions. The results demonstrate that full-length tensile reinforcement yields the most significant improvements in flexural capacity, while intermediate/short bond lengths are governed by bond and anchorage effects at the end of rebars. Compression-side reinforcement influences stability (tortional buckling) and stress redistribution but must be detailed to prevent debonding and splitting. Finally, the chapter translates these findings into allowable-strengthening guidance for Heritage applications by adapting ACI 440.2R concepts to timber and explicitly addressing sudden FRP loss scenarios, thereby providing practical, minimally invasive retrofit recommendations for conservation engineers.

Additional pictures pertinent to Chapter 5 are included in Appendix C.

Status: Preparation (drafts)

Retrofitting Heritage Timber Beams Employing NSM-GFRP: Influence of Rebar Configuration and Length

Reza Abbasi Malekabadi [1], Bara Alseid[2], Ghazanfarah Hafeez [3, *]

[1] Department of Building, Civil and Environmental Engineering, Concordia University, Montréal, Canada, H3G1M8
reza.abbasimalekabadi@mail.concordia.ca

[2] Department of Building, Civil and Environmental Engineering, Concordia University, Montréal, Canada, H3G1M8
bara.alseid@mail.concordia.ca

[3] Department of Building, Civil and Environmental Engineering, Concordia University, Montréal, Canada, H3G1M8
*Correspondence: ghazanfarah.hafeez@concordia.ca ; Tel.: +15148482424; ext.: 8703

Abstract

Heritage buildings are old, yet culturally valued structures. These century-old buildings necessitate structural assessment, maintenance, and strengthening to improve their structural Performance and preserve their cultural value. This study experimentally investigates the flexural Performance of full-scale, 150-year-old Heritage timber beams strengthened with Glass Fibre Reinforced Polymer (GFRP) bars using the Near-Surface Mounted (NSM) technique, which keeps their cultural value with minimum disruption. A total of 18 Heritage timber beams, both intact and fire-affected, were reinforced in 6 different configurations varying in rebar number, length, and location and then tested under a four-point displacement-controlled monotonic bending test. Results demonstrated an increase in flexural capacity ranging from 30% to over 140% with 100% development length (full-length) tensile reinforcement as the most significant enhancement. Fire-affected beams also benefited significantly, although to a lesser extent than intact specimens. Key observations include shifts in the neutral axis, improved load distribution, and altered failure modes, transitioning from brittle tensile rupture to shear-flexural or de-bonding mechanisms, all demonstrating the effectiveness of the technique. Further, the study establishes the maximum allowable strengthening threshold for Heritage timber beams by modifying the ACI-440.2R-wise recommendation to account for potential de-bonding or sudden FRP loss. The findings provide evidence-based guidance for conservation engineers,

highlighting the viability of NSM-GFRP retrofitting as a sustainable and minimally destructive solution for extending the service life of historic timber structures.

Key words: Capacity Gain; Failure Modes; Bond-Slip; Allowable Strengthening; Intact Beam; Charred

5.1 Introduction

Heritage timber buildings are valuable architectural and cultural structures. They have demonstrated accepted longevity and Performance over years of use; however, their Performance can degrade over time due to mechanical fatigue, decay, weathering, moisture fluctuation, and splitting, necessitating performance assessment and strengthening if required. The use of Fibre Reinforced Polymers (FRP) for strengthening timber beams has gained significant attention in recent years due to its potential to enhance the structural Performance of existing timber elements. FRP materials, including Basalt (BFRP), Glass (GFRP), and Carbon (CFRP), provide a lightweight, high-strength solution that can be effectively bonded to timber beams using epoxy adhesives or resins [47,115]. Research has demonstrated that incorporating FRP into timber beams significantly improves their flexural capacity and ductility. For instance, experimental studies have shown that solid and glulam beams reinforced with BFRP and CFRP exhibited enhanced flexural Performance (up to 100%), with improvements in both strength and ductility compared to unreinforced beams [40,42,46,110,116–118]. Strengthening using FRP materials via Near Surface Mounted (NSM) techniques has shown promise in timber applications [119]. In the NSM method, grooves are cut longitudinally in the structural timber element. Then FRPs in the form of rebar or plate are inserted into the grooves already filled with adhesive [10,45]. This method proves particularly useful for Heritage timber beams, as embedded and integrated rebars enhance their structural Performance while addressing sustainability and preservation, with minimal impact on their appearance and preservation of their cultural value.

Research on optimizing the configuration of rebars, including the number, location, and length for Heritage timber beams, remains limited. This study investigates the mechanical Performance of full-scale Heritage beams strengthened with GFRP bars, employing the NSM method, to examine the effect of varying rebar configurations (including ratio) and lengths.

Practically, it will bridge the gap by enhancing guidance for preserving Historic timber structures, addressing the maximum allowable strengthening. The effect of fire on the bending capacity and potential strength regaining is also taken into account.

5.2 Background

Flexural strengthening deploying FRP rods has been explored for the last two decades as a method of strengthening reinforced concrete structures. This method has also recently entered the field of timber construction, including natural and engineered wood products. Experimental investigations for reinforcing solid timber and glulam beams with FRP demonstrated that a small percentage (1.5-2.5%) can enhance the bending capacity up to 90% to 100% respectively [40].

Researchers typically use GFRP to reinforce solid timber beams in various configurations of lengths and locations parallel to the grain [2][34]. It has been identified that the precise location of reinforcement is a crucial factor in creating an effective reinforcement solution. As such, precisely identifying the regions that require reinforcement assures the efficiency and effectiveness of the intervention [2].

NSM-FRP techniques, which involve inserting bars into grooves, have been successfully used to enhance the stiffness and strength of timber [120,121]. This is particularly beneficial for Heritage structures, where maintaining the original aesthetics while enhancing structural Performance is essential. In the NSM process, grooves are cut into the beam that needs strengthening, and then FRP rods are bonded in the grooves using a high-strength epoxy adhesive [122]. The research findings demonstrated that adopting NSM-GFRP bars successfully mitigates the effects of local damage in the timber while significantly enhancing the bending strength of the members, resulting in an enhancement of 18% to 46% [34]. Several investigations have been conducted on the usage of NSM rods as a reinforcing and repair material.

Johnsson et al. (2006) investigated the impact of placing two NSM carbon fibre pultruded rods on the underside of a glulam beam, reaching a reinforcement ratio of around 1.0%. This reinforcement resulted in three benefits: a 44-63% increase in flexural strength, a 10% increase in

stiffness, and a change in failure mode from tensile (brittle) to compressive (ductile in nature) [29]. This increase in flexural capacity, with a reinforcement ratio of approximately 1.0%, was confirmed by Fossetti et al., who achieved a 25% increase [46]. The slightly lower values were the result of failure in the epoxy bond, demonstrating the importance of proper installation. Other researchers investigated BFRP rods as a reinforcing and repair material. Two experiments were completed: the first involved reinforcing a standard glulam beam with two BFRP rods (reinforcement ratio of 1.4%), and the second involved repairing an artificially cracked beam with the same BFRP. The first trial resulted in a 23% improvement in ultimate moment capability. The second experiment showed that FRP rods can be effectively utilized as a repair material to bridge damaged parts of wooden beams [123].

Yeboah and Gkantou used 8mm BFRP (for availability and low price) and GFRP (for being less brittle among other FRPs) bars and epoxy adhesive to strengthen timber beams [10]. Reinforcement ratios of 0.27% to 0.82% have been shown to boost strength by 18% and 46%, respectively [10,34]. Strengthening with BFRP bars yielded a higher capacity (maximum increase of 60%) in comparison with unreinforced solutions [124]. Using CFRP bars has shown that the strength and stiffness of reinforced timber beams increased by 47% and 28% for ρ=0.22% and by 29% and 22% for ρ=0.11%, respectively [44].

Yeboah and Gkantou (2021), in one of their configurations (D1), used two rebars in tension face (reinforcement percentage ρ equal to 0.67%). In the second configuration (D2), an extra bar (reinforcement percentage ρ equal to 1.0%) was added to the compression face [10]. It was claimed to improve strength when 25% and 75% of reinforcement was at the top and bottom of the cross-section, respectively [10,125]. In contrast, it was found that inserting FRP reinforcement at the bottom (consisting of two bars) and top (with one FRP bar) of the beams did not significantly increase the capacity of the NSM beams compared to those with only two FRP reinforcements at the bottom [10].

Bond characteristics and mechanical Performance are sensitive to bar length, placement, and material, but these have not been systematically evaluated for Heritage timber beams strengthened with NSM-GFRP.

5.2.1 *Grooving, Adhesive Application, and Bonding Behaviour*

Embedding FRP rebars in the timber beams requires grooving and the use of a bonding agent. The bonding of FRP to timber is critical to the efficiency of reinforcement. Various bonding approaches, including the use of epoxy resins, have been researched to strengthen the adhesion between FRP and timber, therefore minimizing concerns such as de-bonding during loading [126,127]. The most important structural properties of the adhesive(groove filler) are the ability to transfer shear and tensile strength [10]; hence, the 2-part epoxy is the most applicable in the NSM method [10,34]. They consist of two components: a resin base and a hardener part, also known as a curing agent [50]. Due to overhead application, high modulus, and moisture-tolerant properties, Sikadure 31 is used and addressed in other research [10,48,49].

Grooves and their shape have an impact on the shear load transfer between the bar and the substrate. Grooves, preferred to be circular, demonstrated higher stiffness and load-carrying capacity compared to square grooves [10,48].

Surface-bonded FRP to timber also benefits from good bond behaviour, which is mainly governed by the timber properties rather than adhesives [128]. This latter claim demonstrates the quality of wood in transferring loads, as observed in experimental tests.

Corradi et. al [47], who conducted direct pull-out tests with glued-in composite bars, revealed the influence of bonded length on ultimate capacity. According to their findings, pull-out capacity increased with bond length up to 250 mm. Specimens with shorter bond lengths (150 mm and 200 mm) failed by bar pull-out, while longer bond lengths (250 mm and 300 mm) primarily failed by bar tensile rupture.

5.3 Research significance

Preserving Heritage timber structures may require strengthening solutions to enhance structural Performance. Although various retrofitting techniques exist, a critical shortage of experimental

data specifically addressing Heritage timber beams remains. This study addresses the gap through full-scale experimental testing of Heritage beams strengthened with NSM-GFRP rods, with comparisons to unstrengthened, focusing on the influence of reinforcement configuration, ratio, and length.

The findings provide practical insights into the reliability and effectiveness of reinforcing methodology for Heritage applications, demonstrating its potential to delay failure and improve load distribution. Importantly, this work is the first to define the maximum allowable strengthening level for Heritage timber retrofitting, establishing essential parameters for a safe, sustained, and reversible method.

Beyond technical validation, the research supports the development of performance-based guidelines for the conservation of Heritage timber structures. The results provide evidence-based recommendations to help engineers and conservation specialists select reinforcement strategies that ensure structural safety while preserving historical and cultural values.

5.4 Experimental

The experimental investigation involved reinforced Heritage timber specimens, categorized according to their reinforcement scheme and damage condition. The tested beams are designated with a coding system, where "H" indicates Heritage, "UN" specifies an Undamaged state, and "FD" indicates Fire-Damaged condition. Beams designated "H-UN" serve as control samples representing Heritage timber beams without fire damage, whereas "H-FD" indicates specimens with prior exposure to fire, highlighting the effects of fire-induced damage on structural Performance. Visually, the fire-affected beams were roughly 1mm charred on each side.

The MST-BAR® Grade III GFRP rebars were specifically selected for the purpose of strengthening due to their superior mechanical characteristics, summarized in Table 5.1.

Table 5.1. Mechanical properties of MST-BAR® grade III GFRP reinforcement

Property	Value
Tensile Strength	>1000 MPa
Young’s Modulus (Straight Portion)	>60 GPa

Ultimate strain, ε	>1.7%
Transverse Shear Strength, τ	>220 MPa
Bond Strength to Concrete	≥20 MPa
Glass Transition Temperature (Tg)	125°C

The size(M10) and mechanical properties of FRP are according to ASTM(D7957/D7957M – 17), with an actual diameter of 9.5 mm, the property of which is presented in Table 5.2 [129].

Table 5.2. Mechanical properties of FRP bars

Bar No.	Nominal Dimensions		Measured Cross-Sectional Area Limits mm^2 [$in.^2$]		Minimum Guaranteed Tensile Force kN [kip]
	Diameter mm [in.]	Cross-Sectional Area mm^2 [$in.^2$]	Minimum	Maximum	
M6 [2]	6.3 [0.250]	32 [0.049]	30 [0.046]	55 [0.085]	27 [6.1]
M10 [3]	9.5 [0.375]	71 [0.11]	67 [0.104]	104 [0.161]	59 [13.2]
M13 [4]	12.7 [0.500]	129 [0.20]	119 [0.185]	169 [0.263]	96 [21.6]
M16 [5]	15.9 [0.625]	199 [0.31]	186 [0.288]	251 [0.388]	130 [29.1]
M19 [6]	19.1 [0.750]	284 [0.44]	268 [0.415]	347 [0.539]	182 [40.9]
M22 [7]	22.2 [0.875]	387 [0.60]	365 [0.565]	460 [0.713]	241 [54.1]
M25 [8]	25.4 [1.000]	510 [0.79]	476 [0.738]	589 [0.913]	297 [66.8]
M29 [9]	28.7 [1.128]	645 [1.00]	603 [0.934]	733 [1.137]	365 [82.0]
M32 [10]	32.3 [1.270]	819 [1.27]	744 [1.154]	894 [1.385]	437 [98.2]

The adhesive used for embedding the reinforcement into the timber specimens was Sikadur®-31 [130], CF Normal, a moisture-tolerant, thixotropic, two-component structural adhesive epoxy suitable for bonding wood and other construction materials. It is non-sag in vertical and overhead applications and hardens without shrinkage, making it appropriate for groove-bonded bars in timber. According to the product data sheet, the mixed density at 23 °C is 1.90 ± 0.10

kg/L, and the specified mixing ratio is 2:1 (Component A: Component B) by either weight or volume.

5.4.1 *Material and NSM timber preparation*

The experimental testing campaign followed a structured procedure comprising specimen preparation, reinforcement embedding, and mechanical testing, as illustrated in Fig. 5.1 Heritage timber beams were carefully selected to reflect the actual structural conditions, with some exhibiting signs of fire-induced damage, such as surface charring and superficial cracks. Before reinforcement, the beams were thoroughly cleaned to remove debris, dust, and loose fibres, ensuring a clean surface for adequate bonding. Circular grooves matching the dimensions of the reinforcement bars were precisely milled along the beam lengths, with a minimum diameter of 3mm greater than the FRP bars. Reinforcement configurations varied across specimens, with GFRP bars placed on either the tension or compression side to evaluate performance differences. They were bonded using epoxy resin. Care was taken to ensure full resin coverage and impregnation, minimizing the risk of de-bonding. Three replications of each beam configuration were made. Previous studies have employed 3-5 replicates [10,29–31]. After inserting FRP bars, the beam was left for 14 days for curing before testing. Loading displacement control, quasi-static. Other studies applied monotonic loading at a constant rate of 3 mm/min up to failure [10,131].

(a) (b) (c)

(d)

Fig. 5.1. a: Specimen groups, b: Grooving of the test specimens, c: placement of the reinforcements, d: application of the epoxy

5.4.2 *Test setup*

The comprehensive details of each group's configurations are illustrated in Fig. 5.2 and summarized in Table 5.3. Specimens were systematically varied in terms of the number of reinforcements, length, and position within the cross-section. The tensile zone of the beams was reinforced with either one or two FRP bars, the reinforcement percentage(ρ) of which is 0.0051 and 0.01, respectively. To evaluate the effect of compression rebar in various configurations, an additional bar was added at the top, with a reinforcement percentage (ρ) of 0.51%. These numbers are also used to facilitate comparison with the literature. Note that before increasing the cross-sectional area of the reinforcement, additional considerations such as the distance between neighbouring grooves and edge distances of the timber beams should be addressed [10,119].

The specimens had a span of 2.00 metres and were loaded with a hydraulic jack with a capacity of 300 kN. In a 4-point bending test, the goal is typically to ensure that the bending moment, rather than shear, dominates the behaviour of the beam. To achieve this, the American Society for Testing and Materials (ASTM) provides guidelines for procedures. Up to the failure, the loading type is displacement control, quasi-static monotonic loading applied at a constant rate, close to 3 mm/min, as recommended [131].

Group A consisted of two rebars, each with a 1000 mm length (50% of the specimen length), placed symmetrically on the bottom (tension side) to assess the impact of limited-length tension

reinforcement. Group B also utilized two rebars placed at the bottom tension side, each with a length of 1,500 mm (75%), intended to evaluate the effects of intermediate-length reinforcement. Group C specimens were reinforced with two full-length (2000 mm) rebars positioned at the bottom side, investigating maximum tensile reinforcement potential. Group D explored structural responses with reduced reinforcement ratio, utilizing a single full-length rebar (2000 mm) positioned centrally at the bottom. Group E included two rebars spanning the entire specimen length (2000 mm), placed at both the top and bottom positions, facilitating an analysis of the combined effectiveness of tension and compression reinforcement. Group F, distinctively, had two rebars placed in the tension zone and one rebar placed in the compression zone, each 1,500 mm (75% of the length), to evaluate the influence of compression-zone reinforcement. The carefully designed reinforcement configurations enabled the study to thoroughly investigate optimal GFRP reinforcement strategies, striking a balance between structural enhancements and heritage conservation.

Table 5.3. Specimen details and reinforcement configuration

Group	ID	Number of Rebars	Length of Rebar (mm)	Diameter of Rebar (mm)
Reference Group	H-UN-1	-	-	-
	H-UN-2	-	-	-
	H-FD	-	-	-
Group A	H-UN-A1	2	1000	9.5
	H-UN-A2	2	1000	9.5
	H-FD-A	2	1000	9.5
Group B	H-UN-B1	2	1500	9.5
	H-UN-B2	2	1500	9.5
	H-FD-B	2	1500	9.5
Group C	H-UN-C1	2	2000	9.5
	H-UN-C2	2	2000	9.5
	H-FD-C	2	2000	9.5

Group D	H-UN-D1	1	2000	9.5
	H-UN-D2	1	2000	9.5
	H-FD-D	1	2000	9.5
Group E	H-UN-E	2	2000	9.5
	H-FD-E	2	2000	9.5
Group F	H-FD-F	2	1500	9.5

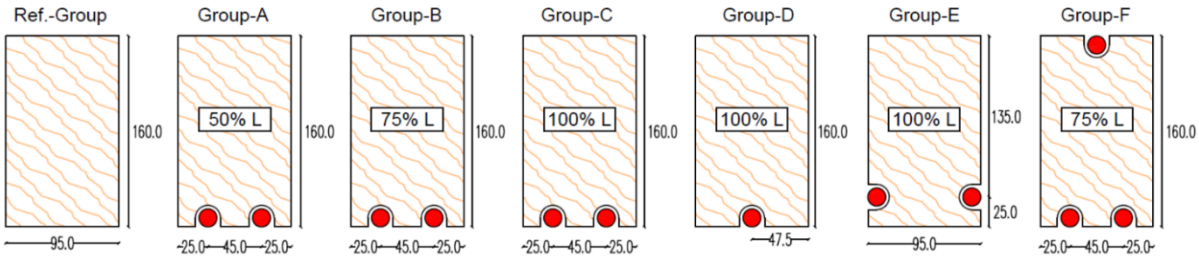

(a)

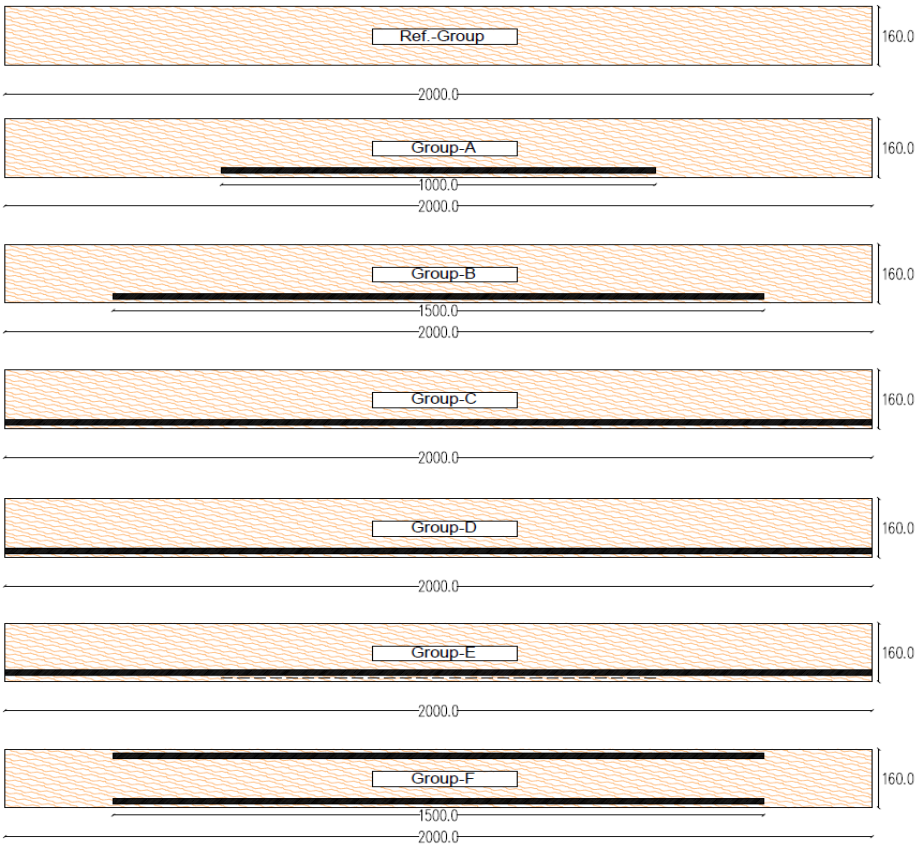

(b)

Fig 5.2. a: Cross-sectional reinforcement placement illustrating rebar position within specimen groups, b: Longitudinal reinforcement layouts demonstrating varying lengths and positions of GFRP reinforcement within each specimen group

For mechanical testing, a standardized four-point bending [106] The setup was used, with roller supports set at a 2000 mm span and a centrally applied load delivered through a hydraulic actuator, as shown in Fig. 5.3. A quasi-static monotonic load was used at a constant rate, close to 3 mm/min, as recommended [131] to allow controlled progression toward failure. Strain gauges were installed at mid-span and along the beam depth to capture strain profiles and detect shifts in the neutral axis. Potentiometers positioned at mid-span recorded vertical deflections. Throughout testing, data were recorded continuously, capturing load, strain, and displacement until failure. This systematic approach ensured accurate, repeatable results to evaluate the flexural Performance and reinforcement effectiveness in heritage timber beams.

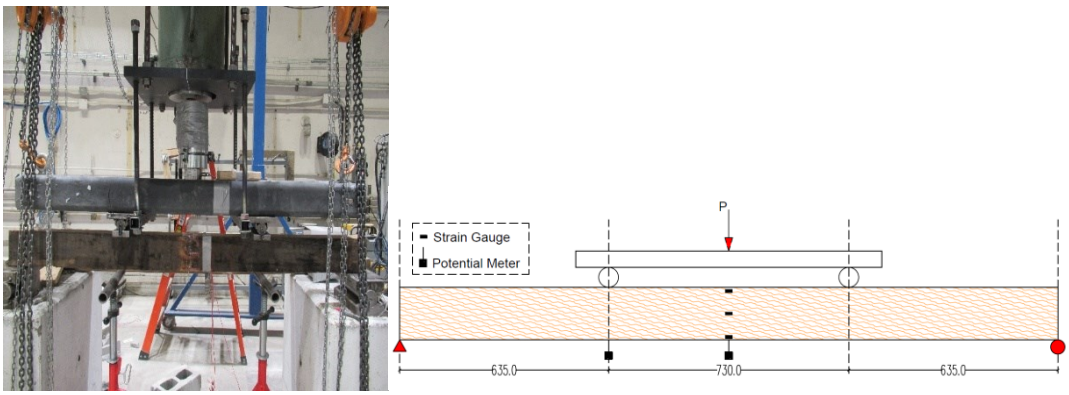

Fig. 5.3. Four-point test setup

5.5 Results and discussion

5.5.1 *Load Deflection Curve and Strengthening Performance (among configurations)*

The experimental results shown in Fig. 5.4 provide substantial insight into the effectiveness of various GFRP reinforcement configurations in Heritage timber beams, particularly when comparing undamaged specimens with those that have been fire-damaged. The reference group provided baseline ultimate loads and deflection values for both intact and fire-damaged conditions. Specifically, the undamaged reference specimens (H-UN-1 and H-UN-2) exhibited ultimate load capacities of 22.62 kN and 26.32 kN, respectively, with maximum deflections of 13.94 mm and 16.03 mm. The fire-damaged control specimen (H-FD) exhibited an ultimate

load of 24.63 kN with a deflection of 15.22 mm. This indicates that the fire-damaged specimens retained substantial load capacity but displayed slightly altered deflection characteristics due to structural deterioration from fire exposure.

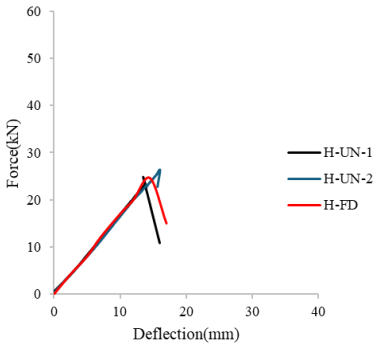

(a)

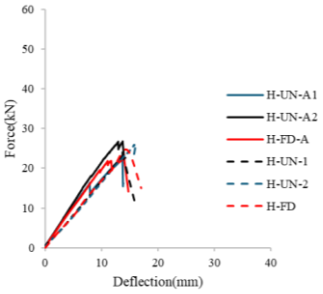

(b)

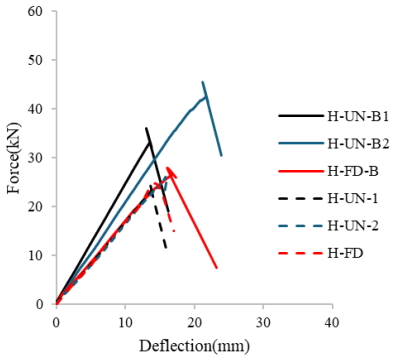

(c)

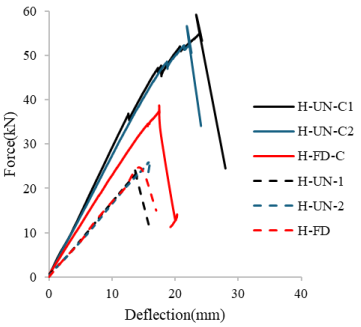

(d)

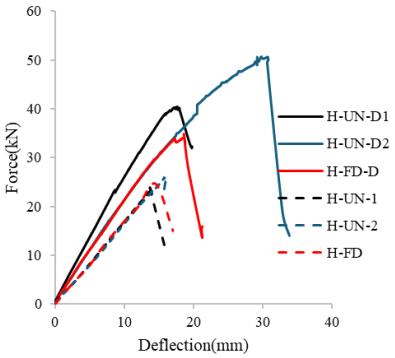

(e)

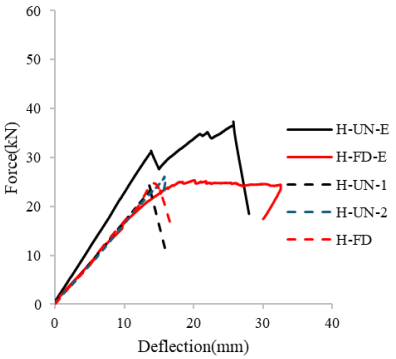

(f)

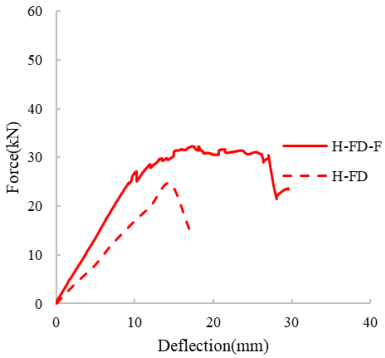

(g)

Fig. 5.4. Comparison of the load-deflection results, a: Reference Group, b: Group A, c: Group B, d: Group C, e: Group D, f: Group E, g: Group F

The Limited-length (50%) GFRP reinforcement in group A resulted in minimal improvements in ultimate load capacities, approximately 1.45% and 1.44% for undamaged specimens H-UD-A1 and H-UD-A2, respectively. The reason behind these results can be attributed to the short bonded/development length, which concentrates stress transfer near the bar ends, producing high interfacial shear and bearing stresses that approach or exceed the parallel-to-grain capacity of the wood and trigger local splitting before the reinforcement can be fully mobilized, where the fire-damaged specimen H-FD-A displayed a slightly higher ultimate load improvement (9.74%). This relatively greater improvement in fire-damaged timber can be attributed to the GFRP reinforcement providing supplementary tensile capacity, thereby partially compensating for internal defects introduced by fire damage. Intermediate-length reinforcement, as obtained for group B, significantly improved the structural capacity of undamaged specimens (H-UD-B1 and H-UD-B2), demonstrating substantial increases of 45.88% and 57.10%, respectively. The notable deflection increase observed for specimen H-UD-B2 (21.95 mm compared to the reference) should, however, not be interpreted as improved material ductility, as GFRP is inherently brittle and non-ductile. Instead, this increase in deflection is primarily attributed to the enhanced load-carrying capacity and a modified failure mode, where reinforcement delays sudden brittle failures, allowing the timber fibres to undergo greater deformation before ultimate rupture occurs. The fire-damaged specimen (H-FD-B) showed only modest improvement (5.27%), indicating the limited effectiveness of intermediate reinforcement lengths in mitigating fire-related brittleness and internal damage. Full-length reinforcement (Group C) yielded the most significant enhancement in ultimate load capacity among bottom-reinforced specimens. For undamaged specimens (H-UD-C1 and H-UD-C2), ultimate capacities increased by 141.29% and 97.26%, respectively. The longer development length distributes bond stresses more uniformly along the groove, keeps the average interfacial shear below the wood's capacity, and allows the CFRP to reach a higher effective strain before timber failure or debonding

initiates, thereby reducing stress concentrations and postponing brittle failure. However, the minimum length is proposed to be ten times the rebar diameter. This marked improvement is primarily attributed to the continuous distribution of tensile reinforcement, which reduced stress concentrations and delayed the onset of brittle failure in the timber. The fire-damaged specimen (H-FD-C) also showed a 50.30% increase in load capacity, indicating the restorative potential of full-length reinforcement even under compromised material conditions.

In Group D, the introduction of a single, centrally positioned full-length rebar significantly improved ultimate load capacities (76.83% and 92.32% increases for H-UD-D1 and H-UD-D2, respectively). The substantial deflection of specimen H-UD-D2 (30.79 mm) does not reflect an increase in material ductility but rather results from delayed timber failure mechanisms due to improved tensile strength provided by the GFRP bar. Such a configuration effectively redistributes stresses, allowing greater elastic deformation and delayed failure, rather than improving inherent ductility. The fire-damaged specimen (H-FD-D) exhibited a substantial yet lower enhancement (38.16%), indicating that reinforcement provides beneficial yet comparatively limited improvements for compromised structural conditions. Group E explored reinforcement in both tension (bottom) and compression (top) zones, achieving considerable increases in ultimate load capacity (62.46%) and flexural enhancement (85.07%) for undamaged specimen H-UD-E. The fire-damaged specimen H-FD-E exhibited negligible ultimate load improvement (1.29%) but demonstrated significant flexural enhancement (113.79%); however, the observed increases in maximum deflection demand require critical evaluation. GFRP is a brittle, high-stiffness material with a linear-elastic behaviour up to failure, and it does not inherently enhance ductility. Therefore, attributing high deflection capacity solely to the presence of GFRP is misleading. The enhanced deflection likely arises from the preservation of timber ductility due to delayed rupture and more distributed cracking, rather than any intrinsic ductility of GFRP itself. In fact, in the absence of early rupture, the timber substrate can undergo a more extended deformation Phase before failure, resulting in higher global deflections. Moreover, full-length reinforcement may have shifted the neutral axis and changed the failure mode from brittle tensile rupture to more gradual crushing or localized delamination, thus indirectly

increasing deformation capacity. Lastly, compression-zone reinforcement (Group F) provided a meaningful improvement for fire-damaged specimen H-FD-F, showing a 30.53% increase in ultimate load capacity and 77.46% improvement in flexural behaviour. The reinforcement in the compression zone enhances overall stability and stiffness, indirectly enabling higher load capacities and extended elastic deformation. Again, this observed behaviour is not due to the improved material ductility of the reinforcement itself, but instead to altered stress distribution and a delayed onset of failure within the timber.

5.5.2 *Strain distribution*

In addition to load-deflection data, experimental strain data were obtained from the tested specimens, as shown in Fig. 5.5. However, reliable strain measurements were obtained only from two specimens, specifically H-UN-1 (unreinforced control) and H-UN-D1 (single, centrally positioned full-length GFRP reinforcement). For several other specimens, unreliable strain signals are attributable to the combined effects of Heritage-timber heterogeneity and environmental sensitivity, such as wood anisotropy, surface coatings, and hygrothermal fluctuations, which produce spatially and temporally non-uniform strains that complicate gauge measurements unless careful consideration is given to gauge placement and protection. Finally, moisture gradients can produce different strain responses at opposing surfaces [132], which is consistent with the observed inconsistencies in some gauges. Despite this, the valid strain profiles confirmed linear distribution across the beam depth, in line with classical bending theory.

A key observation was the shift in the neutral axis by 20 mm in the reinforced specimen (H-UN-D1), moving toward the GFRP side due to increased stiffness. This shift reflects the reinforcement's influence on stress distribution and flexural behaviour. Strain readings showed compression at the top and tension at the bottom near the GFRP, confirming its effectiveness in resisting tensile forces and enhancing load capacity.

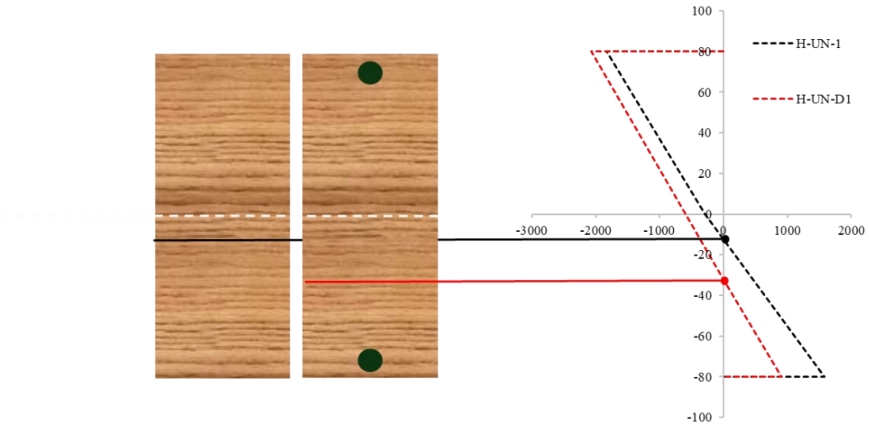

Fig. 5.5. Strain distribution for the recorded test specimens

Further, according to Yeboah and Gkantou (2021), the base of the elastic bending theory, which is plain section theory, is confirmed [10]. It is also reported that some reinforced beams also exhibited non-linear response, and some have somehow lowered neutral axes, which is in line with previous observations [10,48].

5.5.3 *Failure modes*

An essential aspect of structural performance evaluation involves understanding the predominant failure mechanisms observed across specimens. Based on the visual inspection and detailed experimental observations presented (Figs. 5.6a–6r) and summarized in Table 5.4, failure modes varied according to reinforcement configurations and specimen conditions (undamaged vs. fire-damaged). Generally, and in compliance with other research [10], the primary failure modes for both reinforced and non-reinforced beams were brittle tensile failure at the tensile zone

Table 5.4. Failure modes for the different reinforcement configurations

ID.	Failure mode	Possibility of outlier	Figure No.
H-UN-1	Shear/Flexural	-	Figure 3a
H-UN-2	Shear/Flexural	-	Figure 3b
H-FD	Shear/Flexural	yes	Figure 3c
H-UN-A1	Shear/Flexural	-	Figure 3d

H-UN-A2	Shear	-	Figure.3e
H-FD-A	Shear	-	Figure 3f
H-UN-B1	Shear/Flexural	-	Figure 3g
H-UN-B2	Shear/Flexural + Debond-ing	-	Figure 3h
H-FD-B	Shear	yes	Figure.3i
H-UN-C1	Flexural +Debonding	-	Figure 3j
H-UN-C2	Shear + Debonding	yes	Figure 3k
H-FD-C	Shear + Debonding	-	Figure.3l
H-UN-D1	Shear/Flexural	-	Fig-ure.3m
H-UN-D2	Shear	-	Figure 3n
H-FD-D	Shear	-	Figure 3
H-UN-E	Flexural +Debonding	-	Figure 3p
H-FD-E	Shear	yes	Figure.3q
H-FD-F	Shear/Flexural	-	Figure 3

(a) (b) (c)

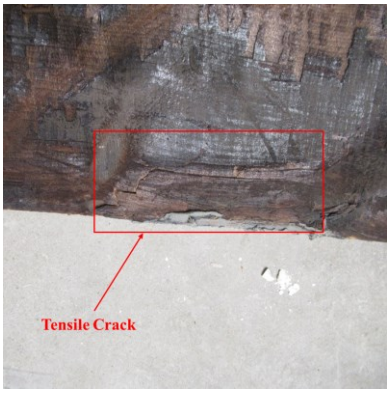
Tensile Crack

(d)

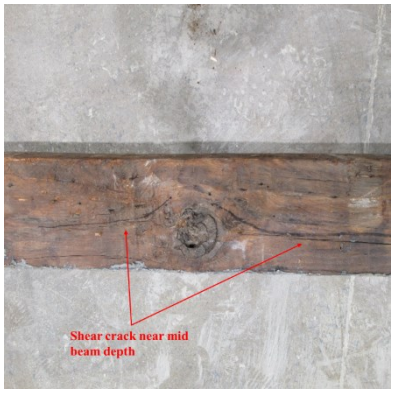
Shear crack near mid
beam depth

(e)

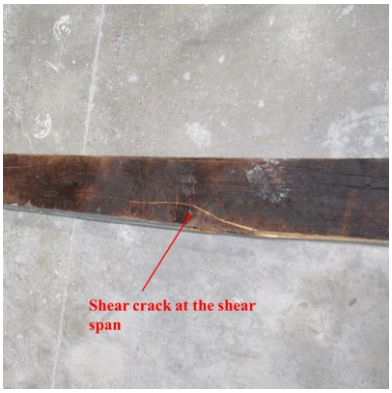
Shear crack at the shear
span

(f)


Shear/ Flexural Failure

(g)

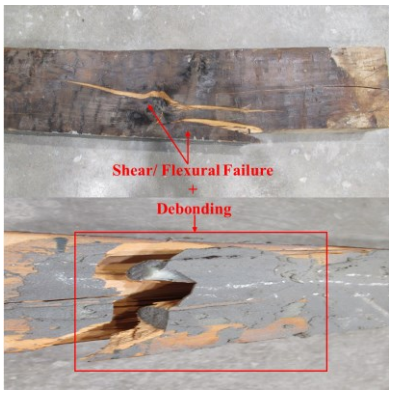
Shear/ Flexural Failure
+
Debonding

(h)


Shear Failure

(i)

(j)

(k)


Shear Failure
+
Debonding

(l)

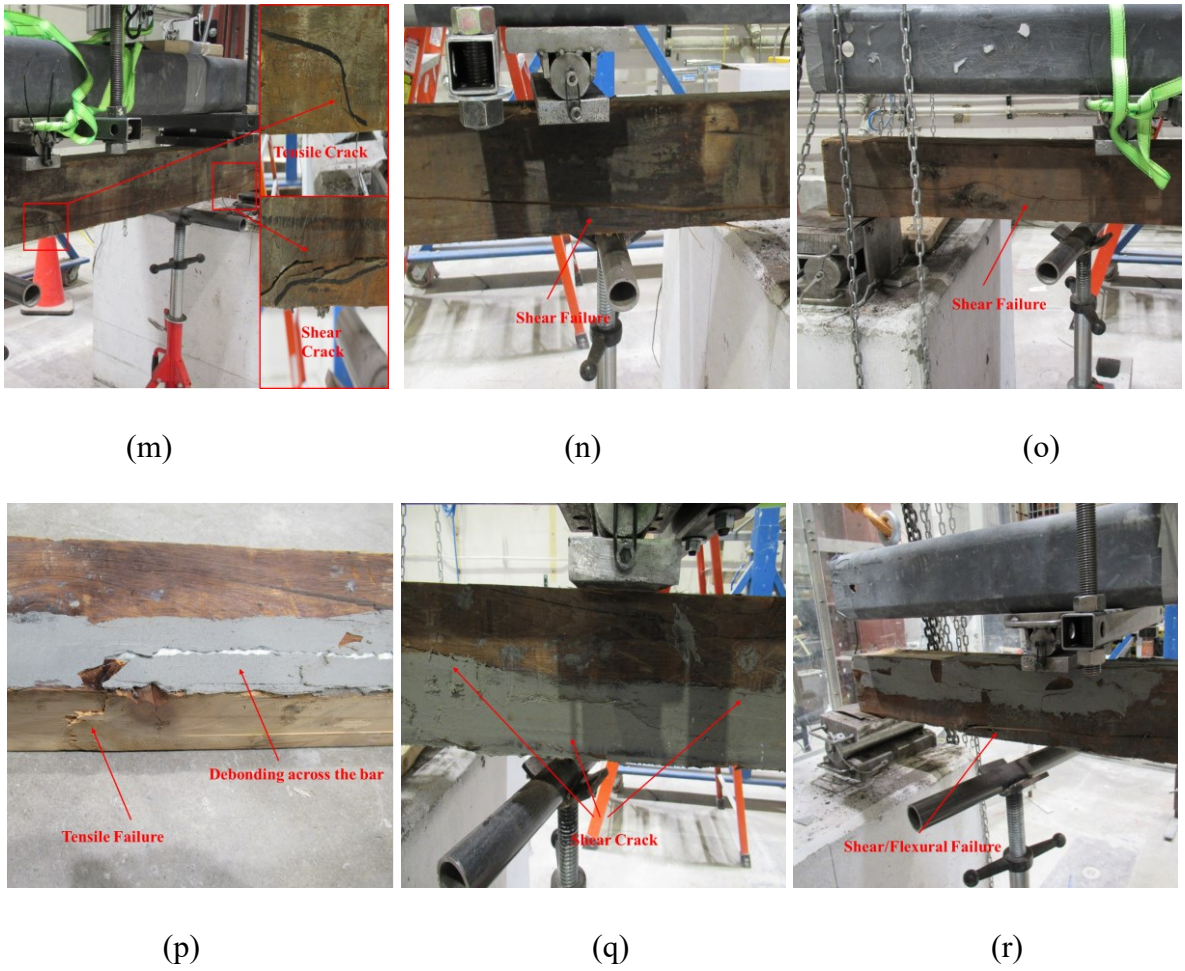

(m) (n) (o)

(p) (q) (r)

Fig. 5.6. Visualization of the failure modes for the different reinforcement configurations

The reference specimens (H-UN-1, H-UN-2, and H-FD) exhibited combined shear and flexural failure modes. Notably, the fire-damaged control specimen (H-FD, Fig. 5.6c) displayed pronounced cracking due to internal deterioration from fire exposure, leading to a more brittle behaviour and highlighting the potential unreliability of timber structures post-fire without reinforcement. Specimens in Group A (H-UN-A1, H-UN-A2, H-FD-A), reinforced with short rebars (50% of beam length), predominantly demonstrated shear-related failures. For instance, H-UN-A2 exhibited evident shear cracking (Fig. 5.6e), indicating that limited-length reinforcement had a minimal impact on altering primary failure mechanisms but contributed slightly to load capacity improvement. Intermediate-length reinforcement (Group B) showed more varied failure characteristics. Specimen H-UN-B1 (Fig. 5.6g) maintained combined shear/flexural failure, similar to reference beams. However, the specimen H-UN-B2 (Fig. 5.6h) exhibited combined shear, flexural, and de-bonding failures. De-bonding, in this case, indicated

inadequate bond interaction between timber and reinforcement at higher load levels, highlighting a critical consideration regarding bond integrity. Conversely, fire-damaged specimen H-FD-B (Fig. 5.6i), despite moderate load capacity enhancement, experienced primarily shear failure, emphasizing the limited influence of intermediate-length reinforcement on changing the brittle nature of fire-affected timber beams.

Group C's full-length reinforcement resulted in distinctive failure modes emphasizing de-bonding and flexural improvements. Specimen H-UN-C1 (Fig. 5.6j) displayed flexural and significant de-bonding failure, suggesting the reinforcement effectively enhanced flexural capacity but experienced bond failures at elevated stress levels. H-UN-C2 and the fire-damaged H-FD-C exhibited shear-dominated failures combined with de-bonding (Fig. 5.6k–6l), reinforcing the observation that full-length reinforcement significantly improved capacity and ductility but also introduced potential de-bonding risks under high loading. For Group D (single rebar, full-length central position), specimens H-UN-D1 and H-UN-D2 exhibited primarily shear/flexural failure modes. However, notably, specimen H-UN-D2, despite significant ductility gains (high deflection at 30.79 mm), still predominantly experienced shear failure (Fig. 5.6n). The fire-damaged specimen H-FD-D (Fig. 5.6o) also displayed apparent shear failure, emphasizing the persistence of brittle shear behaviour in fire-damaged timber despite substantial load capacity gains. In Group E, the dual placement of rebars significantly influenced the failure behaviour. Undamaged specimen H-UN-E predominantly exhibited flexural failure accompanied by de-bonding (Fig. 5.6p). The substantial flexural enhancement (85.07%) was accompanied by clear signs of de-bonding, indicating increased stress transfer between reinforcement and timber. The fire-damaged specimen H-FD-E, despite a negligible improvement in ultimate load, showed extensive shear cracking (Fig. 5.6q), reinforcing earlier observations that fire-induced damage limits the reinforcement effectiveness predominantly in terms of load capacity but may enhance flexural behaviour. Group F's compression-side reinforcement provided a unique insight. The fire-damaged specimen H-FD-F exhibited combined shear and flexural failures (Fig. 5.6r), highlighting the advantage of compression reinforcement in enhancing flexural behaviour and ultimate capacity (30.53% increase). This suggests that compression-side

reinforcement effectively contributes to overall stability, particularly valuable in fire-compromised structural scenarios. The observed failure modes correlate well with measured load-deflection behaviours, as illustrated in the provided load-deflection curves. Specimens experiencing shear and de-bonding failures typically showed sudden drops in load post-peak, highlighting their brittle characteristics despite reinforcement.

In contrast, specimens with pronounced flexural and ductile responses, such as H-UN-D2 and H-UN-E, maintained relatively smoother descending branches on their load-deflection curves, evidencing improved ductility and energy absorption. Furthermore, the significant deflection values recorded, particularly in specimens reinforced full-length or in combined tension-compression schemes, highlight improved deformability, an essential property for heritage structures subjected to variable load conditions. These specimens offered better warning signs before ultimate failure, a vital safety consideration for structural rehabilitation.

5.5.4 *Maximum allowable strengthening*

One of the primary concerns for strengthening Heritage timber buildings is assessing the structure after the sudden removal of the FRP due to de-bonding, fire, vandalism, moisture fluctuation, or any other contributing factors. To address this concern, as there is no guideline in this regard, the wise advice of ACI 440.2R is interpreted in timber beams in Equation (5.1).

ACI suggestion for concrete structures:

$$(\phi R_n)_{ex} \geq (1.1 s_{Dl} + 0.75 s_{Ll})_{new} \tag{5.1}$$

Where R_n is the nominal resistance for the existing element (before strengthening), s_{Dl} and s_{Ll} are service loads due to dead and live loads, respectively, for the new element (after strengthening). As this is a general statement, so considering the flexural behaviour:

$$(\phi M_n)_{ex} \geq (1.1 M_{Dl} + 0.75 M_{Ll})_{new} \tag{5.2}$$

Considering Equation 5.2 for the limit state:

$$(\phi M_n)_{ex} = (1.1 M_{Dl} + 0.75 M_{Ll})_{max} \tag{5.3}$$

And the critical load combination for timber building is also presented in Equation (5.4):

$$(\phi M_n)_{max} = (1.2M_{Dl} + 1.6M_{Ll})_{max} \quad (5.4)$$

From Equation (5.3):

$$(\phi M_n)_{ex} = M_{Dlmax}(1.1+0.75R) \quad (5.5)$$

where $R=M_{Llmax}/M_{Dlmax}$; then from Equation (5.4):

$$(\phi M_n)_{max} = M_{Dl,max}(1.25+1.5R) \quad (5.6)$$

From the combination of Equations (5.5) and (5.6):

$$\frac{(\phi Mn)_{Max}}{(\phi M_n)ex} \leq \frac{1.25+1.5R}{1.1+0.75R} \quad (5.7)$$

By expressing Equation (5.7) in the percentage form:

$$(Max)_{Alw} = \frac{(\phi M_n)_{Max}-(\phi M_n)_{ex}}{(\phi M_n)_{ex}} \quad (5.8)$$

Where $(Max)_{Alw}$ is the maximum allowable of strengthening, so:

$$(Max)_{Alw} = \frac{0.15M_{Dl,max}+0.75M_{Ll,max}}{(1.1M_{Dl})_{max}+(0.75M_{Ll})_{max}} \quad (5.9)$$

By simplifying and dividing Equation (5.9) by M_{Dlmax} :

$$(Max)_{Alw} = \frac{0.15+0.75R}{1.1+0.75R} \times 100 \quad (5.10)$$

Equation (5.10) is the percentage of the maximum allowable for strengthening a given timber structure with FRP.

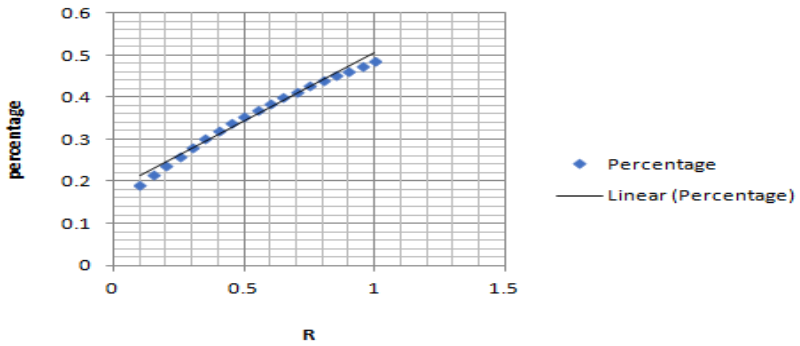

Fig. 5.7. Maximum allowable for strengthening, considering the ACI recommendation

As the final note, if $\frac{(M_{\max})New}{(\phi M_n)_{ex}} \leq (Max)_{Alw}$, strengthening Heritage timber beams (considering only the flexural criterion) with FRP is proposed; otherwise, a combination of dual system, FRP, and local post-tensioning is recommended.

5.6 Conclusion

This study investigated the efficiency of Near-Surface Mounted (NSM) GFRP reinforcement in strengthening 18 full-scale Heritage timber beams. The number of rebars is 1 or 2 ($\rho \approx 0.5$–1.0 %) with the length of 50 %, 75 %, and 100 % of the beam span. The placements were tension-side only, tension plus compression, or single-central bar. The results showed that reinforcement length and configuration had a considerable impact on Performance, with full-length tensile reinforcement yielding the highest capacity improvements. Fire-affected beams also exhibited significant improvement, while their reaction remained somewhat limited. Reinforcement altered structural behaviour by shifting the neutral axis, improving stress distribution, and delaying brittle failure modes.

Importantly, this study established maximum allowed strengthening thresholds for Heritage timber beams, modifying ACI 440.2R regulations to account for unexpected FRP loss. The findings demonstrate NSM-GFRP as a dependable, minimally invasive, and environmentally friendly retrofitting solution for historic timber structures. Beyond technical achievements, the effort promotes conservation practice by balancing structural safety with the preservation of cultural and architectural assets. Future studies should investigate long-term durability, cyclic behaviour, and hybrid retrofitting methodologies to develop safe and reversible solutions for heritage timber conservation. In a straightforward summary:

- Bond length governs efficiency. Short insertion caused rebar pull-out, de-bonding, or substrate failure at the rebar end. Full-span allowed uniform stress and higher effective performance.
- Reinforcement length criteria:
    - Full-length (100%) tensile GFRP: 97% ‑ 141% capacity gain in intact beams; ≈ 50% in fire-affected beams
    - Intermediate (75%): 46%‑57% (intact); ≈ 5% (fire-affected)

    - Short (50%): negligible (1%–2%); only ~ 10% in fire-affected
- Single full-length rebar (group D): 77% - 92% gain (intact); 38% (fire-affected)
- Tension + compression: 62% load and 85% flexural enhancement (intact); negligible load gain, but 110% flexural enhancement (fire-affected)
- Compression-zone rebar (group F): 31% capacity gain and 77% flexural improvement in fire-affected beams
- Fire-affected beams: generally benefited less due to internal damage and micro effects, but still recovered significantly in some cases (strength and/or stiffness)
- Failure mode shift: from brittle tensile rupture/ shear to flexural-shear with delayed cracking or de-bonding
- Neutral axis shift: ~ 20 mm toward the GFRP side (before cracking in the tension zone), reflecting the altered stress distribution
- Deflection increase: may be linked with the delay in timber rupture (not GFRP ductility)
- General performance and significance: 30% - 140% bending capacity improvement while maintaining Heritage appearance and value
- Established maximum allowable strengthening threshold: adapted from ACI 440.2R to ensure safe residual timber-alone capacity if FRP is lost
- Highlighted the need for bond-integrity behaviour and checks, long-term durability, and cyclic-load studies for future work

CHAPTER 6

Analytical Insights into the Bending Capacity Formulation of Heritage Timber Beams

General

Building on the experimental investigation of mechanical performance and strengthening studies reported in the previous chapters, Chapter 6 broadens the scope of this thesis by proposing an analytical formulation and investigating complementary methodologies. While Chapters 3 through 5 provided an empirical foundation for understanding the real behaviour of Heritage timber beams and their reinforcement with NSM-GFRP, Chapter 6 integrates these findings using moment-curvature analysis and simplified equilibrium models to provide theoretical approaches for estimating the bending capacities of strengthened beams. It aligns with the observed results, as other researchers used their experimental results to support their analytical methods [10]. The chapter begins by providing essential background information on strengthened beams before moving on to the proposed formulation for estimating the bending capacity. Furthermore, this chapter proposes future directions, such as combining post-tensioning, commonly employed in the retrofitting of concrete beams, with FRP to create a dual-strengthening system, thereby overcoming the limitations identified in prior chapters and aligning with ACI recommendations. In this way, Chapter 6 acts as both a link between the experimental results and the analytical modelling, as well as a forward-looking component that situates the thesis within the larger body of research and practical applications for sustainable Heritage timber retrofitting.

6.1 Proposed Bending Capacity for Heritage Timber Beams

Bending capacity for unreinforced timber beams is calculated using classical flexure, where plane sections remain plane according to Bernoulli's theory, and a linear stress distribution is assumed across the depth up to failure. Both the compression zone (top fibres) and the tension zone parallel to grain (bottom fibres) contribute to resistance; failure typically occurs when the extreme fibre in tension reaches its tensile strength parallel to grain (brittle rupture) or when

the extreme fibre in compression reaches its compressive limit (local crushing/instability). For a homogeneous rectangular section, the neutral axis is at the centroid, and the nominal bending capacity is taken as the minimum of two governing limits for compression and tension fibres. In the real experimental tests, the amount of flexural capacity often surpasses the theoretical calculation when timber experiences slight nonlinearity. However, in this flexural capacity, considerations of long-term effects, size and moisture modifications, defects/knots, and separate shear and lateral-torsional buckling checks are absent. Handbooks and standards such as CWC O86 [104] provide more accurate formulations to consider the other criteria mentioned above and determine the bending capacity of timber beams within the elastic limit and safety margins.

For the analysis of the enhanced capacity of strengthened beams, there is no standard method [10]. In this proposed methodology, a combined method that includes moment-curvature analysis, equilibrium, and data from experimental studies (Chapter 5) is used to capture the real behaviour of the timber section under bending moment, taking nonlinearity and stress-strain correlation into account.

Fig. 6.1 shows the cross-section of the beam under a moment. Three stages could happen to reach the maximum bending capacity. Before cracking, there is a linear response, so that the initial stiffness of the beam is equal to the slope of the stress-strain curve. In this stage, the entire section resists the bending moment, with the neutral axis located around the mid-depth. Pre-cracking: micro-cracking causes tension stiffness to reduce, and the neutral axis shifts downwards to maintain internal force equilibrium, which is short and temporary. This stage is not considered in the formulation. Post-cracking: Due to cracks, the stiffness in the tension face reduces, and the moment increases with curvature. Consequently, the neutral axis shifts upwards, and the strain line becomes asymmetric.

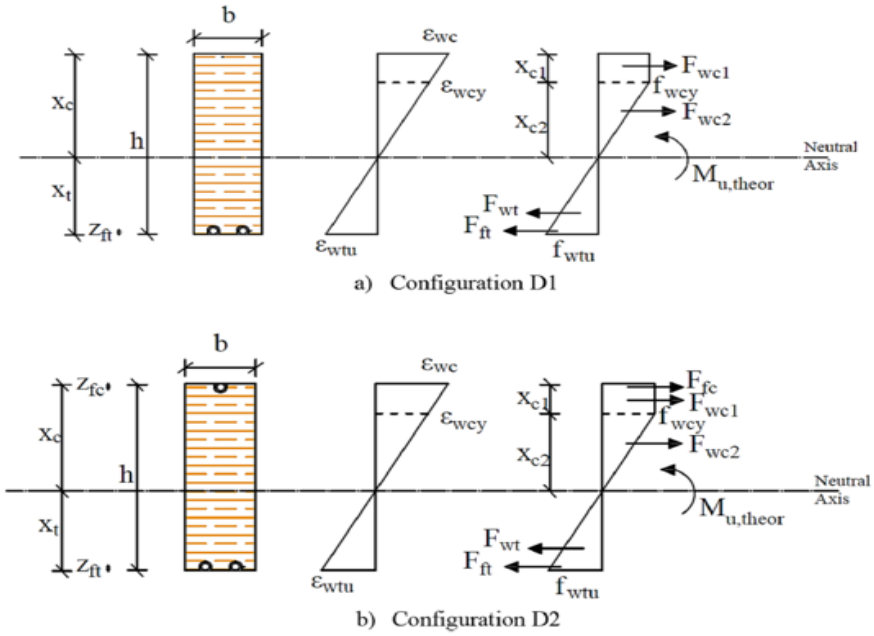

Fig. 6.1 Cross-section of strengthened beam under bending moment [10]

Considering the combination of both force equilibrium and moment-curvature methods, the following steps are being taken. For timber, the compression zone is proposed to be replaced by a rectangular Whitney-type block in a simplified analysis. Timber has a non-linear stress distribution in compression, but a rectangular block can approximate it. Fig. 6.2 shows the proposed stress distribution for the strengthened timber beam with NSM-FRP.

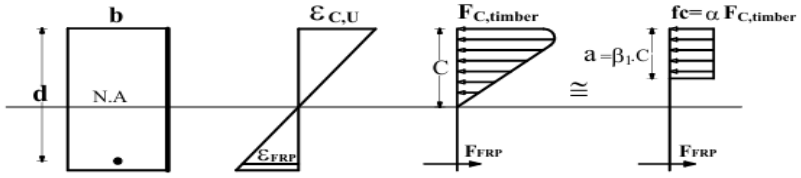

Fig. 6.2 Proposed Whitney-type stress profile of strengthened beam with GFRP

In the stress profile, intensity and height of the stress block can be simplified and expressed in Equations 6.1 and 6.2.

- uniform compression stress:

$$f_c = \alpha \times f_{c,timber} \tag{6.1}$$

$Where\ f_{c,timber}$ is the compressive strength of timber, parallel to the grain; α is an adjustment factor accounting for the non-linear behaviour of timber.

- Depth of compression block (a):

$$a = \beta_1 . c \tag{6.2}$$

where c is the distance from the extreme compression fibre to the neutral axis and β_1 is an adjustment ratio.

To find the location of Neutral Axis (NA), the equilibrium of compression and tension forces is beneficial, so:

$$C = \alpha . f_{c,timber} . b . a \text{ and } T = A_{FRP} . f_{FRP} \tag{6.3}$$

Considering Equation 6.3, it is proposed that timber in tension is cracked; thus, the contribution is ignored. To determine the resistant moment as the bending capacity, Equation 6.4 is constructed by taking the moment around the compression block at the equal load point.

$$M_r = C \times (d - \frac{a}{2}) \tag{6.4}$$

where d is the effective depth of the beam and a is the depth of the compression block, so:

$$C = \alpha \times f_{c,timber} \times b \times a \tag{6.5}$$

$$T = A_{FRP} \times f_{FRP} \tag{6.6}$$

From the equilibrium (C=T):

$$\alpha \times f_{c,timber} \times b \times a = A_{FRP} \times f_{FRP} \tag{6.7}$$

Solving Equation 6.7 for a:

$a = \frac{A_{FRP} \times f_{FRP}}{\alpha \times f_{c,timber} \times b}$ and finally, the moment can be calculated by Equation 6.4. This suggested approach, although very simple and achievable, has some unknown challenges. What exactly are C, β_1, and α.To answer the question, a complete plasticized (in the compression zone) method, followed by the assumption that the contribution of the cracked zone in the timber cross-section due to tension is negligible, is outlined. Hence, all tension is then transferred to the FRP. Note that the perfect bond assumption is a must, which should be satisfied in reality. The plasticized depth (C) can be calculated through the plastic calculation of the section, considering strain compatibility and force equilibrium, as shown in Fig. 6.3.

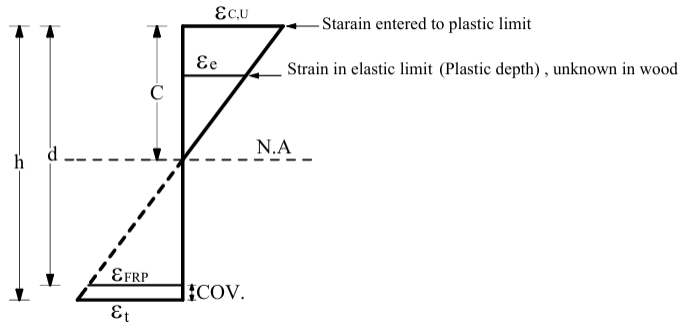

Fig. 6.3 Strain profile and compatibility

Where ε_{cu} is the ultimate strain in the compression zone at the plastic limit, exactly before crushing; ε_e is the strain of wood fibres still in the elastic limit, which is not well-defined in wood; ε_{FRP} and ε_t are the strains in FRP and outer tension wood fibre, respectively; c_p is the plasticized depth, and finally cov. The cover refers to the distance from the outer fibre to the centroid of the FRP in the NSM method.

From moment-curvature analysis:

$$\frac{c_p}{c} = \frac{\varepsilon_{c,u} - \varepsilon_e}{\varepsilon_{c,u}} \Rightarrow c_p = \frac{\varepsilon_{c,u} - \varepsilon_e}{\varepsilon_{c,u}} c \tag{6.8}$$

Also:

$\varepsilon_t = \frac{h-c}{c}\ \varepsilon_{c,u}$ which is assumed to be zero in this methodology, and

$$\varepsilon_{FRP} = \frac{h-c-cov.}{c}\ \varepsilon_{c,u} \tag{6.9}$$

From equilibrium:

$$\Sigma t = \Sigma c \Rightarrow\ f_{FRP} = \left(\alpha . f_{c,timber}\right). a. b \tag{6.10}$$

By taking a moment around N. The ultimate bending capacity is defined in Equation 6.11.

$$Mu = \left(\alpha . f_{c,timber}\right). a. b \left(c - \frac{a}{2}\right) + \sigma_{FRP} A_{FRP} (d - c) \tag{6.11}$$

This formulation, which requires further studies and verifications, is more accurate when the timber cross-section is relatively large and the reinforcement ratio is small. The steps necessary to be taken, considering one of the beams from the destructive tests, are as follows.

The Limitations and assumptions to be addressed in the formulation construction process include: Bernoulli's theory is valid (validated in experimental studies); FRP exhibits linear behaviour (without yielding) up to failure, with a much higher MOE than wood; and timber

behaves linearly until compression failure occurs. Also, E_t and E_f are MOE in timber and FRP, respectively. A_f represents the area of FRP bar(s).

From the transformed section method: $\acute{A}_f = n.A_f$; $n=E_f/E_t$ and from using strain to calculate the position of the neutral axis:

$$\sigma_w = E_w.\varepsilon_w \text{ and } \sigma_{FRP} = E_{FRP}.\varepsilon_{FRP} \quad (6.12)$$

Equations (6.9), (6.12), and (C=T) lead to:

$$0.5bE_wc^2 + A_{FRP}E_{FRP}c^2 - A_{FRP}E_{FRP}d = 0 \quad (6.13)$$

Solving Equation (6.13) reveals the position of NA. Considering Heritage strengthened beam "D":

b=95mm; d=h=160mm; measured MOE_t= 10050 MPa; E_{FRP}=60 GPa; Area of one FRP #3=71mm^2.

Through Equations (6.4) and (6.13):

c=32.3mm and Mu=2.15 kN. m (linear elastic).

By an iterative process and calibrating results with other beams with the same configuration (A, B, C, and the rest of Ds) for convergence and also Equation (6.8):

Plasticized depth, C_p= 11.7mm, meaning that the top 11.73mm of the beam in compression is in plastic stage; then Mu_1=5 kN.m.

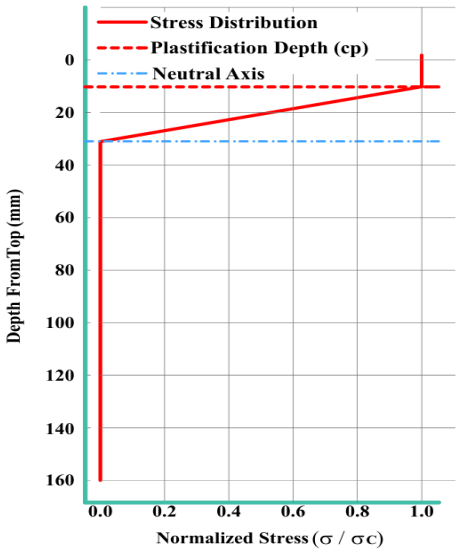

Fig. 6.4 Stress profile in the cross-section of the strengthened beam

Pointing to Fig. 6.4, which shows stress distribution profile in the cross-section of timber Heritage beams strengthened with NSM-FRP, the top 11.7 is fully plasticized and has a constant stress at $F_{c,w}$; from 11.7 to 32.3 is elastic compression, while decreasing linearly; and below 32.3 is the tension zone, where FRP withstand the force (not shown here).

Considering the average maximum resistance of strengthened beam D, Mu = 15.56 kN· m, and defining the strengthening coefficient as 15.56/5.01 = 3.1.

Comparing Cp/C= 11.7/32.3= 0.36, which is close to 1/3=0.33; notably, the plasticized depth at the time of failure is almost one third of the C in experimentally tested beams.

Hemed et. al [133] suggested a linear correlation as:

$$\beta = 2.1 \times h_{cy} + 0.95 \tag{6.14}$$

The parameters are shown in the Fig. 6.5 as follows.

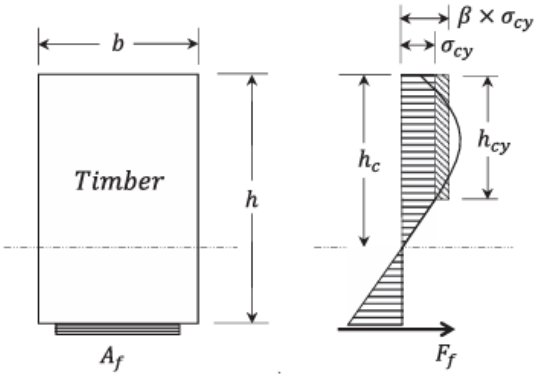

Fig. 6.5 Non-linear Stress profile in the cross-section of the strengthened beam [133]

In this stage, assuming Fcy=10 Mpa, εcu=0.003, and h_{cy}=1⇒ $\beta = 2.1 + 0.95 = 3.05$. The number is very close to 3.1, which has already been obtained. In a nutshell, considering the height of the rectangular block=1 (1/3), then the intensity of pressure in the compression block should be multiplied by 3.1:

$$M_{u,final}=3.01M_{u1} \tag{6.15}$$

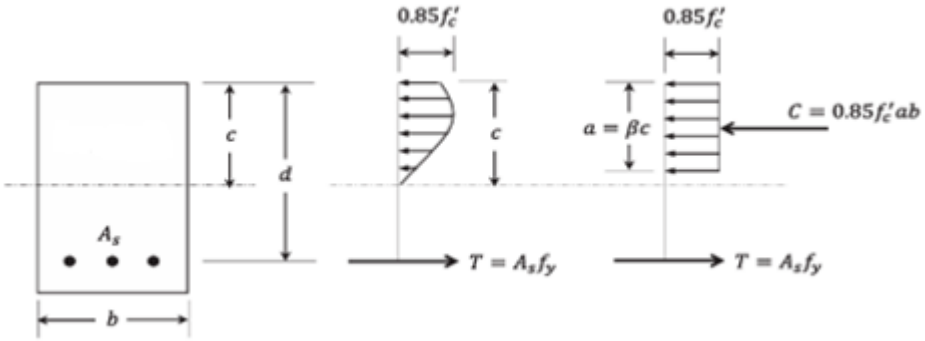

Fig. 6.6 Typical Whitney-type Stress profile in the cross-section of a reinforced concrete beam [133]

Considering the Whitney-type compression stress profile in concrete in Fig. 6.6, the final resistant moment is:

$$Mu = 3.01[(\alpha . f_{c,timber}) . a . b \left(c - \frac{a}{2}\right) + \sigma_{FRP} A_{FRP} (d - c)] \quad (6.16)$$

Now, if the height of this Whitney-type block is 11.7mm, equal to the plastic depth, the intensity of stress is 220.87 MPa. Back to the Equation reported by Hamed et al. [133], manipulating Cp= h_{cy}=11.7mm in Equation (13), reveals $\beta = 2.1 \times 11.7 + 0.95 = 25.52$ and stress concentration, $\beta \times \sigma_{cy} = 25.52 \times 10 \sim 255$ MPa, which is in good agreement with our findings.

As an exact summary, the required steps to be taken to find the ultimate bending capacity of a timber Heritage beam, strengthened by NSM-FRP are:

1-find the neutral axis by the elastic limit

2- Find Cp by plastic analysis

3- Ignore all contributions of wood below the neutral axis and give all tension to FRP

4- Construct the Whitney-type block:

- height= plasticized depth
- intensity= 1.9 Cp

5- Calculate $Mu = [(\alpha . f_{c,timber}) . a . b \left(c - \frac{a}{2}\right) + \sigma_{FRP} A_{FRP} (d - c)]$ (6.17)

6.2 Proposed Dual Strengthening System

This study proposes the post-tensioning technique as a dual strengthening method to enhance the bending performance of Heritage beams. The concept of post-tensioning in timber structures is adapted from concrete engineering, aiming to enhance the performance of timber beams, particularly in terms of strength and deflection. Once the optimum GFRP configuration is determined during the strengthening Phase (discussed in Chapter 5), the beams will then be further post-tensioned to achieve an adequate strength level in compliance with the maximum allowable strengthening limit set by the ACI [9]. This topic is discussed in detail in Chapter 5. The scope of the current study is limited to the validation of the numerical model; however, a proposal is presented to expand the subject matter to include experimental work.

The experimental work is proposed for a range of configurations for two possible scenarios:

1-Applying post-tensioned tendons i) across the entire beam section (span length) and ii) at the support. Fig. 6.7 shows the concept and practical implementation of support stiffening.

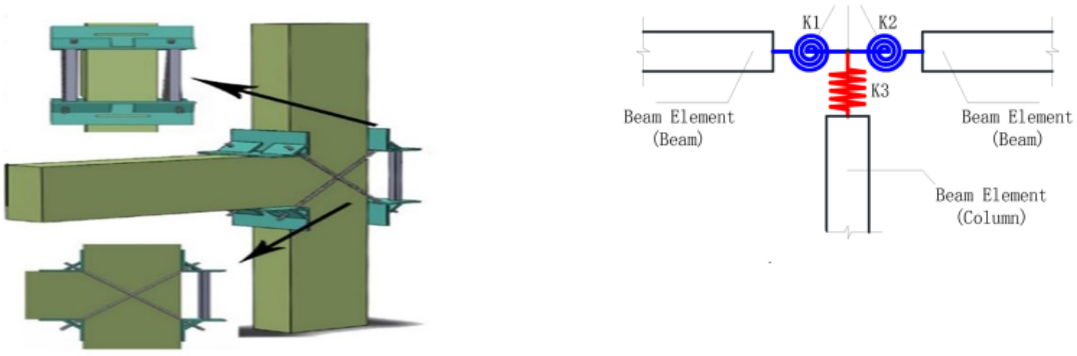

a) Practical implementation [134] b) Concept [69]

Fig. 6.7. Support post-tensioning technique in shear panel

Post-tensioning the beam-column connection enhances joint rotational stiffness and clamping pressure, reducing slip and opening at the interface and changing the boundary condition from near-pinned to semi-rigid/partially fixed. This redistributes internal stresses throughout the beam, reducing mid-span sagging moments and deflections, while increasing end moments and support shear. The stiffer connection typically increases lateral stiffness and enhances drift control, as shown in Fig. 6.9. Decreasing drift is considered a practical benefit

of the method, improving connection rigidity. The unbonded tendons also decrease residual drift (self-centring). In practice, increased stiffness can enhance load resistance capacity at mid-span, but it also concentrates compressive bearing and splitting demands near the support. Therefore, local stiffeners/seat plates, shear panel confinement, and splitting reinforcement are recommended.

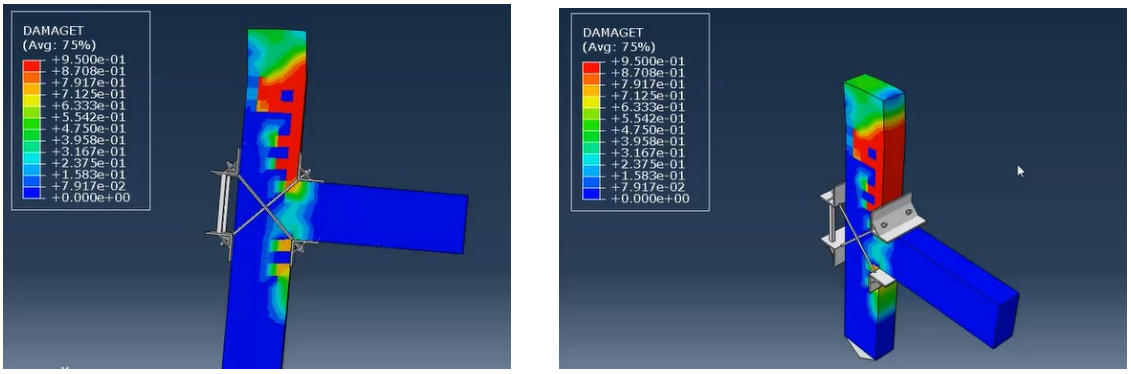

Fig. 6.8. Stiffening connection rigidity as a proposed dual system

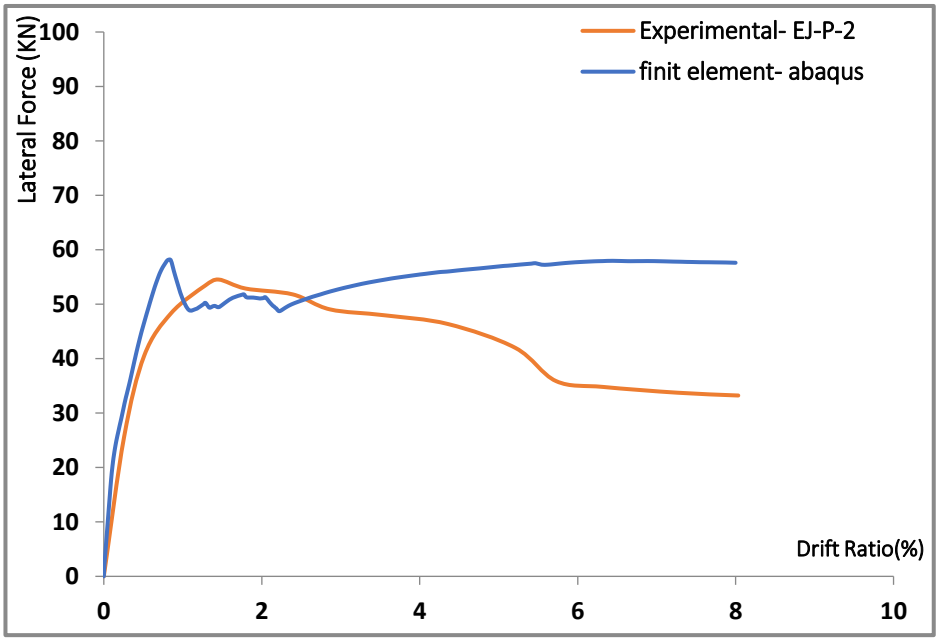

Fig. 6.9. Effect on drift control as a measure of practicality

Additionally, various configurations of the bars around the shear panel are to be explored to determine the optimal configuration for enhancing the structural performance of the beams. Focuses on the deformations within shear panels of timber beam-column joints, providing

lateral resistance as well [55]. However, in either scenario, it is essential to reinforce the support shear panels, beams, and posts with stiffeners to prevent the wood from being crushed or split. The long-term performance and time-dependent prestress losses (creep, relaxation) of post-tensioned timber systems are crucial for ensuring their reliability over time. As such, factors including creep and tension loss in the post-tensioning tendons can negatively impact the structural performance of timber frames. The importance of monitoring these parameters to maintain adequate moment capacity [135,136] and integrating FRP to complement the post-tensioning system with extra reinforcement [137,138] has been documented. Finally, combining FRP and post-tensioning offers enhanced strength, ductility, and energy dissipation capabilities, positioning post-tensioned timber structures as a viable solution for heritage beams, especially in seismic-prone regions.

Expected Results

It is expected to enhance both flexural and deflection properties of timber beams, which are highlighted more in this study. Flexural collapse, which is more important as a structural failure, is expected to shift from brittle-tension failure to a more ductile compression-initiated mode during which its capacity increases up to 46 percent; in the dual system, in fact, FRP will help the suffered timber beam bridge local defects and deficiencies to achieve larger nominal stresses before failure [139].

It is also expected to achieve more ductile load-deflection behaviour as the amount of tensile reinforcement increases, which is attributed to compression yielding at much higher strains [40].

In general terms, the dual strengthening technique is expected to:

- Reducing the amount of sagging and deflection, which affect serviceability, psychological aspects and appearance
- Transferring extra bending moments and relevant tensions beyond the formulated ACI recommendation to lower concentrated spots by means of FRP and post-tensioning technique
- Neutralizing damaged, pyrolyzed, and plastic-deformed or cracked members.

- Improving seismic behaviour of existing buildings to comply with new code requirements

Expected results should be valid for both immediate and long-run effects, so creep, de-bonding, strand relaxation, and local punctures and splitting should be taken into account.

CHAPTER 7

Summary and Conclusions

7.1 Summary

This thesis addresses a persistent need in conservation engineering by demonstrating how to analyze and reinforce in-situ Heritage timber beams using a scientifically sound but least destructive method. The project is divided into two Phases. Phase I (Evaluation) assesses the mechanical performance of full-scale Heritage timber beams through two different approaches: i) developing a correlation between material properties and mechanical performance of in-situ beams by NDTs, and ii) establishing a statistically valid path for indirect performance inference by comparing them to New or Simulated-New Counterparts (SNC). Phase II (Strengthening) experimentally assesses Near-Surface-Mounted (NSM) GFRP retrofits at full scale, then establishes allowable strengthening limits to ensure a safe residual capacity if the FRP contribution is suddenly withdrawn. Complementary analytical formulations (moment-curvature and simplified equilibrium with a Whitney-type compression block) link test findings to design-oriented predictions, suggesting a dual system with local post-tensioning.

Phase I (Evaluation): Data, Assessment, and Inference

i) Chapter 3: The chapter creates a database of full-scale Heritage timber beams, sourced from Eastern Canada (Quebec and Ontario), including density, moisture content, stiffness (MOE), bending strength (MOR), load-deflection response, and failure mechanisms. Bending tests and instrumentation provided the empirical foundation for both direct mechanical performance assessment and indirect measurement, calibration, and correlation. This chapter describes the variability caused by age and flaws, and directly correlates material properties with mechanical performance
ii) Chapter 4: The chapter formulates a Null hypothesis framework and, where market sizes do not match, generates SNC using grade-specified SPF properties and established bending relations to determine whether Heritage beams can be reliably inferred from their "New"

counterparts (references). The approach allows for destructive tests to be done on New equivalent timber beams and results to be attributed to their existing Heritage counterparts

In practice, Phase I provides the methods, dispersion, and acceptance criteria required to convert experimental measurements into defensible mechanical performance for Heritage evaluation and subsequent maintenance and retrofit decisions, and research purposes as well. For many protected buildings, destructive tests of in-situ members are restricted. This Phase, therefore, demonstrates how NDT indices and statistical equivalence to New/SNC beams can be combined to reduce uncertainty without invasive testing, filling a methodological gap noted in current practice and guidance.

Phase II (Strengthening): Full-Scale NSM-GFRP and Allowable Limits

i) Chapter 5: The chapter involves a full-scale NSM-GFRP program on Heritage beams (both intact and fire-affected), with changing rebar number, position(tension/compression), and development length. All beams are subjected to displacement-controlled four-point bending to determine the capacity gain, stiffness change, neutral axis location, and transition of failure modes. A key finding is that full-length tensile reinforcement produces the most significant capacity gains, but intermediate/short development lengths are governed by bond/anchorage effects. Fire-affected members benefit significantly, although less so than intact beams, and failure modes shift from brittle tension rupture to shear-flexural or debonding processes as reinforcement increases. Capacity improvements vary based on the configurations.

   As Heritage conservation must remain safe in the event of retrofit failure (e.g., sudden debonding, fire, vandalism), this chapter also modifies ACI 440.2R-specific recommendations to determine a maximum allowable strengthening for timber beams. This provides practitioners with a clear, top-bound on FRP contribution, ensuring that a residual wood-only load path remains adequate even if FRP efficacy is suddenly withdrawn. The acceptable limit is presented as a percentage of demand; the thesis also includes a decision rule for

when to use a dual system (FRP + local post-tensioning). The strengthening results guide the selection of development length, bond/anchorage, and placement (tension vs. compression side), as well as the importance of local measures to prevent splitting and debonding at rebar ends, particularly in members with pre-existing defects or those that have suffered fire damage.

ii) Chapter 6: The chapter includes analytical and complementary work. To bridge the gap between test results and design, chapter 6 proposes simplified analytical models for FRP-strengthened beams. It combines moment-curvature and force equilibrium for strengthened sections, with compression represented by a rectangular Whitney-type block as a practical approximation to nonlinearity. The effort estimates the ultimate bending moment using concepts of neutral-axis location and plasticized depth.

In the simplified model, the analytical technique assumes plane sections, linear FRP, and timber nonlinearity up to compression failure; it performs best at low reinforcement ratios and relatively large sections.

Furthermore, the chapter proposes a dual strengthening system, as future work, that combines NSM-FRP with local post-tensioning at supports or beam-column joints to increase rotational restraint, limit residual drift (self-centring with unbonded tendons), and handle cases where the required demand would exceed the allowable FRP capacity. The approach is consistent with the conservation premise of reversibility and residual capacity.

7.2 Conclusions

The following are the main conclusions derived from this PhD thesis.

1- Built a full-scale database of Heritage beams (density, MOE, MOR, load–deflection, failure modes

2- Combined NDT and destructive testing to correlate and determine MOE/MOR and flexural capacity of in-situ members, aiding conservation decisions where destructive testing is limited

3- NSM-GFRP delivered substantial and configuration-dependent flexural enhancements at full scale. Capacity gains from 30% to 140% were observed, with full-length tensile reinforcement consistently most effective; intermediate/short development lengths require careful bond/anchorage detailing. Fire-affected beams responded positively but to a lesser extent, and failure modes shifted toward shear-flexural or debonding as reinforcement increased
4- The moment–curvature plus a Whitney-type compression block methodology captured the principal experimental phenomena (neutral-axis shifting, compression plasticization) and provides acceptable estimates for strengthened beams, subject to explicit assumptions about linearity and reinforcement ratios
5- Adapted ACI 440.2R, the wise concept to timber, yielded an upper bound on FRP contribution that preserves a residual wood-only load path under sudden FRP loss, translating a core Heritage requirement into a clear design rule
6- Dual FRP plus post–tensioned systems warrant targeted development. Where required demand exceeds the allowable FRP limit or where drift control and self-centring are priorities, the proposed local post-tensioning concept can raise support rigidity, reduce mid-span resistance demand, and improve residual drift, provided detailing addresses shear-panel confinement, splitting, and time-dependent prestress losses

All in all, the thesis delivers (i) a field-calibrated database of Heritage beam properties, (ii) an equivalence-based assessment route that is compatible with conservation constraints, (iii) full-scale evidence and detailing guidance for NSM-GFRP retrofits, (iv) a maximum-allowable FRP limit that operationalizes residual-capacity requirements, and (v) analytical tools that make these results usable in preliminary design and screening. Together, these outcomes provide a coherent, conservation-aligned framework for assessing and upgrading Heritage timber beams, and a reasoned path toward hybrid (FRP + post-tensioning) solutions where needed.

7.3 Recommendations and Future Work

- Developing and verifying analytical methods to calculate the bending capacity of strengthened beams
- Developing post-tensioning as a dual method to address the required bending capacity beyond the ACI recommendation
- Evaluating thermal softening and bond retention under standard fire curves and realistic Heritage coverings. Developing detailing that protects both aesthetics and rating demands

References

[1] J. Brol, A. Wdowiak-Postulak, Old Timber Reinforcement with FRPs, Materials (Basel). 12 (2019). https://doi.org/10.3390/ma12244197.

[2] M.J. Morales-Conde, C. Rodríguez-Liñán, P. Rubio-de Hita, Bending and shear reinforcements for timber beams using GFRP plates, Constr. Build. Mater. 96 (2015) 461–472. https://doi.org/10.1016/j.conbuildmat.2015.07.079.

[3] A historic building, (n.d.). https://images.app.goo.gl/ZoAtCtXDv5SrXfBY9.

[4] A well-maintained ancient building, (n.d.). https://images.app.goo.gl/pXAtaynm9BFUsLKg6.

[5] Layers of history: Building in Istanbul reflects Roman, Byzantine, Ottoman eras, n.d. https://www.turkiyetoday.com/culture/unique-building-istanbul-66513/.

[6] O. Citizen, Kingston heritage building collapses overnight, n.d. https://ottawacitizen.com/news/local-news/kingston-heritage-building-collapses-overnight.

[7] 2023 CBC, Halifax development on hold after heritage building destroyed, (n.d.). https://www.cbc.ca/news/canada/nova-scotia/halifax-development-on-hold-after-heritage-building-destroyed-in-crane-move-1.6772583.

[8] Z. Xin, C. Guan, H. Zhang, Y. Yu, F. Liu, L. Zhou, Y. Shen, Assessing the density and mechanical properties of ancient timber members based on the active infrared thermography, Constr. Build. Mater. 304 (2021) 124614. https://doi.org/10.1016/j.conbuildmat.2021.124614.

[9] P.S. and R. Kanitkar, ACI 440.2R and The New Seismic Strengthening Guidelines

Using FRP, ACI Symp. Publ. 327 (n.d.). https://doi.org/10.14359/51713341.

[10] D. Yeboah, M. Gkantou, Investigation of flexural behaviour of structural timber beams strengthened with NSM basalt and glass FRP bars, Structures. 33 (2021) 390–405. https://doi.org/https://doi.org/10.1016/j.istruc.2021.04.044.

[11] M. Eder, O. Arnould, J.W.C. Dunlop, J. Hornatowska, L. Salmén, Experimental micro-mechanical characterisation of wood cell walls, Wood Sci. Technol. 47 (2013) 163–182. https://doi.org/10.1007/s00226-012-0515-6.

[12] W.A. Côté, Chemical Composition of Wood BT - Principles of Wood Science and Technology: I Solid Wood, in: F.F.P. Kollmann, W.A. Côté (Eds.), Springer Berlin Heidelberg, Berlin, Heidelberg, 1968: pp. 55–78. https://doi.org/10.1007/978-3-642-87928-9_2.

[13] L.A. Donaldson, Lignification and lignin topochemistry — an ultrastructural view, Phytochemistry. 57 (2001) 859–873. https://doi.org/https://doi.org/10.1016/S0031-9422(01)00049-8.

[14] J. Barros, H. Serk, I. Granlund, E. Pesquet, The cell biology of lignification in higher plants., Ann. Bot. 115 (2015) 1053–1074. https://doi.org/10.1093/aob/mcv046.

[15] Ö. Gezici-Koç, S.J.F. Erich, H.P. Huinink, L.G.J. van der Ven, O.C.G. Adan, Bound and free water distribution in wood during water uptake and drying as measured by 1D magnetic resonance imaging, Cellulose. 24 (2017) 535–553. https://doi.org/10.1007/s10570-016-1173-x.

[16] E.E. Thybring, M. Fredriksson, S.L. Zelinka, S. V Glass, Water in Wood: A Review of

Current Understanding and Knowledge Gaps, Forests. 13 (2022). https://doi.org/10.3390/f13122051.

[17] Mechanical Properties of Woods, YFILIOS Solut. (n.d.). http://www.yfilios-solution.com/2024/07/mechanical-properties-of-woods.html.

[18] D.E.K. David W. Green, Jerrold E. Winandy, Mechanical properties of wood. Wood handbook : wood as an engineering material, 1999.

[19] J. Brol, S. Dawczyński, A. Malczyk, K. Adamczyk, Testing timber beams after 130 years of utilization, 2012.

[20] N. Thaler, M. Humar, Performance of oak, beech and spruce beams after more than 100 years in service, Int. Biodeterior. Biodegradation. 85 (2013) 305–310. https://doi.org/10.1016/j.ibiod.2013.08.020.

[21] Z. Xin, D. Ke, H. Zhang, Y. Yu, F. Liu, Non-destructive evaluating the density and mechanical properties of ancient timber members based on machine learning approach, Constr. Build. Mater. 341 (2022) 127855. https://doi.org/10.1016/j.conbuildmat.2022.127855.

[22] K. Kránitz, M. Deublein, P. Niemz, Strength estimation of aged wood by means of ultrasonic devices, in: Futur. Qual. Control Wood Wood Prod. Proc. Final Conf. COST Action E53‘Quality Control Wood Wood Prod. 4–7th May 2010, Edinburgh, UK, Edinburgh Napier University, 2010: pp. 425–433.

[23] I. and U. 2020 (2020) GlobalABC, GlobalABC Roadmap for Buildings and Construction 2020-2050, IEA, Paris, Licence: CC BY 4.0, 2020.

https://www.iea.org/reports/globalabc-roadmap-for-buildings-and-construction-2020-2050.

[24] S. Swiss Society of Engineers and Architects SIA, Zurich, Normentwurf SIA 269:2009, Grundlagen der Erhaltung von Tragwerken (Draft Standard SIA 269:2009 Basis of Maintenance of Structures), 2009.

[25] C.S.N. ISO, 13822 Bases for design of structures-Assessment of existing structures, Int. Organ. Stand. (2010).

[26] Swiss Society of Engineers and Architects, SIA 269/5:2011, Existing Structures – Timber Structures, Schweizer Norm, Zurich,Switzerland, 2011.

[27] A.T. Council, Seismic evaluation and retrofit of multi-unit wood-frame buildings with weak first stories, Federal Emergency Management Agency, National Earthquake Reduction Program, 2012.

[28] P. LUECHINGER, J. FISCHER, C. CHRYSOSTOMOU, G. DIETEREN, F. LANDON, S. LEIVESTAD, N. MALAKATAS, G. MANCINI, J. MARKOVA, S. MATTHEWS, New European Technical Rules for the Assessment and Retrofitting of Existing Structures., 2015.

[29] H. Johnsson, T. Blanksvärd, A. Carolin, Glulam members strengthened by carbon fibre reinforcement, Mater. Struct. 40 (2007) 47–56.

[30] Q. Xu, L. Chen, K.A. Harries, F. Zhang, Z. Wang, X. Chen, Experimental study and numerical simulation of long-term behavior of timber beams strengthened with near surface mounted CFRP bars, Mater. Struct. 50 (2017) 1–13.

[31] X. Xueyu, W. Yiqingzi, X. Rongjun, L. Xuanxing, Experimental study and theoretical analysis on flexural mechanical propertiesof reinforced timber beams, Adv. Compos. Lett. 27 (2018) 096369351802700103.

[32] R.A. Barnes, G.C. Mays, Fatigue performance of concrete beams strengthened with CFRP plates, J. Compos. Constr. 3 (1999) 63–72.

[33] E.J. Biblis, Analysis of wood-fiberglass composite beams within and beyond the elastic region, FPJ. 15 (1965) 81–88.

[34] C. Gentile, D. Svecova, S.H. Rizkalla, Timber beams strengthened with GFRP bars: development and applications, J. Compos. Constr. 6 (2002) 11–20.

[35] D. Svecova, R.J. Eden, Flexural and shear strengthening of timber beams using glass fibre reinforced polymer bars—an experimental investigation, Can. J. Civ. Eng. 31 (2004) 45–55.

[36] P. de la Rosa García, A.C. Escamilla, M.N.G. García, Bending reinforcement of timber beams with composite carbon fiber and basalt fiber materials, Compos. Part B Eng. 55 (2013) 528–536.

[37] N. Plevris, T.C. Triantafillou, FRP-reinforced wood as structural material, J. Mater. Civ. Eng. 4 (1992) 300–317.

[38] S. Gómez, D. Svecova, Behavior of split timber stringers reinforced with external GFRP sheets, J. Compos. Constr. 12 (2008) 202–211.

[39] A. Yusof, A.L. Saleh, Flexural strengthening of timber beams using glass fibre reinforced polymer, Electron. J. Struct. Eng. 10 (2010) 45–56.

[40] K.-U. Schober, A.M. Harte, R. Kliger, R. Jockwer, Q. Xu, J.-F. Chen, FRP reinforcement of timber structures, Constr. Build. Mater. 97 (2015) 106–118.

[41] M. Hanafi, E. Aydin, A. Ekinci, Engineering properties of basalt fiber-reinforced bottom ash cement paste composites, Materials (Basel). 13 (2020) 1952.

[42] R. Kliger, M. Johansson, R. Crocetti, M. Al-Emrani, Strengthening timber with CFRP or steel plates–short and long-term performance, in: Proc. World Conf. Timber Eng. Miyazaki, Japan, 2008.

[43] A. André, R. Kliger, Strengthening of timber beams using FRP, with emphasis on compression strength: a state of the art review, in: Proc. Second Off. Int. Conf. Int. Inst. FRP Constr. Asia-Pacific Reg. APFIS, 2009: pp. 193–202.

[44] H. Al-hayek, Flexural behaviour of post-tensioned timber beams, (2014).

[45] W. Lu, Z. Ling, Q. Geng, W. Liu, H. Yang, K. Yue, Study on flexural behaviour of glulam beams reinforced by Near Surface Mounted (NSM) CFRP laminates, Constr. Build. Mater. 91 (2015) 23–31.

[46] M. Fossetti, G. Minafò, M. Papia, Flexural behaviour of glulam timber beams reinforced with FRP cords, Constr. Build. Mater. 95 (2015) 54–64.

[47] M. Corradi, L. Righetti, A. Borri, Bond Strength of Composite CFRP Reinforcing Bars in Timber., Mater. (Basel, Switzerland). 8 (2015) 4034–4049. https://doi.org/10.3390/ma8074034.

[48] G.M. Raftery, C. Whelan, Low-grade glued laminated timber beams reinforced using improved arrangements of bonded-in GFRP rods, Constr. Build. Mater. 52 (2014) 209–

220.

[49] J. Fiorelli, A.A. Dias, Fiberglass-reinforced glulam beams: mechanical properties and theoretical model, Mater. Res. 9 (2006) 263–269.

[50] M.D. Banea, L.F.M. da Silva, Adhesively bonded joints in composite materials: an overview, Proc. Inst. Mech. Eng. Part L J. Mater. Des. Appl. 223 (2009) 1–18.

[51] P. Alam, M.P. Ansell, D. Smedley, Mechanical repair of timber beams fractured in flexure using bonded-in reinforcements, Compos. Part B Eng. 40 (2009) 95–106.

[52] H.J. Dagher, High-performance wood composites for construction, Vii Ebramem. 154 (2000) 154–163.

[53] A.S. Wheeler, A.R. Hutchinson, Resin repairs to timber structures, Int. J. Adhes. Adhes. 18 (1998) 1–13.

[54] M. Romani, H.J. Blaß, Design model for FRP reinforced glulam beams, in: Proc. Int. Counc. Res. Innov. Build. Constr. (CIB), Work. Comm. W18 Timber Struct. Meet., 2001.

[55] A. Rahmzadeh, A. Iqbal, Finite Element Modelling of Post-Tensioned Timber Beam-Column Joints Designed for Seismic Loading, in: Proc. 12th Can. Conf. Earthq. Eng. Quebec City, Canada, 2019.

[56] A.G. Woodside, Releasing the death-grip of null hypothesis statistical testing (p<. 05): Applying complexity theory and somewhat precise outcome testing (SPOT), J. Glob. Sch. Mark. Sci. 27 (2017) 1–15.

[57] W.W. Tryon, Evaluating statistical difference, equivalence, and indeterminacy using

inferential confidence intervals: an integrated alternative method of conducting null hypothesis statistical tests., Psychol. Methods. 6 (2001) 371.

[58] N. Balluerka, J. Gómez, D. Hidalgo, The controversy over null hypothesis significance testing revisited, Methodology. 1 (2005) 55–70.

[59] F.S. Nathoo, M.E.J. Masson, Bayesian alternatives to null-hypothesis significance testing for repeated-measures designs, J. Math. Psychol. 72 (2016) 144–157. https://doi.org/https://doi.org/10.1016/j.jmp.2015.03.003.

[60] A.G. Patriota, On some assumptions of the null hypothesis statistical testing, Educ. Psychol. Meas. 77 (2017) 507–528.

[61] A.J. Harrison, S.A. McErlain-Naylor, E.J. Bradshaw, B. Dai, H. Nunome, G.T.G. Hughes, P.W. Kong, B. Vanwanseele, J.P. Vilas-Boas, D.T.P. Fong, Recommendations for statistical analysis involving null hypothesis significance testing, Sport. Biomech. 19 (2020) 561–568.

[62] D.J. Murdoch, Y.-L. Tsai, J. Adcock, P-values are random variables, Am. Stat. 62 (2008) 242–245.

[63] F. Emmert-Streib, M. Dehmer, Understanding statistical hypothesis testing: The logic of statistical inference, Mach. Learn. Knowl. Extr. 1 (2019) 945–962.

[64] A. Cavalli, D. Cibecchini, M. Togni, H.S. Sousa, A review on the mechanical properties of aged wood and salvaged timber, Constr. Build. Mater. 114 (2016) 681–687.

[65] H. Pretzsch, P. Biber, G. Schütze, J. Kemmerer, E. Uhl, Wood density reduced while wood volume growth accelerated in Central European forests since 1870, For. Ecol.

Manage. 429 (2018) 589–616. https://doi.org/https://doi.org/10.1016/j.foreco.2018.07.045.

[66] M.I. Carrillo Gómez, J.R. Sotomayor Castellanos, D. Raya González, Structural analysis of wood beams by non-destructive methods in restoration works of the Cathedral of Morelia, Mexico, Int. Arch. Photogramm. Remote Sens. Spat. Inf. Sci. 42 (2019) 263–270.

[67] A. Kandemir-Yücel, A. Tavukçuoğlu, E.N. Caner-Saltık, Soundness assessment of structural timber elements in traditional timber dwellings: the combined use of quantitative IR thermograhy and ultrasonic testing, (n.d.).

[68] V. Nasir, H. Fathi, A. Fallah, S. Kazemirad, F. Sassani, P. Antov, Prediction of Mechanical Properties of Artificially Weathered Wood by Color Change and Machine Learning, Materials (Basel). 14 (2021) 6314. https://doi.org/10.3390/ma14216314.

[69] M. Lyu, X. Zhu, Q. Yang, Condition assessment of heritage timber buildings in operational environments, J. Civ. Struct. Heal. Monit. 7 (2017) 505–516. https://doi.org/10.1007/s13349-017-0239-2.

[70] L.P. Perlin, R.C. de A. Pinto, Â. do Valle, Ultrasonic tomography in wood with anisotropy consideration, Constr. Build. Mater. 229 (2019) 116958. https://doi.org/https://doi.org/10.1016/j.conbuildmat.2019.116958.

[71] P. Xu, C. Guan, H. Zhang, G. Li, D. Zhao, R.J. Ross, Y. Shen, Application of Nondestructive Testing Technologies in Preserving Historic Trees and Ancient Timber Structures in China, Forests. 12 (2021). https://doi.org/10.3390/f12030318.

[72] F. Liu, P. Xu, H. Zhang, C. Guan, D. Feng, X. Wang, Use of Time-of-Flight Ultrasound to Measure Wave Speed in Poplar Seedlings, Forests. 10 (2019). https://doi.org/10.3390/f10080682.

[73] D. Diamantidis, Report 32: probabilistic assessment of existing structures-a publication for the Joint Committee on Structural Safety (JCSS), RILEM publications, 2001.

[74] M. Riggio, D. D'Ayala, M.A. Parisi, C. Tardini, Assessment of heritage timber structures: Review of standards, guidelines and procedures, J. Cult. Herit. 31 (2018) 220–235. https://doi.org/https://doi.org/10.1016/j.culher.2017.11.007.

[75] C. Group, ISO 13822:2010 Bases for design of structures -- Assessment of existing structures, 2010.

[76] S. Swiss Society of Engineers and Archi tects SIA, Zurich, Normentwurf SIA 269/5:2009 Erhaltung von Tragwerken– Holzbau (Draft Standard SIA 269/5:2009 Existing Structures– Timber Structures), 2009.

[77] N. Macchioni, C. Bertolini Cestari, T. Tannert, Review of Codes and Standards, in: 2011: pp. 115–121. https://doi.org/10.1007/978-94-007-0560-9_14.

[78] Canada, Parks, 2010, Standards and Guidelines for the conservation of historic places in Canada., 2017. https://www.historicplaces.ca/media/18072/81468-parks-s+g-eng-web2.pdf.

[79] R. Yadav, J. Kumar, Engineered wood products as a sustainable construction material: A review, Eng. Wood Prod. Constr. 10 (2021).

[80] M. Gong, Lumber-based mass timber products in construction, in: Timber Build.

Sustain., IntechOpen, 2019.

[81] S. He, X. Zhao, E.Q. Wang, G.S. Chen, P.-Y. Chen, L. Hu, Engineered wood: sustainable technologies and applications, Annu. Rev. Mater. Res. 53 (2023) 195–223.

[82] C.C. on B. and F. Codes, National Building Code of Canada: 2015, (2015). https://doi.org/10.4224/40002005.

[83] M. Piazza, M. Riggio, Visual strength-grading and NDT of timber in traditional structures, J. Build. Apprais. 3 (2008). https://doi.org/10.1057/jba.2008.4.

[84] R. Anthony, K. DUGAN, D. ANTHONY, A Grading Protocol for Structural Lumber and Timber in Historic Structures, 40 (2009).

[85] C. Osuna-Sequera, D.F. Llana, G. Íñiguez-González, F. Arriaga, The influence of cross-section variation on bending stiffness assessment in existing timber structures, Eng. Struct. 204 (2020) 110082. https://doi.org/https://doi.org/10.1016/j.engstruct.2019.110082.

[86] R. by the I. 14th G. Assembly, No TiICOMOS CHARTER- PRINCIPLES FOR THE ANALYSIS, CONSERVATION AND STRUCTURAL RESTORATION OF ARCHITECTURAL HERITAGE (2003) tle, 2003. http://www.international.icomos.org/.

[87] M. Zielińska, M. Rucka, Non-destructive Testing of Wooden Elements, IOP Conf. Ser. Mater. Sci. Eng. 1203 (2021) 32058. https://doi.org/10.1088/1757-899X/1203/3/032058.

[88] M.G. Barker, Steel girder bridge field test procedures, Constr. Build. Mater. 13 (1999) 229–239. https://doi.org/https://doi.org/10.1016/S0950-0618(99)00013-6.

[89] A. Marzo, B. Carpani, G. Marghella, C. Tripepi, A Methodology to Manage and

Correlate Results of Non-Destructive and Destructive Tests on Ancient Timber Beams: The Case of Montorio Tower, NDT. 2 (2024) 311–329. https://doi.org/10.3390/ndt2030019.

[90] A. Ceccotti, M. Togni, NDT on large ancient timber beams: assessment of the strength/stiffness properties combining visual and instrumental methods, 1996.

[91] A. Josifovski, N. Todorović, J. Milošević, M. Veizović, F. Pantelić, M. Aškrabić, M. Vasov, A. Rajčić, An Approach to In Situ Evaluation of Timber Structures Based on Equalization of Non-Destructive and Mechanical Test Parameters, Buildings. 13 (2023). https://doi.org/10.3390/buildings13061405.

[92] T. Nowak, F. Patalas, A. Karolak, Estimating Mechanical Properties of Wood in Existing Structures—Selected Aspects, Materials (Basel). 14 (2021). https://doi.org/10.3390/ma14081941.

[93] A. Firmanti, E.T. Bachtiar, S. Surjokusumo, K. Komatsu, S. Kawai, Mechanical stress grading of tropical timbers without regard to species, J. Wood Sci. 51 (2005) 339–347. https://doi.org/10.1007/s10086-004-0661-z.

[94] D. Van Duong, J. Matsumura, Within-stem variations in mechanical properties of Melia azedarach planted in northern Vietnam, J. Wood Sci. 64 (2018) 329–337. https://doi.org/10.1007/s10086-018-1725-9.

[95] J. Moore, A. Lyon, S. Lehneke, Effects of rotation length on the grade recovery and wood properties of Sitka spruce structural timber grown in Great Britain, Ann. For. Sci. 69 (2012). https://doi.org/10.1007/s13595-011-0168-x.

[96] O. Carpentier, E. Antczak, F. Brachelet, T. Descamps, L. VanParys, 12th International Conference on Quantitative InfraRed Thermography, (2014).

[97] A. Zziwa, Y. Ziraba, J. Mwakali, Strength properties of selected Uganda timbers, Int. Wood Prod. J. 1 (2010). https://doi.org/10.1179/002032010X12759166444887.

[98] D. Ponneth, A. Vasu, J.C. Easwaran, A. Mohandass, S.S. Chauhan, Destructive and non-destructive evaluation of seven hardwoods and analysis of data correlation, Holzforschung. 68 (2014) 951–956. https://api.semanticscholar.org/CorpusID:100901035.

[99] A. Cavalli, L. Bevilacqua, G. Capecchi, D. Cibecchini, M. Fioravanti, G. Goli, M. Togni, L. Uzielli, MOE and MOR assessment of in service and dismantled old structural timber, Eng. Struct. 125 (2016) 294–299. https://doi.org/https://doi.org/10.1016/j.engstruct.2016.06.054.

[100] Y.S.S.A.Y. Yoshihiko HirashimaMina, Strength properties of old wood (Part 3), Ournal Wood Sci. Soc. (2005). https://doi.org/https://doi.org/10.2488/jwrs.51.146.

[101] Z. Cai, M. Hunt, R. Ross, L. Soltis, Static and vibration moduli of elasticity of salvaged and new joists, For. Prod. J. 50 (2000) 35–40.

[102] ASTM D2395-17; Standard Test Methods for Density and Specific Gravity (Relative Density) of Wood and Wood-Based Materials, in: B. Stand. Vol. 04.10, 2017: p. 13. https://doi.org/10.1520/D2395-17.

[103] J. Bodig, B.A. Jayne, Mechanics of Wood and Wood Composites, Van Nostrand Reinhold, 1982. https://books.google.ca/books?id=GsFRAAAAMAAJ.

[104] CWC O86, Title: Engineering design in wood, Published by CSA Group, 2019.

[105] ASTM International. (2021). ASTM D2395-17, Standard test methods for density and specific gravity (relative density) of wood and wood-based materials, n.d. https://doi.org/https://doi.org/10.1520/D2395-17.

[106] ASTM D198-21a; Standard Test Methods of Static Tests of Lumber in Structural Sizes, 2022. https://doi.org/10.1520/D0198-21A.

[107] F. Arriaga, X. Wang, G. Íñiguez-González, D.F. Llana, M. Esteban, P. Niemz, Mechanical Properties of Wood: A Review, Forests. 14 (2023). https://doi.org/10.3390/f14061202.

[108] F. Divos, T. TANAKA, Relation Between Static and Dynamic Modulus of Elasticity of Wood, Acta Silv. Lignaria Hungarica. 1 (2005) 105–110. https://doi.org/10.37045/aslh-2005-0009.

[109] F. Arriaga, C. Osuna-Sequera, I. Bobadilla, M. Esteban, Prediction of the mechanical properties of timber members in existing structures using the dynamic modulus of elasticity and visual grading parameters, Constr. Build. Mater. 322 (2022) 126512. https://doi.org/https://doi.org/10.1016/j.conbuildmat.2022.126512.

[110] T.P. Nowak, J. Jasieńko, D. Czepiżak, Experimental tests and numerical analysis of historic bent timber elements reinforced with CFRP strips, Constr. Build. Mater. 40 (2013) 197–206. https://doi.org/https://doi.org/10.1016/j.conbuildmat.2012.09.106.

[111] B. Zhang, Q. Xie, J. Xue, Study on the flexural behavior evolution of timber beams with natural shrinkage cracks in historic timber structure, Structures. 73 (2025) 108429.

https://doi.org/https://doi.org/10.1016/j.istruc.2025.108429.

[112] H. Sousa, J. Branco, P. Lourenco, Use of bending tests and visual inspection for multi-scale experimental evaluation of chestnut timber beams stiffness, J. Civ. Eng. Manag. 22 (2015). https://doi.org/10.3846/13923730.2014.914083.

[113] ISO 178, 2019.

[114] F. Gravetter, L. Wallnau, L.-A. Forzano, Essentials of Statistics for The Behavioral Sciences, 9th ed., Wadsworth Publishing, 2017.

[115] A. Wdowiak-Postulak, Natural Fibre as Reinforcement for Vintage Wood., Mater. (Basel, Switzerland). 13 (2020). https://doi.org/10.3390/ma13214799.

[116] A. Borri, M. Corradi, A. Grazini, A method for flexural reinforcement of old wood beams with CFRP materials, Compos. Part B Eng. 36 (2005) 143–153. https://doi.org/https://doi.org/10.1016/j.compositesb.2004.04.013.

[117] Y.-F. Li, Y.-M. Xie, M.-J. Tsai, Enhancement of the flexural performance of retrofitted wood beams using CFRP composite sheets, Constr. Build. Mater. 23 (2009) 411–422. https://doi.org/https://doi.org/10.1016/j.conbuildmat.2007.11.005.

[118] K.C. Johns, S. Lacroix, Composite reinforcement of timber in bending, Can. J. Civ. Eng. 27 (2000) 899–906. https://doi.org/10.1139/l00-017.

[119] L. De Lorenzis, J.-G. Teng, Near-surface mounted FRP reinforcement: An emerging technique for strengthening structures, Compos. Part B Eng. 38 (2007) 119–143.

[120] M.M. Bakalarz, P.G. Kossakowski, P. Tworzewski, Strengthening of Bent LVL Beams with Near-Surface Mounted (NSM) FRP Reinforcement, Materials (Basel). 13 (2020).

https://doi.org/10.3390/ma13102350.

[121] K. Saad, A. Lengyel, Inverse Calculation of Timber-CFRP Composite Beams Using Finite Element Analysis, Period. Polytech. Civ. Eng. (2020). https://doi.org/10.3311/PPci.16527.

[122] R.E.-H. and S.H. Rizkalla, Near-Surface-Mounted Fiber-Reinforced Polymer Reinforcements for Flexural Strengthening of Concrete Structures, ACI Struct. J. 101 (n.d.). https://doi.org/10.14359/13394.

[123] G.M. Raftery, F. Kelly, Basalt FRP rods for reinforcement and repair of timber, Compos. Part B Eng. 70 (2015) 9–19. https://doi.org/https://doi.org/10.1016/j.compositesb.2014.10.036.

[124] A. Gand, D. Yeboah, M. Khorami, A. Olubanwo, R. Lumor, Behaviour of strengthened timber beams using near surface mounted Basalt Fibre Reinforced Polymer (BFRP) rebars, Eng. Solid Mech. 6 (2018) 341–352. https://doi.org/10.5267/j.esm.2018.7.001.

[125] S. Franke, B. Franke, A.M. Harte, Failure modes and reinforcement techniques for timber beams–State of the art, Constr. Build. Mater. 97 (2015) 2–13.

[126] Moein Ramezanpour Kami, Vahab Toufigh, Ultrasonic evaluation for the detection of contact defects of the timber and fiber-reinforced polymer, Struct. Heal. Monit. 22 (2022) 2868–2887. https://doi.org/10.1177/14759217221130499.

[127] Q. Liu, S. Ma, X. Han, Study on the flexural behavior of poplar beams externally strengthened by BFRP strips, J. Wood Sci. 66 (2020). https://doi.org/10.1186/s10086-020-01887-y.

[128] W. Jing, S.S. T., Q. Pizhong, C. Fangliang, Experimental Investigation on FRP-to-Timber Bonded Interfaces, J. Compos. Constr. 18 (2014) A4013006. https://doi.org/10.1061/(ASCE)CC.1943-5614.0000418.

[129] J.J. Myers, D. Gremel, A. Ericson, C. Van Kampen, New ACI 440.11 code adopted for design of concrete reinforced with glass-fiber-reinforced polymer bars., PCI J. 68 (2023).

[130] Sika Ireland, "Sikadur®-31 CF Normal," Sika Ireland, 2024. [Online], (2025). https://www.bing.com/ck/a?!&&p=cd97c3d94ae59e14598c1a956e0e45b4ef0173ac9477fcba96bd8d5edf7fdda5Jmlt-dHM9MTc1NzQ2MjQwMA&ptn=3&ver=2&hsh=4&fclid=1c1e32f5-5a92-656e-2ca2-20425ba9647c&psq=si-kador+31&u=a1aHR0cHM6Ly9jYW4uc2lrYS5jb20vZW4vY29uc3Ry-dWN0aW9uL2FuY2hvc.

[131] H. Alhayek, D. Svecova, Flexural stiffness and strength of GFRP-reinforced timber beams, J. Compos. Constr. 16 (2012) 245–252.

[132] W. Anaf, A. Cabal, M. Robbe, O. Schalm, Real-Time Wood Behaviour: The Use of Strain Gauges for Preventive Conservation Applications., Sensors (Basel). 20 (2020). https://doi.org/10.3390/s20010305.

[133] H. Hoseinpour, M.R. Valluzzi, E. Garbin, M. Panizza, Analytical investigation of timber beams strengthened with composite materials, Constr. Build. Mater. 191 (2018) 1242–1251. https://doi.org/https://doi.org/10.1016/j.conbuildmat.2018.10.014.

[134] Ö. Yurdakul, Ö. Avşar, Strengthening of substandard reinforced concrete beam-column

joints by external post-tension rods, Eng. Struct. 107 (2016) 9–22.

[135] G. Granello, C. Leyder, A. Palermo, A. Frangi, S. Pampanin, Design Approach to Predict Post-Tensioning Losses in Post-Tensioned Timber Frames, J. Struct. Eng. 144 (2018). https://doi.org/10.1061/(asce)st.1943-541x.0002101.

[136] A. Di Cesare, F. Ponzo, N. Lamarucciola, D. Nigro, EXPERIMENTAL SEISMIC POST-TENSIONING PERFORMANCE AND LONG-TERM EFFECTS OF A POST-TENSIONED TIMBER FRAMED MODEL WITH DISSIPATIVE SYSTEMS, 2021. https://doi.org/10.7712/120121.8761.18994.

[137] S. Osman, S. Aldabagh, M.S. Alam, S. Sheikh, Performance-Based Seismic Design of Hybrid GFRP–Steel Reinforced Concrete Bridge Columns, Collect. Tech. Pap. - AIAA/ASME/ASCE/AHS/ASC Struct. Struct. Dyn. Mater. Conf. 27 (2023). https://doi.org/10.1061/JCCOF2.CCENG-3991.

[138] E. McConnell, D.O. Mcpolin, S. Taylor, Post-tensioning glulam timber beams with basalt FRP tendons, Proc. Inst. Civ. Eng. Constr. Mater. 168 (2015) 232–240. https://doi.org/10.1680/coma.14.00032.

[139] C. Gentile, D. Svecova, W. Saltzberg, S.H. Rizkalla, Flexural strengthening of timber beams using GFRP, in: Proc. 3rd Int. Conf. Adv. Compos. Mater. Bridg. Struct. Ottawa, Canada, 2000: pp. 637–644.

Appendix A

Table A.1. Results of full-scale Heritage beams under bending test (pertinent to Chapters 3 and 4)

Geometry			Destructive			Non-destructive	
No.	bxh (cm)	Span (mm)	Fmax (N)	Def (mm)	Failure mode	Dens. (kg/m^3)	MOE (MPa)
S1	14x19	1800	39668	16.326	shear	425	8645
B2	8.5x19.5	1800	22105	12.8	bending	374	6980
B3	8x20.5	1800	34798	21.6	bending	430	7730
S4	9.5x9.5	1100	26761.99	15.033	shear	544	9979
S5	9.5x9.5	1100	24234.02	12.036	shear	380	5818
S6	7.5x12	1100	23941.31	11.92	shear	405	7429
S7	7x20	1100	39321.96	10.984	shear	473	8491
B8	7x19.5	1050	25910.46	8.42	bending	481	8054
S9	7x20	1070	52307	15.06	shear	448	7835
SB10	7.5x20	1030	30885	9.48	shear/bend.	429	7159
B11	7.5x19	1080	34931.29	9.146	bending	418	7377
S12	9x9	1140	10396.76	9.502	shear	373	6004
S13	9.5x9.5	1150	16703	11.58	shear	443	7567
SB14	8.5x9	1130	17954	17	shear/bend.	364	6218
S15	9.5x10	1130	19071.6	11.67	shear	418	7675
B16	7.5x19.5	1180	32137	9.9	bending	412	6862
B17	8.5x20	1300	19832.2	10	bending	398	7021
S18	8.3x20	1300	35357	10.9	shear	442	7510
S19	9.5x10	1300	22797.1	16.1	shear	398	7535
S20	9.5x9.5	1300	23249.45	15.83	shear	353	5699
S21	7.5x12	1300	20508.6	16.79	shear	418	7779
SB22	9.5x9.5	1300	24340	20.154	shear/bend.	378	6084

S23	7.5x12	1350	24154.2	21.4	shear	444	7548
S24	9.5x10	1350	22397.9	21.64	shear	407	6232
S25	9.5x9.5	1380	20774.71	19.825	shear	564	11872
S26	7.5x11.5	1450	23100	23	shear	382	6431
B27	7.5x11.8	1450	22451.15	23.5	bending	415	7702
B28	7x11.3	1450	20162.6	23.5	bending	428	7991
SB29	13.5x19	1500	60600	14.7	shear/bend.	433	7361
B30	6.5x20	1550	15827	10.98	bending	350	6183
S31	10x9.5	1570	22211	27.39	shear/bend.	390	6853
B32	7.2x11.2	1600	14142.4	18.86	bending	428	7940
B33	9.8x10	1630	21173	31.8	bending	412	7330
B34	9.8x10	1670	18985.4	32.66	bending	462	7436
B35	9.8x10	1700	17545.2	33.75	bending	398	6368
SB36	9.6x9.8	1700	21700	49.4	shear/bend.	413	8003
B37	7x20	1700	13456.9	9.25	bending	428	6961
S38	9.6x9.8	1800	14245.6	24.6	shear	417	7732
SB39	10x9.6	1800	18396.7	44.4	shear/bend.	389	6632
B40	9.4x10	1780	20286	41.9	bending	427	7833
B41	7.5x11.6	1780	21164.2	35.49	bending	431	7635
S42	14x19	1830	43020.8	15.15	shear	416	7331
B43	8x20.5	2030	27021.65	22.59	bending	391	6663
B44	6.8x20.2	2000	23143	24.15	bending	412	6946

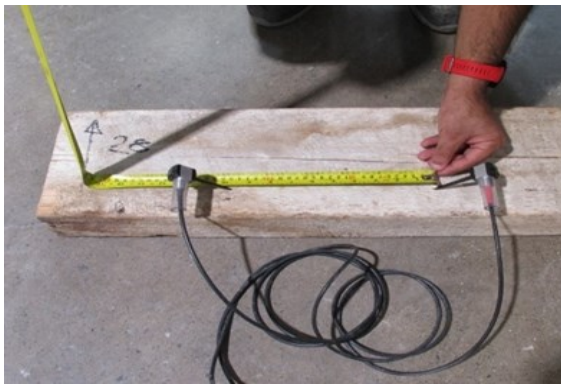

a-1

a-2

a-3

a) NDTs

b-1

b-2

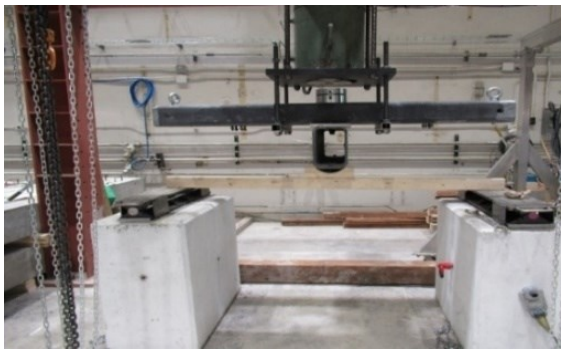

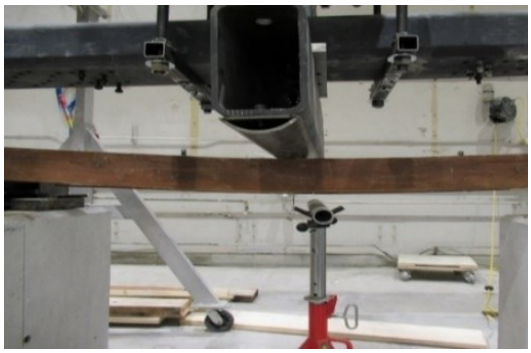

b-3 *b-4*

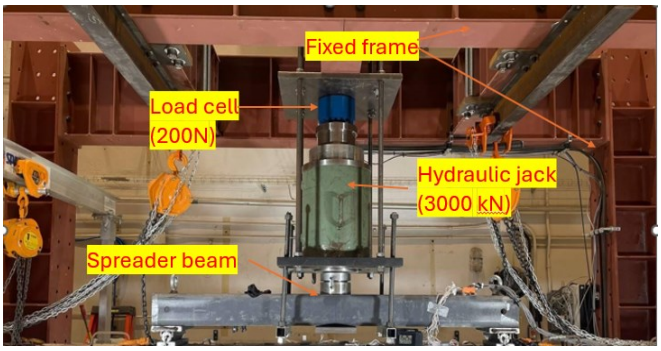

b-5

b) Destructive tests

Fig. A.1. Destructive and NDTs (pertinent to Chapters 3 and 4); a) NDTs, b) Destructive tests

Appendix B

B.1. Procedure to Simulate New Beams

Before starting the Null hypothesis, data are generated for the new beams by simulating them. This task is required since the desired lumber dimensions were unavailable in the market.

First, the material and mechanical properties of the SPF beams are identified. By performing the oven test, the dry density was calculated as 468.9 kg/m^3, followed by an ultrasonic test, which revealed MOE=6.96 GPa. By referring to CWC O86 for SPF timber grades 2 and better, Fb= 11.8 GPa and MOE= 9.5 GPa, while as released by tests, MOE=6.96 GPa; all steps are done several times with Fb=7-11.8 GPa and to be on the safety margin, one lower grade and Fb= 7.6 GPa is chosen conservatively (to be verified later) for the Null hypothesis purpose. Continuing the required calculations based on the above data (Table A.1 in Appendix A- chapter 3):

I (moment of inertia) =bh3/12 =4860000mm4 presented in column no. 4. Also, it is known that Fb=mc/I where m is the moment at failure, c is half of the height, and I is the moment of inertia, so that, m=FbI/c=820800. From here, predicted Fmax (from formulation) = m/(0.25l)= 1356.7MPa reflected in column no. 6. Note that this latter formulation is derived from the simple maximum moment in the middle of the span as: m=pl/4=0.25pl, where l is the span of the beam. Now, moving to the test results from the experiment: Fmax=4240N. The safety factor, SF=4240/1356.7=3.125. In the meanwhile, for a Heritage beam with the cross-section of b=140 and h=190 mm (beam No. 1) Fmax=39668N and by following and redoing the same explained procedure, Fmax(analytical)=14226N; now the concept of safety factor, SF=39668/14226=2.8 which is very close to 3.1 already obtained from new beams stating that it is almost following the same rule and also emphasizes the real strength of Heritage beam is 2.8 times of its analytical new counterpart. This single piece of evidence is not strong enough to conclude; however, the Null hypothesis will give it power.

Now to check the results with CWC O86 and to verify the assumption of Fb= 7.6 GPa, a new beam close to the existing bending tables is chosen so that b=75mm, and h=116mm; from the

CWC O86 tables (interpolation) and analytics Fmax= 6022N and Fmax= 7986N respectively. from the table of Heritage beams (beam no. 41) and bxh =75x116 mm, Fmax= 21164.2N. by calculating the ratio (R) of Heritage/New: R1=21164.2/7986=2.65 and R2=21164.2/6022=3.5 and the Ravg= (3.5+2.65)/2=3.1, almost equal to 3.125, so the assumed Fb= 7.6 GPa is accurate enough and is acceptable.

The final step is multiplying all Fmax (analytics/predicted from formulations) by 3.18 to simulate the final Fmax for all similar new beams to their Heritage counterparts. Results are presented in Table B.1.

Table B.1. Results of destructive tests on Heritage and SNCs (pertinent to Chapter 4)

Heritage Beams(H) (Experimental)					Simulated New Counterparts (SNC)			
No	Area (mm2)	Span (mm)	Fmax(N)	Frequency	No	Area (mm2)	Span (mm)	Fmax(N) (experiment)
H1	7312-8100	1450-1600	14142-20162	2	SNC1	7312-8100	1450-1600	9932-9095
H2	13000-13736	1550-2020	15827-214	2	SNC2	13000-13736	1550-2020	22353-27026.6
H3	8050-8850	1450	22451-23100	2	SNC3	8050-8850	1450	11021-11604
H4	8700	1780	21164.2	1	SNC4	8700	1780	9135
H5	9000	1300-1350	20508-24154	2	SNC5	9000	1300-1350	12890-13385.5
H6	9000	1100	23941	1	SNC6	9000	1100	15819.05

H7	13300-15000	1050-1180	25910-5207	6	SNC7	13300-15000	1050-1180	38940.2-46928.2
H8	14000	1700	1456.9	1	SNC8	14000	1700	26537.4
H9	7650-8100	1130-1140	10396-17954	2	SNC9	7650-8100	1130-1140	9816.9-10303.2
H10	16600-17000	1300	1982-35357	2	SNC10	16600-17000	1300	41147.6-42139
H11	15600-17425	1800-2030	22105-34798	3	SNC11	15600-17425	1800-2030	26684-30093.6
H12	9025-9500	1100-1150	16703-26762	4	SNC12	9025-9500	1100-1150	12012.2-13545.5
H13	9025-10000	1300-1670	18985-24340	8	SNC13	9025-10000	1300-1670	7902.8-11774.2
H14	9024-10000	1700-1800	14245.6-21700	5	SNC14	9024-10000	1700-1800	8249.3-9288.1
H15	25650-26600	1500-1830	39668-60600	3	SNC15	25650-26600	1500-1830	44497.3-52348

Table B.2. Results of destructive tests on New beams

New(N) Beams (Experimental)				
No	Area (mm2)	Span (mm)	Fmax(N)	Fre-quency
N1	4200	1200	6240	1
N2	7200	2420	4240	1
N3	6750	2420	3920	1
N4	8100	2420	4958	1
N5	9450	1500	12500	1
N6	18225	1500	28119	1

Appendix C

c-1

c-2

c-3

c-4

c-5

c-6

c-7

c-8

c-9

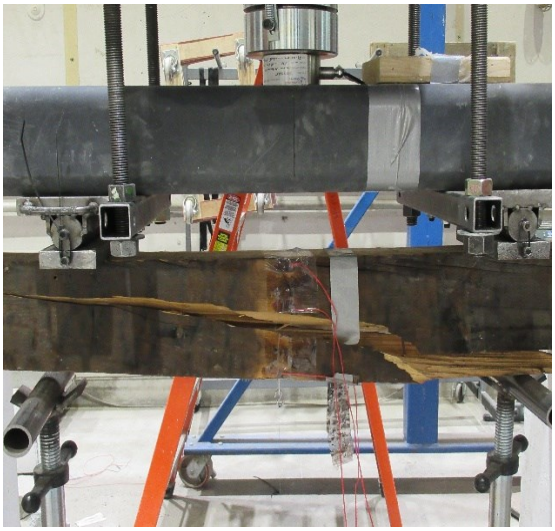

c-10

c-11

Fig. C.1. Experimental pictures of strengthened Heritage beams, along with associated failures